AD-A269 553

Exploratory Study of Joi for Ceramic Underwater Pressure Housings

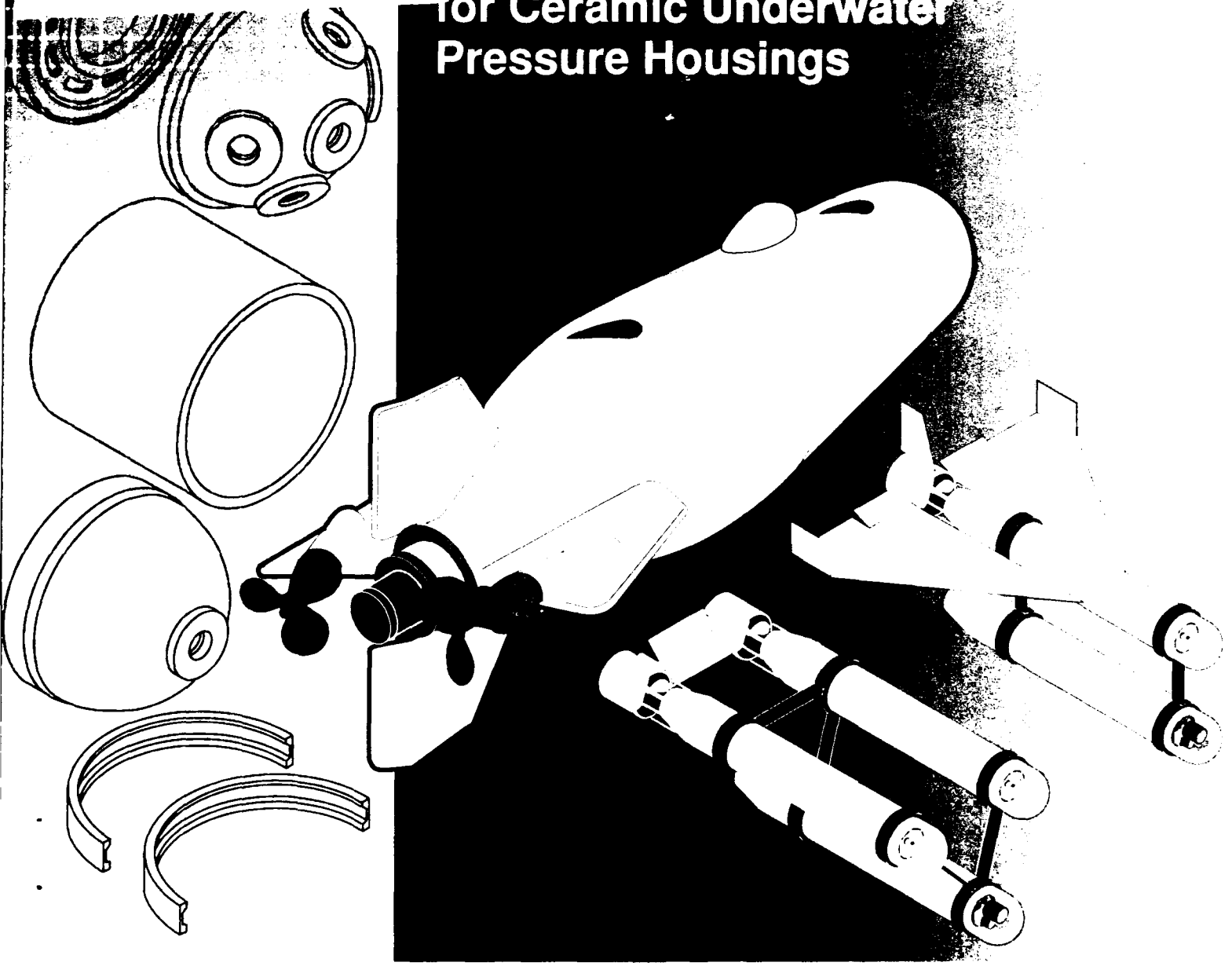

R. P. Johnson
R. R. Kurkchubasche
J. D. Stachiw

Technical Report 1586
May 1993

Approved for public release; distribution is unlimited.

93-21960

Technical Report 1586
May 1993

Exploratory Study of Joint Rings for Ceramic Underwater Pressure Housings

R. P. Johnson
R. R. Kurkchubasche
J. D. Stachiw

Accesion For
NTIS CRA&I
DTIC TAB
Unannounced
Justification
By
Distribution/
Availability Codes
Dist | Avail and/or Special
A-1

DTIC QUALITY INSPECTED 1

NAVAL COMMAND, CONTROL AND OCEAN SURVEILLANCE CENTER
RDT&E DIVISION
San Diego, California 92152–5001

J. D. FONTANA, CAPT, USN
Commanding Officer

R. T. SHEARER
Executive Director

ADMINISTRATIVE INFORMATION

This work was performed by the Marine Materials Technical Staff, RDT&E Division of the Naval Command, Control and Ocean Surveillance Center, for the Naval Sea Systems Command, Washington, DC 20362.

Released by
J. D. Stachiw, Head
Marine Materials
Technical Staff

Under authority of
N. B. Estabrook, Head
Ocean Engineering
Division

ES

SUMMARY

The use of ceramics to construct underwater pressure resistant housings requires techniques that can be used to adjoin ceramic hull components together. The Naval Command, Control and Ocean Surveillance Center (NCCOSC) RDT&E Division (NRaD) has pioneered the use of epoxy-bonded metallic joint rings for the purpose of assembling adjacent ceramic housing sections. These joint rings act to transfer load through joint interfaces, while also providing a means of sealing and maintaining closure. Additionally, joint rings can be designed to provide additional stiffness to the housing assembly to increase buckling resistance.

This report summarizes issues that must be considered when designing metallic joint rings for ceramic underwater housings. Selection of the joint ring material and joint ring bonding adhesives are addressed. The effect of various joint ring design parameters on the structural performance of the ceramic housing assembly are also discussed. The report concludes with a description of four different alumina-ceramic pressure housings that were designed and pressure tested to destruction. The purpose of these tests was to validate the structural performance of various joint ring designs for consideration in future ceramic underwater pressure resistant housings.

CONTENTS

FIGURES

TABLES

INTRODUCTION

Figure 1[1] shows three cross sections of designs that could be used to assemble a ceramic cylindrical hull for an underwater pressure housing. These joining techniques differ in the configuration of metallic joint rings that are used at the interface of adjacent ceramic components. Joint rings may serve a variety of different functions to the housing, but all share certain primary functions essential to their successful application in ceramic underwater pressure housings.

Joint rings act to transfer load between adjacent ceramic sections without having the bearing surfaces at the end of one ceramic part bear directly against the bearing surface of an adjacent ceramic part. Early attempts to join ceramic components without the protection of joint rings (reference 11) resulted in short-term cyclic fatigue failure initiated by cracks that originated from the region of direct ceramic-to-ceramic contact. Protecting the ends of ceramic components with metallic joint rings allows transfer of pressure-induced interface loads between hull sections without causing fretting failure of ceramic ends.

Joint rings also provide local attachment points for mounting internal or external hardware such as tie rods, payload rails, and electrical cable raceways. The means for achieving joint seals and joint closure can also be designed into joint rings. By integrating these features into the joint ring, the localized loads associated with handling, assembling, and sealing the pressure housing can be directed onto the metallic end rings and not on the more sensitive ceramic hull components.

Additionally, it may be advantageous to design the joint rings to provide additional stiffness to increase the buckling resistance of the pressure-housing assembly. Manufacturing constraints may limit techniques that the designer can use to stiffen individual ceramic hull components. In these cases, metallic joint rings can be configured to provide the required ceramic component end support needed to achieve the operating depths for which the housing is intended.

1. Figures and tables are placed at the end of the text.

JOINT RING FUNCTION

The first housing configuration shown in figure 1 would appear to be the simplest way to construct a ceramic cylindrical hull section for an underwater pressure housing. This assembly consists of a single monocoque ceramic cylinder with appropriate metallic end caps for mating with the end closures. But for many housing configurations, a single monocoque cylinder hull may not be a viable design approach. Large housings (reference 6), with outer diameters of 25 inches or larger and hull lengths corresponding to L/D ratios greater than two, may simply not be manufacturable. Fabrication of these large parts may be limited by the size of available isopress equipment, kilns, and grinding machines. Additionally, cylinder length may be limited by other constraints such as slumping of the green body during firing. Successful construction of such large cylindrical housings requires assembling a number of shorter cylinders together using joint rings or other bonding techniques.

Brazing a number of ceramic rings together has been demonstrated to be one potential approach to building up longer cylindrical hull sections that may not be fabricated as one piece (reference 11). Six-inch outer-diameter (OD) cylinders (L/D = 1.5) have been constructed by metallizing the ends of ceramic rings and then brazing the rings together. The shortcoming of this and similar techniques such as diffusion bonding is that the size of cylinder that can be constructed this way is limited by the size of the fabrication equipment that is available. Brazing furnaces that are big enough to handle larger ceramic components may not exist or be of limited access.

Another technique for joining ceramic cylinders involves using a metallic coupling ring like that shown in the second housing configuration in figure 1. This technique involves epoxy bonding an H-shaped ring to the ends of adjacent ceramic cylinders. Assembling cylinders in this way can be performed using relatively simple handling fixtures and is not size limited. Pressure testing of

cylindrical hulls constructed using coupling rings has demonstrated the viability of this approach. Analysis and testing has shown that the structural performance of the coupling ring configuration matches or exceeds the performance of the single monocoque cylinder it replaces. As mentioned previously, the presence of coupling rings also provides a means of accommodating local internal and external attachments to the pressure housing walls. The general structural behavior of ceramics is such that they are well suited to bearing the primarily compressive membrane stresses that exist in the walls of underwater pressure housings under depth loading. On the other hand, ceramics will not perform as well in areas where localized stresses exist due to local attachments and/or joint interfaces. For this reason, metallic coupling rings are advantageous in helping to buffer the ceramic hull against these extraneous stresses.

In addition to manufacturing considerations that may limit their use, there are a number of housing configurations where a monocoque cylinder design is undesirable for structural reasons. The structural integrity of cylinders with large values of L/D subjected to high hydrostatic pressure may depend on their ability to resist buckling. For this type of monocoque hull, the wall thickness that is required to resist buckling may have to be substantial. While the thick hull may be capable of avoiding collapse by buckling, it could be understressed to the point that the high compressive strength of the ceramic material is not being utilized. This approach would result in a housing with a higher weight-to-displacement (W/D) ratio and would give lower performance than could be achieved with other housing designs.

Designing a more efficient housing by using integral stiffening ceramic ribs would be a more efficient approach from a weight-savings point of view, but unfortunately is restricted because fabrication is not economical because of manufacturing constraints. To have stiffening ribs in large cylinders made from ceramic materials such as alumina, one would have to isopress a very thick walled cylinder, and then create ribs by grinding out the excess material between the ribs once the ceramic body has been fired. This would be an exorbitantly expensive and risky operation. Green machining this excess material prior to firing is not an option because of thermal-expansion mismatch problems and the potential for high residual stresses that would occur at the rib/hull interface during firing. A typical alumina-ceramic green body that is fabricated by isopressing can shrink as much as 20% during the firing process.

The prospect for integral ribs is much better for cermet hull components made by alternative fabrication techniques (reference 12). An example of this would be silicon carbide-reinforced alumina-ceramic matrix composites made by directed metal oxidation process. This material process results in less than a one-percent dimensional change during fabrication which, in theory, should allow for near net-shape fabrication of housing components with features like integral ribs. An additional benefit that cermet materials could have for underwater pressure housings is that the shell wall could transition to a metal-rich composition toward the ends of the hull section. This would allow the cermet cylinder ends to be designed with features such as O-ring glands, attachment points, and flanges for closure. The size and shape of housings made to date by this process are limited to 12-inch OD monocoque cylinders with L/D = 1.5.

Given these current limitations in fabricating stiffened ceramic hull components, alternative approaches to increasing the buckling resistance of ceramic housings are required. One such technique is to integrate stiff metallic joint rings into the housing assembly design. These rings can be designed to support the cylinder ends in such a way as to raise the collapse pressure of the housing by increasing the external pressure required to bend the ceramic hull into a buckled configuration. The last of the three housing configurations shown in figure 1 uses a central metallic joint ring assembly designed to stiffen the ceramic hulls. The use of stiff joint rings to help bear the external hydrostatic load allows the designer to build up cylindrical hulls by using a number of cylinders which have a reduced wall thickness compared to the single monocoque cylinder they replace. This composite structure of stiff metallic joint rings and ceramic hulls allows the designer to achieve the required buckling resistance of the assembly while

tailoring down the ceramic wall thickness to utilize ceramic's excellent compressive strength. This allows structures to be optimized to have a minimum W/D ratio by taking advantage of the material properties of each of the housing's components.

JOINT RING MATERIAL

In the design of joint rings for underwater ceramic pressure housings, material selection is driven by the specific criteria that govern the individual housing design. The use of ceramics is attractive for underwater housing designs where low W/D ratios are needed to provide maximum buoyancy. Ceramics are an excellent candidate for this purpose because of their high specific compressive strength and specific modulus. Consequently, the selection of a joint ring material for these types of applications would require metals that also have high specific strengths to help keep the structural weight of the housing assembly to a minimum. In cases where the metallic joint rings are designed to provide additional stiffness to increase the buckling resistance of the housing assembly, the specific modulus of the joint ring material becomes an important concern.

An additional benefit of using ceramic for major underwater hull components is its excellent resistance to corrosion in seawater. Likewise, materials used for joint rings should be capable of withstanding the marine environment without degradation due to any type of corrosive failure.

A number of ceramic materials like beryllia exhibit outstanding heat conductivity which make them attractive for applications in housings that require heat dissipation to keep internally packaged components such as electronics at low ambient temperatures. For these types of applications, it may also be desirable to select materials with high thermal conductivities to fabricate the joint rings in order to offer an additional path through which internally generated heat can be dissipated.

In situations where underwater housings require the capability to operate over a wide range of temperatures, matching the thermal expansion coefficients between the ceramic used in the hull and the material used in the joint ring becomes important. The closer the coefficents are to each other, the less thermally induced stress will occur at the interface between the two materials under thermal cycling. Stresses induced by thermal loading may be of concern specifically in cases where the bearing surfaces of the ceramic ends are placed in localized tension. In such cases, the potential for cracks to propagate from any local tensile regions would exist if the housing was subjected to high numbers of thermal cycles. If high temperatures are part of the operating environment for the ceramic housing, special care must be given to the type of materials used for the joint rings as well as the type of bonding adhesives and seals that are selected.

Another localized stress that may appear at the interface between the ceramic hull and metal joint ring is caused by a Poisson's-type effect that occurs under hydrostatic pressure loading of the housing assembly (reference 7). External pressure on underwater housings results in substantial compressive membrane strains in the housing components. This meridional and circumferential compression leads to radial expansion of the housing wall under depth load. The amount of radial expansion depends on the elastic moduli and Poission's ratio of the housing material and the magnitude of the membrane stresses. At discontinuities in the housing-wall material and geometry such as at the interface between a ceramic hull and a metallic end cap, a mismatch in radial expansion will occur. Typically, the metallic end cap will undergo greater radial expansion than the relatively stiff adjacent ceramic shell and thereby place the ceramic bearing surface region into localized tension. This effect can be of concern when the underwater housing assembly is required to complete a high number of dive cycles. The tensile stresses present at the ceramic bearing surface may be large enough to initiate cracks that propagate into the ceramic wall from bearing surface flaws under repeated loading.

In addition to material properties, consideration of relative material and manufacturing costs for joint rings for ceramic underwater pressure housings are obviously important. The machinability rating of the material becomes an issue especially when

fabricating joint rings for large housings (reference 6). Ceramic housing joint rings used at the Naval Command, Control and Ocean Surveillance Center (NCCOSC) RDT&E Division (NRaD) are machined from solid rolled-ring forgings which require substantial material removal to create the U-shaped joint ring used to encapsulate the ceramic ends. In joint ring designs requiring external or internal lugs or ears for attachment points, the weldability of the material may become an important criteria. Since the structural performance of pressure housings can be sensitive to geometric imperfections, welding techniques that minimize distortion in the finished parts should be pursued.

The choice of material for use in a joint ring depends on the performance criteria selected for each specific application. Both titanium alloy Ti-6Al-4V and high-strength 7000-series aluminum alloys have been successfully employed at NRaD for use in joint rings for ceramic underwater pressure housing assemblies. Titanium alloys are especially attractive because of their high specific strength, high specific modulus, corrosion resistance, thermal expansion coefficient match with alumina ceramic, and weldability.

JOINT RING BONDING MATERIALS

As mentioned previously, there are a number of techniques that can be used to join adjacent ceramic housing components. When metallic joint rings are selected as the means of attachment, procedures for bonding the joint ring to the ends of each ceramic hull component must be developed. Two-part epoxy adhesives had been selected by NRaD for this purpose, and a description of the bonding procedure currently used by NRaD is given in appendix A. The use of two-part epoxies for joint ring assembly may not be an acceptable choice in cases where there are high operating temperatures. The top assembly shown in figure 2 shows a cross-section view of a ceramic cylinder, metallic joint ring for mating and sealing with an end closure, and the epoxy bond filling the annular and axial spaces between these two parts. A general discussion on important considerations to be used for selection of a suitable bonding adhesive is as follows.

The bonding material should offer compliance to eliminate point loadings on the bearing surface of the ceramic ends caused by imperfections in the ceramic surface. The bonding material must be capable of transferring the high compressive loads between the ceramic hull and its metallic joint ring without degradation. The joint ring design and the adhesive selected must perform this load transfer without the adhesive extruding, fracturing, delaminating, or exhibiting any other type of permanent failure. The use of small chamfers or radii at the edges of the ceramic hull component ends aids in reducing the stresses on the bonding material as well as reducing the chance for chipping the edge of the ceramic part during assembly.

The bond between the joint ring and hull component must also withstand external pressure and the marine environment without any leakage. As discussed in appendix A, one way of ensuring that no water penetrates the epoxy bond in the joint is by applying an RTV sealant over the epoxy where it is exposed to water as shown in the top assembly of figure 2. This design may be of use when the pressure housing is intended to undergo a large number of dive cycles or extended submersion and the potential for water intrusion becomes more likely. Other techniques for sealing the epoxy include replacing a bead of RTV with a urethane coating or mechanical seal like the one shown in the bottom assembly of figure 2. This seal is an elastomeric boot that is "rubber banded" into place and offers the benefit of being removed for easier inspection of the underlying ceramic hull.

Another advantage already noted is that joining ceramic components with epoxy bonded metallic joint rings is an economically feasible approach that can be performed using simple assembly fixtures and is not constrained by the size of the housing components. The existence of these simple joining techniques that perform reliably during service are essential to the continued success of ceramic underwater pressure housings.

Another potential bonding technique involves placing a brazing alloy between the ceramic hull and metallic joint ring and heating this assembly in a furnace to obtain a brazed joint. A number of

techniques have been developed for ceramic-to-metal brazed joints including sintered metal powder process, active filler metal process, and vapor coating process (reference 9). A typical active filler metal process brazing alloy requires a minimum furnace temperature of 600 degrees Celsius to form, which requires a good match in thermal expansion coefficients between the ceramic and metal joint ring to avoid residual stress problems once the brazed joint has been cooled.

Residual stresses that result from brazing can have catastrophic effects if their result is to place the ceramic hull ends in a state of tensile stress. Failure by static fatigue due to residual tensile stresses in the ceramic can occur. The larger the diameter of the ceramic hull component, the larger the potential for thermal deflection differences during brazing and, consequently, the greater the chance for residual stress problems. One approach to dealing with thermal expansion mismatch between the ceramic hull and metallic joint ring is to add an interlayer of a metal that has an intermediate thermal expansion coefficient, but this necessitates an additional joint as well as additional risk and cost. Other ceramic-to-metal bonding techniques such as fusion welding, diffusion bonding, and glass sealing exist, but are, as yet, untested for use in ceramic underwater pressure housings.

JOINT RING DESIGN

The detailed design of metallic joint rings for ceramic underwater pressure housings is obviously dependent on the specific application for which the housing is intended. Nonetheless, general recommendations can still be made about certain details the engineer will have to consider when designing metallic joint rings.

Figure 3 shows three options for joint rings based on a Naval Ocean Systems Center (NOSC)[2] type Mod 1 (hereafter called Mod 1) design for a service joint between a ceramic cylindrical hull and a ceramic hemispherical end closure. The primary functions of the metallic joint rings for this case are to protect the bearing surfaces of the ceramic ends and to provide a means of assembly and sealing. Protection of ceramic ends is especially important when there are substantial differences in radial deflection between adjacent hull components under external hydrostatic pressure. Fretting between unprotected ceramic ends would be more severe, the greater the mismatch in displacements of adjoining ceramic ends. Since the hemispherical end closure acts to support the end of the cylinder against buckling, designing the joint rings for additional stiffness would not be considered. The first assembly of figure 3 shows various dimensioning variables that define the joint ring design. Selection of appropriate values for these variables are determined by their impact on factors such as hardware cost, ability to be assembled, and effect on structural performance of the joint interface.

Selection of the length of the joint ring flange L is driven by a number of such considerations. The longer the flange (i.e., the greater the bond length between cylinder and joint ring), the more expensive the part becomes to fabricate. Other shortcomings of long flanges are the potential of increased difficulty of assembly due to misalignment and a reduction in the portion of the ceramic shell that can be nondestructively evaluated with techniques such as ultrasonics. Intermittent nondestructive evaluation of the ceramic housing wall to ensure structural integrity may be desirable in cases where the hull undergoes a high number of dives to design pressure. Additionally, longer-length flanges may be undesirable from a weight point of view when maximum buoyancy of the housing assembly is desired.

The advantages of using a longer flange are primarily based on their observed effect of increasing the structural performance of the housing assembly under cyclic load. As mentioned previously, cracks that propagate from the localized tensile stress regions caused by Poisson's effects at the bearing surfaces of ceramic ends can

2. NOSC is now Naval Command, Control and Ocean Surveillance Center (NCCOSC) RDT&E Division (NRaD).

eventually degrade the performance of ceramic underwater pressure housings. These circumferential cracks have been observed to run in a more-or-less meridional orientation from the bearing surface of the ceramic ends. Failure could occur if these cracks propagated to the point that they break through the inner or outer diameter of the ceramic hull wall and a portion of compressive load-bearing hull spalls off or leaks occur. The presence of a long flange length L acts to contain this spalling effect by encapsulating the ceramic ends where the cracks may appear. Additionally, finite-element analysis (FEA) indicates that the presence of longer flange lengths also has the effect of decreasing the localized tensile stresses that may occur at the ceramic's ends and, thus, reduces the chance of crack propagation. Metallic joint rings designed for ceramic hemispheres and cylinders at NRaD are typically chosen to have a flange length between two and three times the thickness of the shell wall they encapsulate.

The other primary variable that determines the shape of the flange is its thickness, TF. FEA indicates that thinner flange thickness results in lower tensile stresses occurring at the bearing surfaces of the ceramic component ends. Manufacturing joint rings with thinner flanges may require tighter dimensional tolerances, and thinner flanges may be undesirable if attachment points for additional hardware are needed at the flange surfaces. Flange thickness may also be constrained by the amount of material needed to contain the high hydrostatic stresses that occur in the trapped epoxy under an external pressure load. The forces exerted on the flanges of the joint ring by the epoxy become more critical the greater the amount of axial clearance, TA, that exists between the ceramic ends and the bearing surface on the joint ring.

The amount of TA and radial clearance, TR, between the ceramic shell and its metallic joint rings affects the ease of joint ring assembly and the structural performance of the joint interface. The amount of nominal TR used at NRaD is on the order of 1/1000 of the OD of the ceramic hull components. Obviously, the ability to achieve this clearance in actual assembly depends on using proper assembly fixtures and also on the dimensional tolerances to which the joint ring and ceramic hull are fabricated. Higher tolerances on the ceramic piece parts implies higher monetary costs, but also provides greater ease of assembly and higher structural reliability. The additional cost for tighter tolerances is due to the additional work required to finish grind the inner and outer surfaces of the ceramic hull. This grinding process can be used to fabricate ceramic piece parts which are very concentric and of uniform wall thickness. Typical tolerances for 12-inch OD cylinders (L/D = 1.5) procured by NRAD are on the order of plus or minus .005 of an inch on wall thickness and OD. FEA indicates that using radial clearances of 1/1000 of the OD of the ceramic hull will result in minimum interface stresses in the ceramic at the joint. Higher values of radial clearance than this could also result in higher potential for the epoxy to extrude from the metallic joint ring under the nigh loads associated with substantial external hydrostatic pressure.

Controlling the TA between the bottom of the U-shaped metallic joint ring and the bearing surface at the end of the ceramic shell depends on the relative flatness of these interfacing surfaces and the use of standoffs during assembly. A standoff of equivalent thickness to the desired axial clearance can be used during assembly to maintain spacing between the ceramic bearing surface and bottom of the U-shaped metallic joint ring. Cured epoxy standoffs or 125-pound manila stock (see figure A-1 of appendix A) can be used for this purpose. FEA indicates that variations in TA also effect the interface stresses in the joint region. The challenge of applying the results of FEA for an actual joint is to develop manufacturing tolerances and assembly techniques that achieve the desired TA spacing.

Assembling the joint interface to eliminate epoxy in the TA may also improve the structural performance of housings required to achieve a high number of dive cycles to design depth. Keeping the bearing surface of the ceramic ends free of epoxy can be accomplished by covering the bearing surface with a gasket (references 6 and 13). It is hypothesized that under high hydrostatic loads the epoxy could flow into surface flaws in ceramic

and the high hydrostatic pressure of the epoxy in the flaw could then act to initiate cracks that could propagate under repeated loading.

A number of material candidates for use in ceramic bearing surface gaskets have been evaluated experimentally (reference 13) to determine their effect on the cyclic fatigue life of ceramic underwater pressure housings. The most promising gasket material tested based on these studies is graphite fiber reinforced (GFR) PEEK composite. NRaD has used .040-inch-thick GFR PEEK gaskets consisting of eight graphite fiber plys laid up in a (0/90) configuration. In addition to keeping the ceramic bearing surface free of epoxy, it is hypothesized that the tailored mechanical properties of the GFR PEEK gasket are well suited for application as a protective gasket. The graphite fibers provide relatively good in-plane stiffness to the gasket which helps reduce the Poisson's effect-induced stresses on the ceramic bearing surface described previously. Yet, the PEEK matrix also provides the gasket with tough, yet compliant, properties in the axial direction which aids in reducing localized stresses on the ceramic bearing surface ends due to surface irregularities.

The benefits of having service joints that can be mechanically disassembled are numerous. Service joints allow for internal access to ceramic underwater pressure housings to package or unpackage payloads. They allow for separate housing components to be pressure tested individually before the entire assembly is tested. They allow for hull components to be inspected individually or to be more easily replaced. The use of service joints also requires additional sealing techniques and a means of maintaining closure. Figure 3 shows three examples of sealing and closure configurations that can be used for service joints for ceramic underwater pressure housings.

The first assembly shown in figure 3 utilizes split V-band clamp bands to join adjacent housing sections. Clamp bands aid in sealing a joint-ring interface by maintaining uniform compression of O-ring face seals during assembly. These figures also show a redundant radial seal machined into the extended lip of the hemisphere joint ring. For larger housings, pulling a slight internal vacuum on the housings during assembly to compress the O-ring face seal may help for assembling the V-band coupling. The location of the O-ring glands in the joint rings should be placed as far as possible from the bearing surfaces of the ceramic hull components. This minimizes the effect that the potentially high localized stresses that occur in the joint ring around the O-ring gland under external pressure loading will have on the adjacent ceramic. For this reason, the O-ring glands in the joint rings shown in figure 3 are located in the external flange of the hemispherical end-cap joint ring. The second and third assemblies shown in figure 3 use circumferential bolts and tie rods to maintain closure. Tensioned internal or external tie rods between joint rings of the cylindrical hull have the benefit of helping to bear the handling loads on the pressure housing assembly that would otherwise be born by the joint ring/shell epoxy bonds only. Using tensioned tie rods to precompress the ceramic hull to reduce tensile stresses that may occur in the ceramic during handling is also an option. The use of bolts or tie rods to maintain closure also requires more space than split V-band clamp bands, which may be of concern if tight packaging volume requirements exist.

Figure 4 shows four detailed views of joint-ring designs based on those discussed earlier and shown in figure 1. The first two designs are permanent joints that could be used where disassembly is not required. The first design shows a coupling ring that could be used to assemble multiple cylinders together to create a longer hull for cases when the ceramic cylinder cannot be fabricated as a single unit. The second design shows a coupling ring with an integral internal T-shaped stiffening ring to provide additional structural support. The last two configurations shown in figure 4 are options when both disassembly and additional stiffness are required for a joint-ring design. The fourth option has the additional advantage that the inner stiffening I-ring is not externally exposed, which offers the designer a greater selection of material choices from which to fabricate the I-ring. Materials

which have high specific modulus, but are susceptible to sea water corrosion, can now be considered.

Selection of the assembly tolerances and encapsulating flange dimensions discussed earlier for service joint rings also apply to the joints shown in figure 4. The design of joint rings, like those in the final three assemblies of figure 4, that provide additional structural support for buckling resistance is the next issue to be addressed.

JOINT RING DESIGN FOR INCREASED STRUCTURAL STABILITY

Structural instability can occur in underwater pressure housings under external hydrostatic load if there exists a means by which the strain energy associated with compression of the shell membrane can be converted to strain energy associated with bending of the shell membrane. Typically, the in-plane membrane stiffness of a shell is substantially greater than its bending stiffness. Consequently, if the strain energy in the membrane can be converted to bending energy, the subsequent bending of the shell can result in very large deflections. These large deflections associated with bending of the pressure-housing shell wall is known as buckling and is one of the primary failure mechanisms for ceramic underwater pressure housings. Utilizing stiffening rings like those in the last three assemblies of figure 4 increases the buckling resistance of the housing assembly because the inertia created by a deep joint-ring web can result in substantial bending stiffness.

The use of a joint ring with radial depth to provide additional buckling resistance is predicated on the available external and internal packaging volume that exists for each housing. Optimally, the major portion of mass of the T-shaped portion of a central stiffened joint ring would be concentrated in an internal flange that is offset from the shell wall via a deep relatively slender web. External pressure housings can also be stiffened with external ribs, but this approach is not as structurally efficient as an internal rib configuration. The larger the diameter of the web and flange of the stiffening ring, the less stable it becomes under compressive load, and, consequently, the less structural support it will provide to the hull assembly.

Once volume constraints are established, stiffened joint rings require structural analysis techniques to verify the integrity of the design. Stress analysis should be performed to verify that stresses in the stiffened joint ring are well below levels that would cause yielding of the metal to occur. If yielding occurs before buckling, a stability analysis that can account for material nonlinearities is required. Additionally, stability analysis must be performed to ensure that the stiffened joint rings provide adequate resistance against failure by general instability of the housing (long wave length), as well as failure by local instabilities such as local flange or web crippling (short wave length). In designs where multiple stiffened joint rings are used, inner bay buckling (intermediate wave length) also must be checked. An optimized hull design incorporating stiffened joint rings would have all of these three potential failure modes occur at the same external pressure load.

The amount of stiffness that a joint ring provides a housing depends on both its geometry and location with respect to the shell wall, as well as the material that is used. For this reason, high modulus materials or high specific modulus materials where weight is a concern are most attractive. NRaD has utilized both titanium alloy (Ti-6Al-4V) and high-strength 7000 series aluminum alloys to fabricate stiffened joint rings. Stiffened joint rings that utilize ceramics as part of their design also have been considered. A stiffened joint ring that could utilize ceramic's outstanding specific modulus would be ideal where weight savings are of concern.

JOINT RING TEST CASES

Four ceramic underwater pressure housings were assembled and tested to destruction to validate potential joint-ring designs for full-scale 26- and 33-inch OD ceramic deep-submergence pressure housings designed by NRaD (reference 6). All four test housings utilized alumina-ceramic cylinders purchased from COORS Ceramics Company as

the primary hull structures. 99.8 percent alumina was used for the case 1 housing, while 94 percent alumina was used for the other three housing assemblies. All metallic joint rings used in these tests were machined from Ti-6Al-4V that was subsequently bonded to the alumina hull components with a two-part epoxy as described in appendix A.

Joining two alumina cylinders together using a central coupling ring or a stiffened central joint ring were two of the concepts that were studied for the designs of the 26- and 33-inch housing cylindrical hulls. The intent of these four test cases was to compare their predicted performance based on structural analysis calculations to their actual tested performance. Specifically, predictions of the external pressure required for each of the housings to fail by buckling was to be compared to tested collapse pressures, although finite-element stress analysis calculations were compared to strain gage data for test case 4 (reference 13).

Figure 5 shows the final assembled housing used for test case 1, and figure 6 shows an internal view of the case 1 housing prior to bonding of the second ceramic hull to the central coupling ring. Dimensions for each of the ceramic hulls used in this assembly are given in figure 7, and the dimensions of the titanium central coupling ring are provided in figure 8.

Both ceramic shell components for the case 1 assembly have a nominal seven-inch-long cylindrical section with an integral hemisphere at one end. A nominal wall thickness of .2 of an inch is used for both the cylindrical and hemispherical portions of each ceramic hull. Each of the ceramic components were fabricated by a slip casting process with no finishing operations performed. Fabricating the part without any finish grinding results in a lower cost part at the expense of looser dimensional tolerances. Loose dimensional tolerances for the ceramic components requires either loose tolerances for the coupling ring or making the effort to custom fit the coupling ring to the measured dimensions of the as-fabricated ceramic hull ends. Loose dimensional tolerances also add more uncertainty to predicting failure by buckling. To compensate for this increased uncertainty, additional shell wall thickness may be required for an additional safety margin.

A cross-sectional view of the test case 2 assembly is shown in figure 9. This configuration consists of two alumina-ceramic cylinders shown in figure 10 joined together using the titanium coupling ring shown in figure 11. The remaining cylinder ends are encapsulated with the end cap joint rings shown in figure 12 that are designed to mate with the flat-steel end plates shown in figure 13.

The case 3 assembly is shown in figure 14 and utilizes two ceramic cylinders with the same dimensions and alumina composition as used for the case 2 assembly (figure 10). These two cylinders are joined together using the central stiffened joint ring shown in figure 15 and their remaining ends are encapsulated with the end-cap joint rings machined to the dimensions shown in figure 12. The central stiffened joint ring acts to couple the two ceramic cylinders together and also provides additional buckling resistance through its integral T-shaped ring at its inner wall. Existing titanium hemispheres shown in figure 16 from an earlier NRaD program were used as end closures for the case 3 housing. Figure 17 shows an end-cap joint ring and a stiffened central joint ring before assembly. Figure 18 shows each alumina cylinder with a bonded end-cap joint ring prior to epoxy bonding the stiffened central joint ring in place.

The configuration of the test case 4 assembly is covered in great detail in reference 13. The top assembly drawing along with the joint rings used are shown again in figures 19, 20, 21, and 22. The central stiffened joint ring is similar to the one used for test case 3. The short thick web shown for the integral T-shaped ring does not represent an optimally designed stiffener because of constraints that were set for maximizing internal packaging volume while loading the housing from one end only. An alternative stiffener could be designed for the same weight as the part shown in figure 20 which would provide substantially more external pressure capacity if packaging volume constraints did not exist.

PROCEDURES FOR CALCULATING STRUCTURAL STABILITY FOR JOINT RING TEST CASES

Structural stability analysis requires selecting the operating requirements (service depth) and desired margins of safety for the housing design. Traditional buckling analysis involves calculating the elastic bifurcation buckling pressure based on perfect housing geometry to ensure the housing design meets the selected requirements. The margin of safety used for the buckling analysis is an important consideration and should depend largely on the amount of geometric imperfection that exists in the finished housing components. The increased uncertainty in the buckling calculations brought about by greater geometric imperfection may require more design margin to ensure the performance on the hull design.

Preliminary predictions of critical buckling pressures for cylindrical pressure housings can be performed using equations derived for closed-ended vessels under uniform external pressure. The following equation assumes that the ends of the cylinder are simply supported, i.e., the ends are rigidly supported in the radial direction, but meridional rotations are allowed.

This equation (equation 1),

$$P_c = \left\{ \frac{1}{3}\left[n^2 - 1 - \left(\frac{\pi D}{2L}\right)^2 \right]^2 \frac{2E}{1-\nu^2}\left(\frac{t}{D}\right)^3 - \frac{2E\frac{t}{D}}{\left[n^2\left(\frac{2L}{\pi D}\right)^2 + 1 \right]^2} \right\} \frac{1}{n^2 + \frac{1}{2}\left(\frac{\pi D}{2L}\right)^2}$$

(reference 1)

where n=# of lobes formed, t=cylinder wall thickness, D=outer diameter of cylinder, L=simply supported length of cylinder, E=elastic modulus of cylinder material, and v=Poisson's ratio of cylinder material, can be used for initial predictions of collapse pressure for housings such as those indicated in cases 1 and 2. Derivation of equation 1 is based on linear differential equations where deflections of the shell structure are assumed to be small. Consequently, applications of this formula to housings that exhibit nonlinearities due to large deformations and/or material nonlinearities would result in less accurate predictions of failure by buckling.

A solid flat-end plate with a short lap interface with the cylinder, such as used in case 2, is reasonably approximated to be a simply supported boundary condition. In cases where the cylinder is capped at both ends by hemispheres, equation 1 can still be employed using an effective length (L) equal to the simply supported length of the cylinder, plus one third the depth of each hemisphere. The logic for using an effective length follows since a hemisphere represents a more compliant end constraint than a flat plate and, thus, would be expected to decrease the collapse pressure for a cylindrical housing in the same way that lengthening the cylindrical portion of a housing would also decrease the collapse pressure. Further, it has been shown (reference 8) that varying the wall thickness of the hemisphere or using a different modulus material for the hemisphere does relatively little to change the collapse pressure of the housing assembly. Thus, increasing the effective length (L) of the housing by one third the depth of each hemisphere regardless of hemisphere design details is a reasonable first approach.

Since the hemispheres in case 1 are integral end closures to the cylinders, the use of equation 1 which assumes simply supported boundary conditions at cylinder ends would be expected to give conservative results. Yet, the presence of additional boundary conditions at the cylinder ends has relatively little influence on collapse pressures due to general instability failure modes for the entire cylindrical housing assembly unless the length of the cylindrical section is relatively short.

Equation 1 also can be used when separate cylindrical sections are joined with coupling rings such as in cases 1 and 2 by assuming that the cylindrical portion of the housing behaves as a monocoque cylinder with length (L) equal to sum of the length of the two cylinders and the web thickness of the coupling ring. For the coupling rings used in cases 1 and 2, this has been shown to be a conservative means of calculating the collapse pressure since the increased inertia associated with the

flanges of the coupling ring actually help to increase buckling resistance of the housing. While equation 1 may be used to help predict the general instability of housings joined by coupling rings, other techniques need to be used to ensure that the flanges of the coupling ring are substantial enough to resist local crippling under external pressure.

The increase in buckling resistance afforded by adding more material to the flanges of the coupling ring motivates the design of the joint rings used in cases 3 and 4. If the stiffness of the joint ring was substantial enough to approximate its support of the cylinder as being simply supported, then equation 1 could be used to predict innerbay buckling for each of the cylinders. For the stiffened central joint rings used in cases 3 and 4, the critical collapse mode is by general instability for the entire cylindrical assembly (two cylinders joined by a stiffened central joint ring). Hand calculation techniques for predicting failure for this type of assembly are limited such that stability analysis requires the use of more comprehensive tools such as the BOSOR4 computer program.

BOSOR4 is a structural analysis program for computing stress, buckling, and vibration of complex shells of revolution that was developed by David Bushnell at Lockheed Missiles and Space Co., Inc. BOSOR4 is written using FORTRAN IV, and predictions are based on finite difference energy minimization with constraint conditions for the structure under study. The meridian of the shell of revolution is modeled by using a number of segments with material, geometric, and boundary condition properties representative of the real structure.

BOSOR4 predictions of collapse pressure for the four test cases presented here were based on elastic bifurcation analysis. All housing materials were modeled as linear elastic, but nonlinear effects due to large deflections were considered. Bifurcation analysis searches for the external pressure load at which the axisymmetric deformation of the housing structure ceases to be stable. For externally pressurized cylindrical housings like the four test-case assemblies presented here, the post buckling behavior is unstable such that once the bifurcation pressure is reached, the housing cannot continue to carry additional external pressure which results in catastrophic collapse of the hull.

For real housing structures, there is no such thing as true bifurcation buckling. All real housings have imperfections which lead to discrepencies between predicted failure by bifurcation theory and the actual tested failure. The amount of discrepency is dependent on the amount of initial imperfection in the housing components. Cylindrical housings subjected to external pressure are imperfection sensitive, meaning the presence of initial imperfections act to reduce the pressure capacity of the housing as predicted by bifurcation theory. Cylindrical housings subjected to hydrostatic external pressure typically have general instability failure modes characterized by long axial wavelengths and relatively few circumferential wavelengths (N=2 or N=3 for test cases discussed in this report). Consequently, global imperfections such as uniform out-of-roundness would be expected to have more deleterious effects than any localized imperfections.

A linear elastic bifurcation analysis of externally pressurized housings is appropriate when there is relatively little bending energy stored in the housing up until the bifurcation point is reached. This is the case in housings where there is a good radial deflection match between adjacent housing components implying the axisymmetrically deformed housing has the same approximate shape as the undeformed housing prior to loading. Conversely, if substantial bending energy exists in the cylindrical housing subjected to external pressure due to relatively rigid boundary conditions such as occurs at the interface with flat bulkhead end closures or at stiff joint rings, then a nonlinear analysis may be required. The power of programs like BOSOR4 is that they allow the designer of underwater pressure housings to perform buckling analysis based on different modeling assumptions (i.e., linear or nonlinear geometric or material effects) as appropriate for each particular housing design case.

RESULTS OF JOINT RING STRUCTURAL STABILITY CALCULATIONS

The buckling capacity of the four test-case housing assemblies were predicted using BOSOR4 and hand calculation techniques where applicable. The results of these calculations are shown in table 1. The material properties for the ceramic cylinders used for each housing assembly are listed in the table along with the housing dimensions used for calculating collapse pressure for cases 1 and 2 using equation 1 shown above. All titanium joint rings were modeled using material property values of 16.4 million for the compressive elastic modulus and .31 for the Poisson's ratio. Equation 1 was programmed in FORTRAN to calculate collapse pressure of the first two test cases for values of N=2, 3, and 4. The results of pressure tests performed with each of the housings are listed for comparison at the bottom of table 1.

The BOSOR4 models were constructed to allow for meridional rotations at the joints between cylinders and end closures under external pressure as occurs in cases 2 through 4. The central coupling rings and central stiffened joint ring were modeled with their own discrete branched-shell segments. Detailed modeling of these central joint rings allows for prediction of any local instabilities in the ring as well as more accurate predictions of general instability modes for the entire housing.

Results of hand calculations show prediction of the collapse pressure based on equation 1 to be 11,582 psi, which is off by more than 20 percent from the actual tested value of 9,200 psi for case 1. The simply supported length (L) used in equation 1 for the case 1 housing was 16.16 inches (7.00 inches for each ceramic cylinder section, plus 1.02 inches for each ceramic hemisphere section equal to one third the depth of hemisphere, and .12 of an inch for coupling ring web). The BOSOR4 model for the case 1 housing consisted of seven segments. Two segments were used to model each ceramic hull component, and a total of three segments were used to model the web and two flanges of the central coupling ring. BOSOR4 calculations for the case 1 housing predicted a collapse pressure of 10,512 psi, which also was higher than the actual tested value. Some of this difference could be attributed to the deleterious effect of geometric imperfections that existed in the ceramic hull components that were used.

The ceramic components used in the test case 1 housing had maximum deviations from true circular shape equal to about 10 percent of the nominal shell wall thickness. BOSOR4 models for all four test cases were run using nominal housing component dimensions and the assumption that no geometric imperfections were present. Additionally, the use of equation 1 assumes meridional rotations can occur between the end closure and the cylindrical hull which does not hold for case 1 since the hemispheres are integral to the cylinder sections of the housing.

Both hand calculations and the BOSOR4 model predict that the case 1 housing would fail with two circumferential lobes forming as the housing buckled. Figure 23 shows BOSOR4 graphical output for the predicted failure mode for case 1. This figure shows the meridian of the shell before pressure loading (dashed lines) and its buckled configuration as it fails (solid lines). Obviously, the formation of lobes is not an axisymmetric deformation such that the buckled configuration shown in figure 23 represents a sectioned view through the major axis of a single circumferential wave. As a comparison, a BOSOR4 model was constructed that contained a single monocoque cylinder with an equivalent length to the two-cylinder/coupling-ring configuration of case 1 (outer diameter and wall thickness of the ceramic monocoque cylinder was kept constant). Collapse by buckling was predicted to occur at 10.201 psi for this single-cylinder replacement which indicates the presence of this particular coupling ring slightly increases the external pressure capacity of the case 1 assembly (10,201 psi to 10,512 psi). This indicates that a cylindrical hull could be built up using a number of cylinders joined by coupling rings without necessarily degrading the structural performance of the cylindrical hull assembly.

Calculations based on equation 1 and a BOSOR4 model both under-predict the buckling capacity for the case 2 housing, although both values are still

within a reasonable margin of the tested value. Use of equation 1 predicts a collapse pressure of 8,413 psi, and a BOSOR4 model predicts a collapse pressure of 9,558 psi as compared to the tested result of a critical pressure of 10,250 psi. The simply supported length (L) used in equation 1 for the case 2 housing was 29.03 inches (15.00 inches for each cylinder, plus .25 of an inch for coupling ring web, and minus .61 of an inch for supported length at each flat-steel end plate). The model used for the case 2 housing consisted of seven segments. One segment was used to model each end plate, and one segment was used to model each ceramic cylinder. Three segments were used to model the web and two flanges of the central coupling ring. Initially, additional segments were used to model both end-cap joint rings, but they were eliminated in the final model since their presence had virtually no effect on the general instability modes for the entire assembly. The BOSOR4 model for the case 2 housing accounts for the increased support associated with the stiffness supplied by the flanges of the coupling ring and gives a more accurate prediction than obtained with equation 1 where the coupling ring flanges are unaccounted for.

Both techniques predict that failure should occur for the case 2 assembly with three circumferential waves occurring at collapse. Figure 24 shows the BOSOR4 graphical output for the predicted failure mode for the case 2 assembly. Figure 25 shows the case 2 coupling ring after the test housing was pressurized to failure. Visual inspection of the deformed coupling ring indicated that it was slightly triangular in shape as would be expected for an N=3 failure. The eventual formation of circumferential lobes results in bending the housing shell wall to the point that rupture occurs. In figure 25, the external flange of the coupling ring can be seen to have blown outward at an assumed location of one of the three circumferential lobes that formed as the housing failed. Figure 26 shows the end-cap joint rings from the failed case 2 test housing. These joint rings showed substantially less permanent deformation than occurred with the central coupling ring as would be expected since the predicted maximum deflections for the case 2 assembly should occur at the mid-bay location of the central coupling ring prior to failure.

Buckling predictions were not made with equation 1 for cases 3 and 4 because of the complicating presence of the central stiffened joint rings utilized in both these assemblies. However, predictions were made based on BOSOR4 models for these case 3 and case 4 housings which gave excellent results. The case 3 housing was predicted to fail with two lobes forming (N=2) at an external pressure of 9,603 psi compared with the tested failure pressure of 9,550 psi. The BOSOR4 model for this test case used a total of nine segments. One segment was used to model each titanium hemisphere, and one segment was used to model each ceramic cylinder. A total of five segments was used to model the three flanges and two webs that make up the central stiffened joint ring.

Figure 27 shows BOSOR4 graphical output for the predicted mode of failure for case 3. Figure 28 shows the hardware that was retrieved after pressure testing the housing to failure. The remains of a wood plug used to mitigate the effects of the implosion on the titanium hemispheres can be seen. Figure 29 shows the remnants of the central stiffened coupling ring which clearly validates the prediction that failure occurred with two circumferential lobes forming due to an N=2 general instability. It is apparent from this picture that the wooden implosion mitigation plug did relatively little to resist snap-through of the stiffened central joint ring as the housing assembly buckled.

Detailed BOSOR4 modeling of the geometry of the central stiffened joint ring also allows the designer to predict any buckling failures that may occur due to local instabilities such as crippling of joint ring flanges or webs. BOSOR4 calculations predicted that local buckling of the central stiffened joint ring for case 3 would occur at external pressures substantially greater than that required to initiate failure by general instability. Ideally, the design of the central stiffened joint ring would be optimized such that local crippling would occur at the same external pressure that causes a general instability failure. But as mentioned earlier, packaging constraints limited the geometry of the central

stiffened joint ring and, thus, prevented an optimized design.

Prior to pressurizing the case 3 housing to failure, the housing assembly was equipped with strain gages on the interior and exterior surfaces at mid-bay of each ceramic cylinder as well as on various locations of the central stiffened joint ring as indicated in figure 30. Varying numbers of gages were located around the circumference of the housing for each axial location shown. Eleven pressure cycles to 9,000 psi were completed, and strains were recorded for each gage at 1,000 psi intervals until an external pressure of 8,500 psi was reached whereby the recording interval was reduced to 100 psi increments. Table 2, Sheets 1 through 6 show strain gage measurements recorded during testing in units of micro inches/inch. Plots of this data are presented in figures 31 through 34. These plots reveal that the measured strains increase as a linear function of pressure until an external pressure of 8,500 psi is reached. At external pressures greater than 8,500 psi, the strains recorded for the various circumferential gages at each axial location begin to diverge.

The initiation of this nonlinear behavior indicates that circumferential waves are forming. It is of value to note that the onset of lobes occurs well before the housing assembly finally collapses. Specifically for the case 3 housing, lobes have begun to form at an external pressure equal to 1,000 psi less than the collapse pressure. As expected, the formation of circumferential waves is most accentuated in the data for the inner flange of the central stiffened joint ring shown in figure 33. The additional bending of the shell associated with the formation of lobes either acts to increase or reduce the measured strains depending upon the location of the gage with respect to the waves that form. It is this bending which accounts for the nonlinearities that appear in the data near the collapse pressure for this particular housing assembly.

The BOSOR4 prediction of a critical buckling pressure of 12,208 psi for the case 4 housing assembly compared very well with the tested collapse pressure of 11,930 psi. The BOSOR4 model for the case 4 housing utilized a total of 15 segments to define the complete assembly. Three segments were used to model each hemisphere to account for the spherical, conical, and cylindrical portions of the hemisphere design. One segment was used to model each ceramic cylinder, and seven segments were used to model the central stiffened joint ring. Again, additional segments were used to model the cylinder and hemisphere end-cap joint rings to check for local instabilities, but were removed for the final model because of their negligible impact on the general instability failure modes for the whole assembly. Appendix B contains the BOSOR4 input file for the case 4 housing for reference of the modeling techniques used for all four test cases presented in this report.

Figure 35 shows the BOSOR4 graphical output for the N=2 predicted failure for this particular housing. Figure 36 shows the case 4 housing as it is being loaded into the vessel for pressurization to failure. Figure 37 shows the central stiffened joint ring after collapse. The case 4 housing was partially filled with water prior to pressurizing to failure to mitigate the effects of the implosion. This resulted in substantially less deformation in the central stiffened joint ring than in the case 3 housing. Subsequent measurements determined that the joint ring was oval in shape, corresponding to the formation of two lobes (N=2 failure).

The N=3 failure mode for the case 3 and 4 housings occur at external pressures substantially higher than the pressure required for the housings to fail in an N=2 mode. None the less, it is interesting to note the differences in the way the housings fail for these two modes. The N=3 failure mode occurs with antisymmetric inner-bay lobes forming where the three lobes formed in one cylinder are out of phase with the three lobes formed in the adjacent cylinder as shown in figure 38. For this N=3 mode, the stiff central coupling ring merely twists and has little impact on the collapse pressure, and the shell wall thickness of the cylinders controls the buckling capacity. This type of failure mode is referred to as "rolling" and is caused by compression of the web of the internally central stiffened joint ring. This implies that an optimal housing consisting of two cylinders and a stiff central coupling ring can be designed such that failure pressure would be equal for both the N=2 and N=3 mode shapes. The central coupling ring would be

sized to provide adequate bending resistance against N=2 failure, and the cylinder wall thickness would be sized to be adequate for N=3 failure. Of course, the final design of the coupling ring and cylinders also must be satisfactory from a stress analysis point of view and checked for any local instabilities.

As an interesting comparison, a BOSOR4 model was constructed where the case 4 cylindrical hull consisting of two ceramic cylinders with stiffened central joint rings was replaced by a single monocoque cylinder of equivalent length (cylinder wall thickness and outer diameter were held constant). This new cylindrical hull with case 4 end closures was predicted to buckle at 8,234 psi. Thus, the integration of the case 4 central stiffened joint ring into the cylindrical hull assembly increases the buckling capacity by approximately 48 percent (8,234 psi to 12,208 psi).

CONCLUSION

The use of epoxy-bonded metallic joint rings to assemble ceramic hull sections has proven to be an economically viable as well as structurally reliable means of constructing ceramic underwater pressure housings without size limitations. Accurate predictions of the structural performance of composite housings consisting of ceramic shells joined by metallic joint rings can be made using both commercially available structural analysis software as well as hand calculation techniques. Metallic joint rings also provide engineers with a way to integrate design features such as local attachment points, additional buckling resistance, and a means of sealing and maintaining closure between adjacent housing sections. The continued development of simple joining techniques like epoxy-bonded metallic joint rings is essential to the continued success and acceptance of ceramic underwater pressure housings.

GLOSSARY

AUTB	Advanced Ultrasonic Test Bed
FEA	finite element analysis
FEM	finite element model
GFR	graphite-fiber-reinforced
GFRP	graphite-fiber-reinforced plastic
ID	inner diameter
IED	independent exploratory development
Kpsi	one thousand psi
L	length
L/D	length/diameter
MEK	methyl ethyl ketone
MOR	Modulus of rupture
ND	nondestructive
NDE	nondestructive evaluation
NDT	nondestructive test
NOSC	Naval Ocean Systems Center
OD	outside diameter
PEEK	poly-ether-ether-ketone
rms	root mean square
SAM	Scanning Acoustic Microscopy
S.F.	safety factor
t	ceramic shell thickness
TA	axial clearance
t/D	thickness/diameter
TF	flange thickness
TR	radial clearance
t/Ro	thickness/external radius
W	width
W/D	weight-to-displacement

REFERENCES

1. Bickell, M. B. and Dr. M. Ruiz. "Pressure Vessel Design and Analysis," St. Martin's Press.
2. Brush, Don O. and Bo O. Almroth. 1975. "Buckling of Bars, Plates, and Shells," McGraw-Hill Company.
3. Bushnell, David. "BOSOR4 User's Manual," Lockheed Missiles & Space Co., Inc.
4. Bushnell, David. 1981. "Buckling of Shells-Pitfall for Designers," AIAA Journal, Vol. 19 (Sep), pg. 1183.
5. Bushnell, David. 1981. "Computerized Buckling Analysis of Shells," Applied Mechanics Laboratory, Lockheed Palo Alto Research Laboratory (Dec).
6. Johnson, R. P., R. R. Kurkchubasche, and J. D. Stachiw. 1993. "Design and Structural Analysis of Alumina Ceramic Housings for Deep Submergence Service Fifth Generation Housings," NRaD TR 1583 (Mar), NCCOSC *RDT&E Division, San Diego, CA.*
7. Johnson, R. P. "Stress Analysis Considerations for Deep Submergence Ceramic Pressure Housings," ROV 92.
8. Kurkchubasche, R. R. "Elastic Stability Consideratins for Deep Submergence Ceramic Pressure Housings," ROV 92.
9. Santella, M. L. 1992. "A Review of Techniques for Joint Advance Ceramics," American Ceramic Society Bulletin, Vol. 71, No. 6.
10. Stachiw, J. D. 1990. "Exploratory Evaluation of Alumina Ceramic Housings for Deep Submergence Service—Fourth Generation Housings," NOSC TR 1355 (Jun), Naval Ocean Systems Center, San Diego, CA.
11. Stachiw, J. D., and J. L. Held. 198[illegible] "Exploratory Evaluation of Alumina Veramic Cylindrical Housings for Deep Submergence Service—The Second Generation NOSC Ceramic Housings," NOSC TR 1176 (Sep), Naval Ocean Systems Center, San Diego, CA.
12. Stachiw, J. D., T. J. Henderson, and C. A. Andersson. 1991. "Novel Ceramic Matrix Composites for Deep Submergence Pressure Vessel Applications," NOSC TD 2222 (Oct), Naval Ocean Systems Center, San Diego, CA.
13. Stachiw, J. D., R. P. Johnson, and R. R. Kurkchubasche. 1993. "Evaluation of Scale Model Ceramic Pressure Housing for Deep Submergence Service," NRaD TR 1582 (Mar), NCCOSC RDT&E Division, San Diego, CA.
14. Young, Warren C. 1989. "Roark's Formulas for Stress and Strains, Sixth Edition," McGraw-Hill Company.

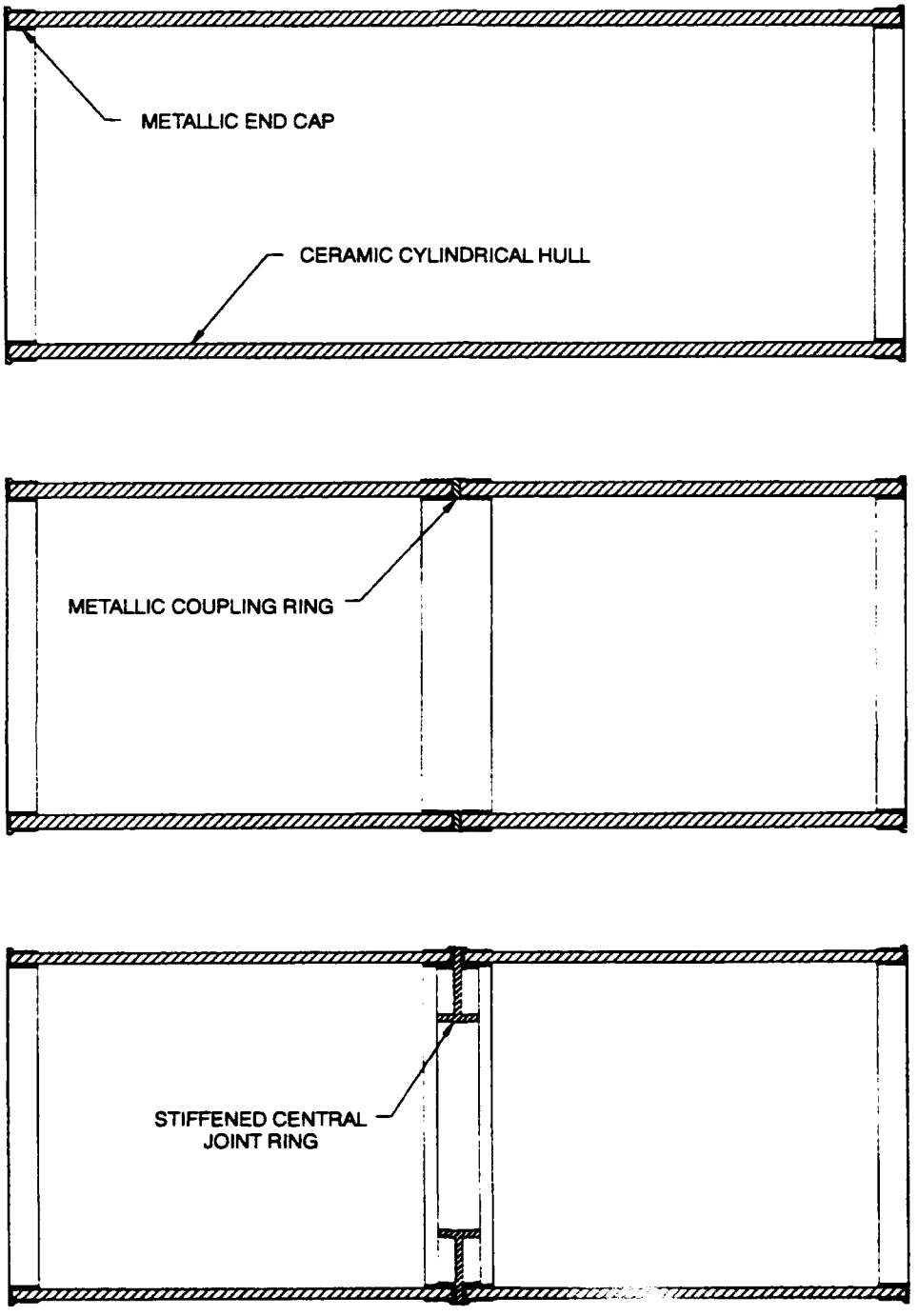

Figure 1. Three potential cylindrical hull assemblies for ceramic underwater pressure housings.

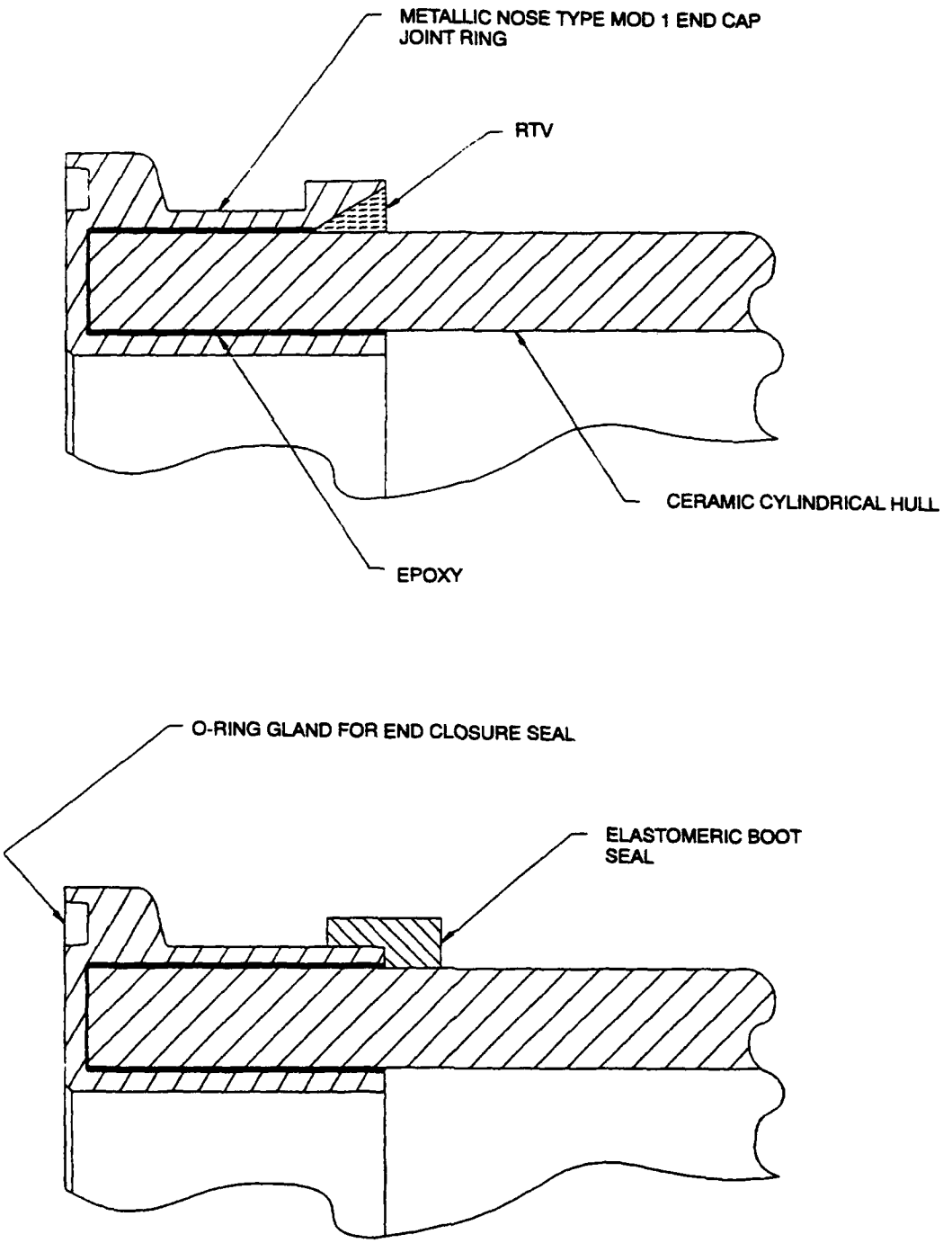

Figure 2. Epoxy bond between joint ring and ceramic hull.

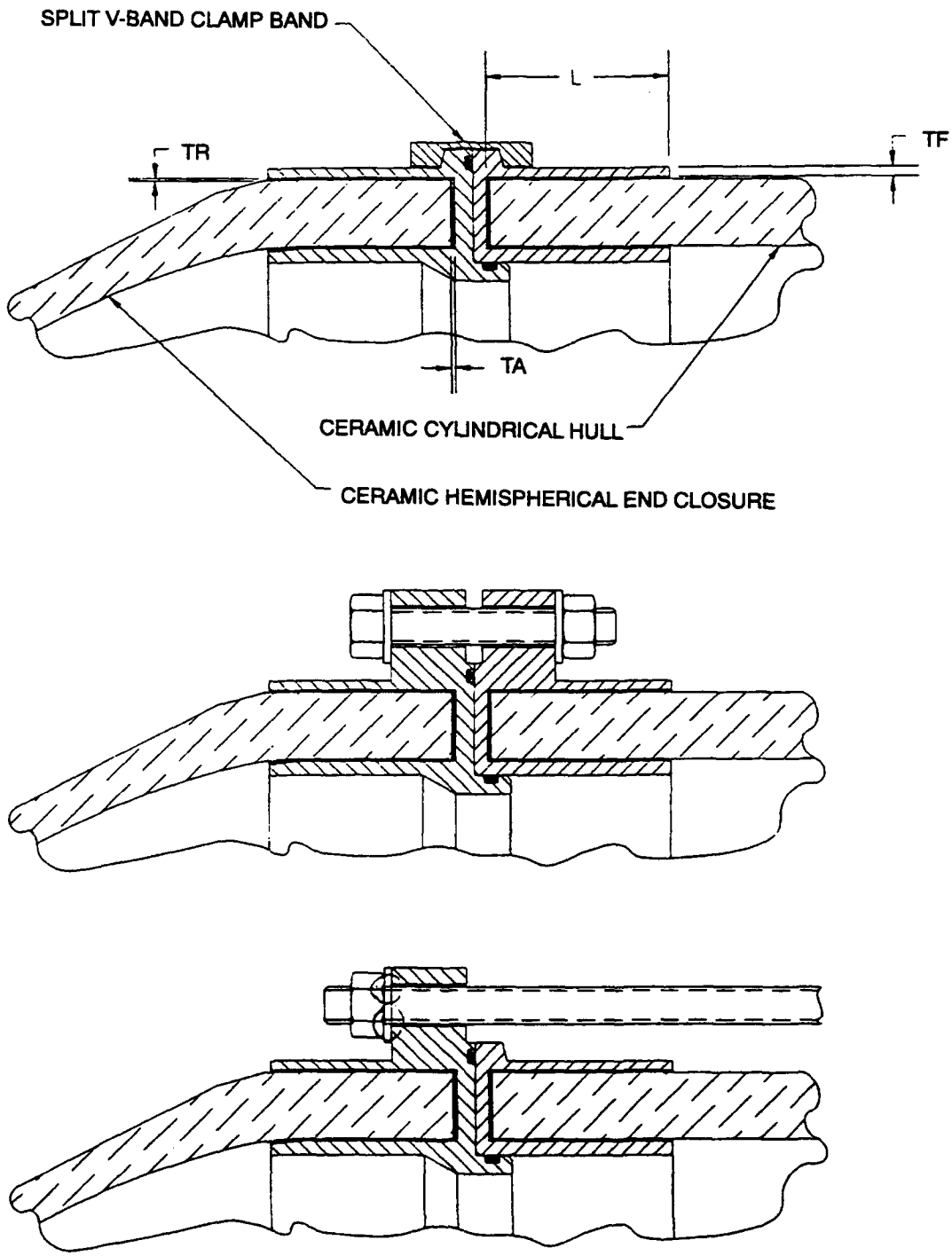

Figure 3. Service joints between ceramic cylinders and ceramic hemispheres.

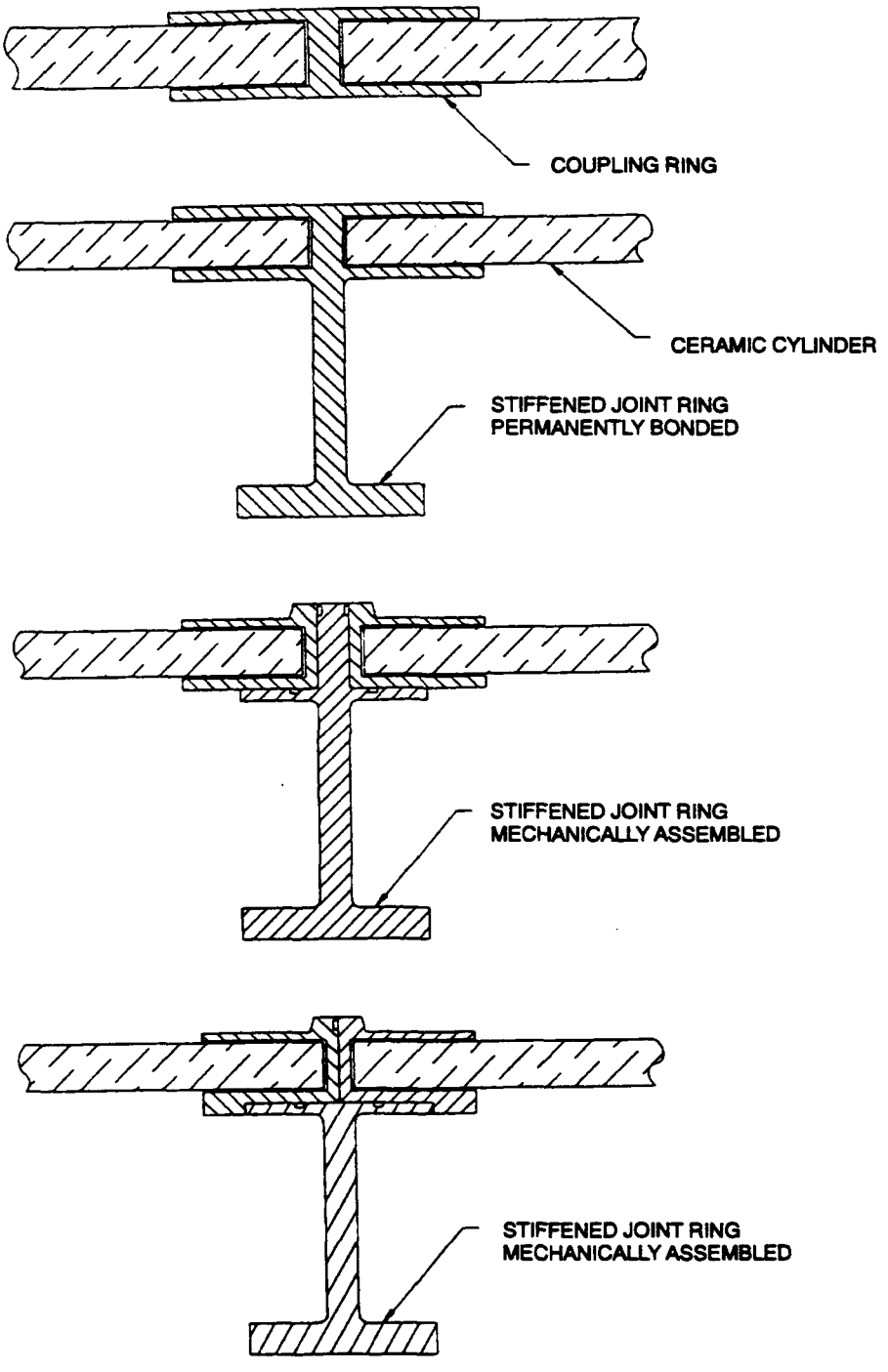

Figure 4. Stiffened joint ring designs.

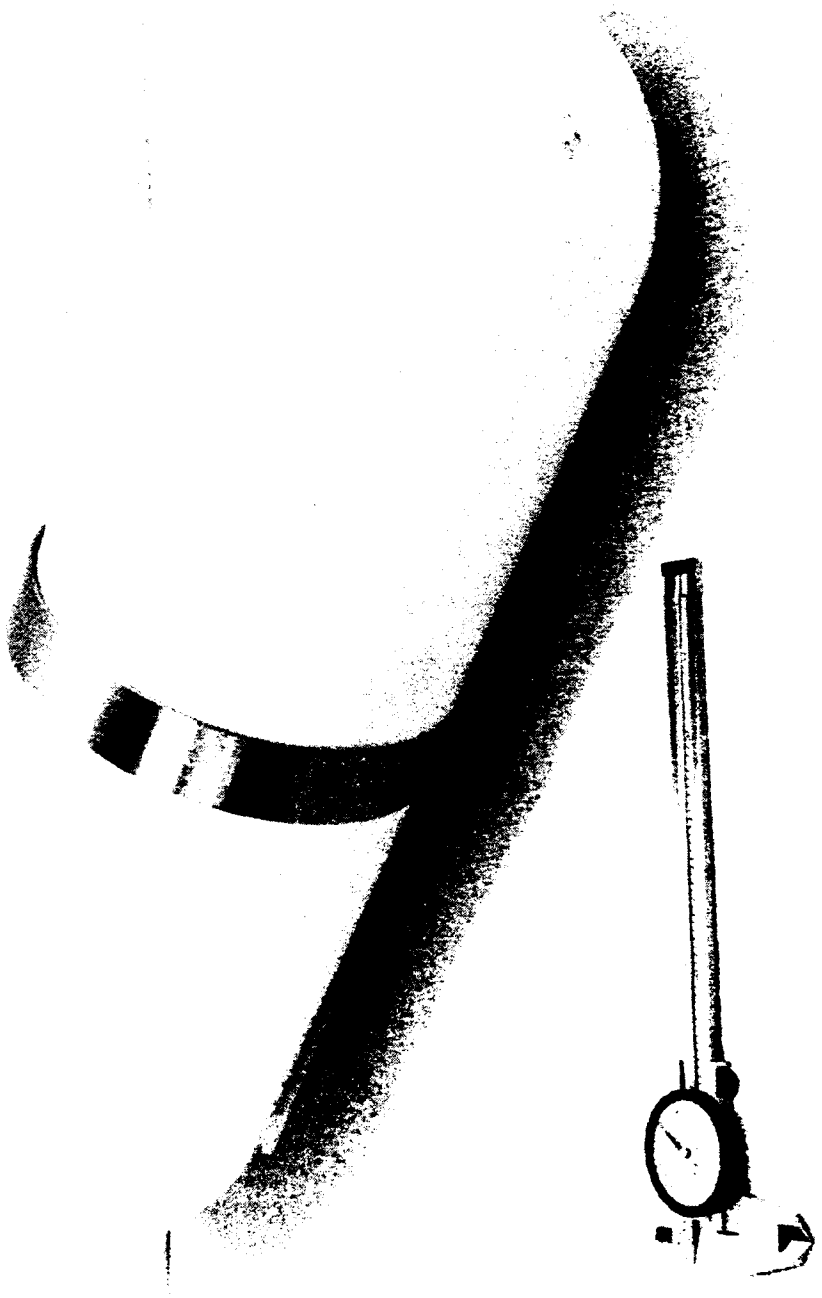

Figure 5. Case 1 test assembly for evaluation of coupling rings.

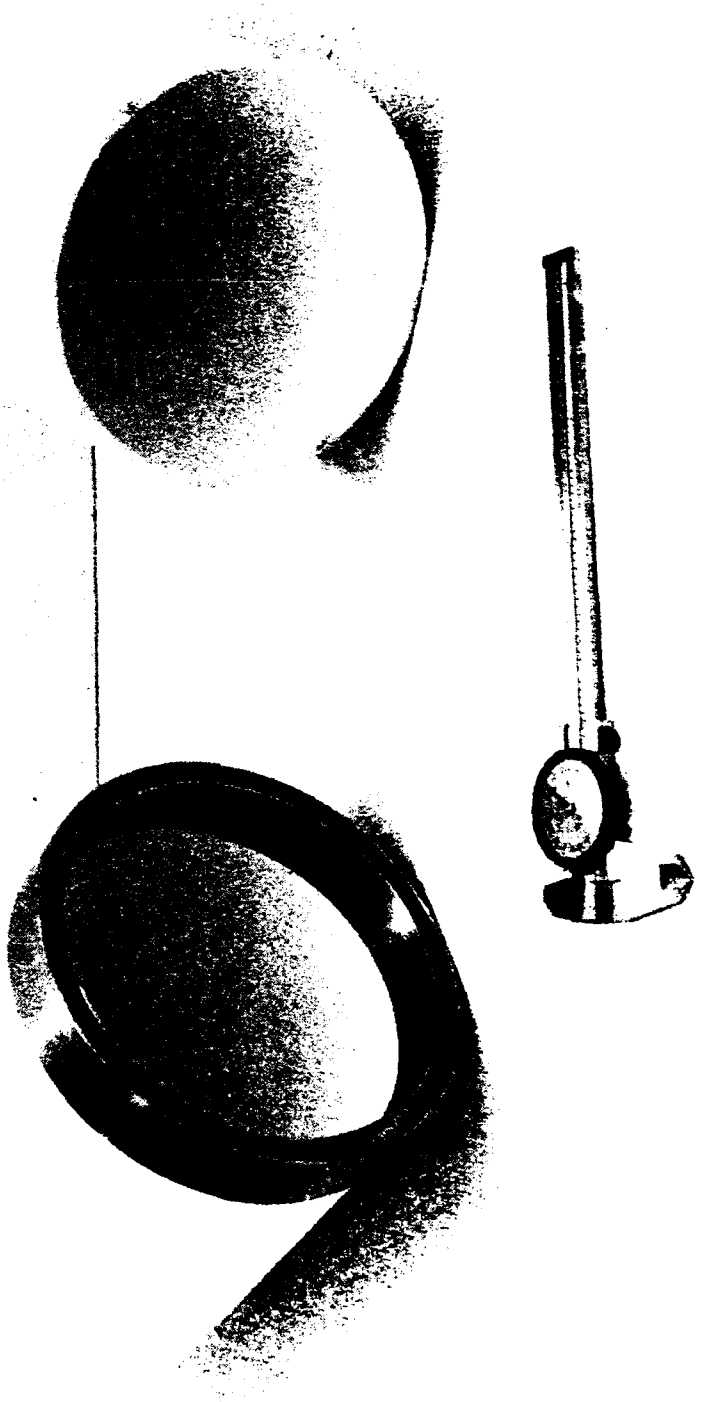

Figure 6. Case 1 test assembly ceramic hull components.

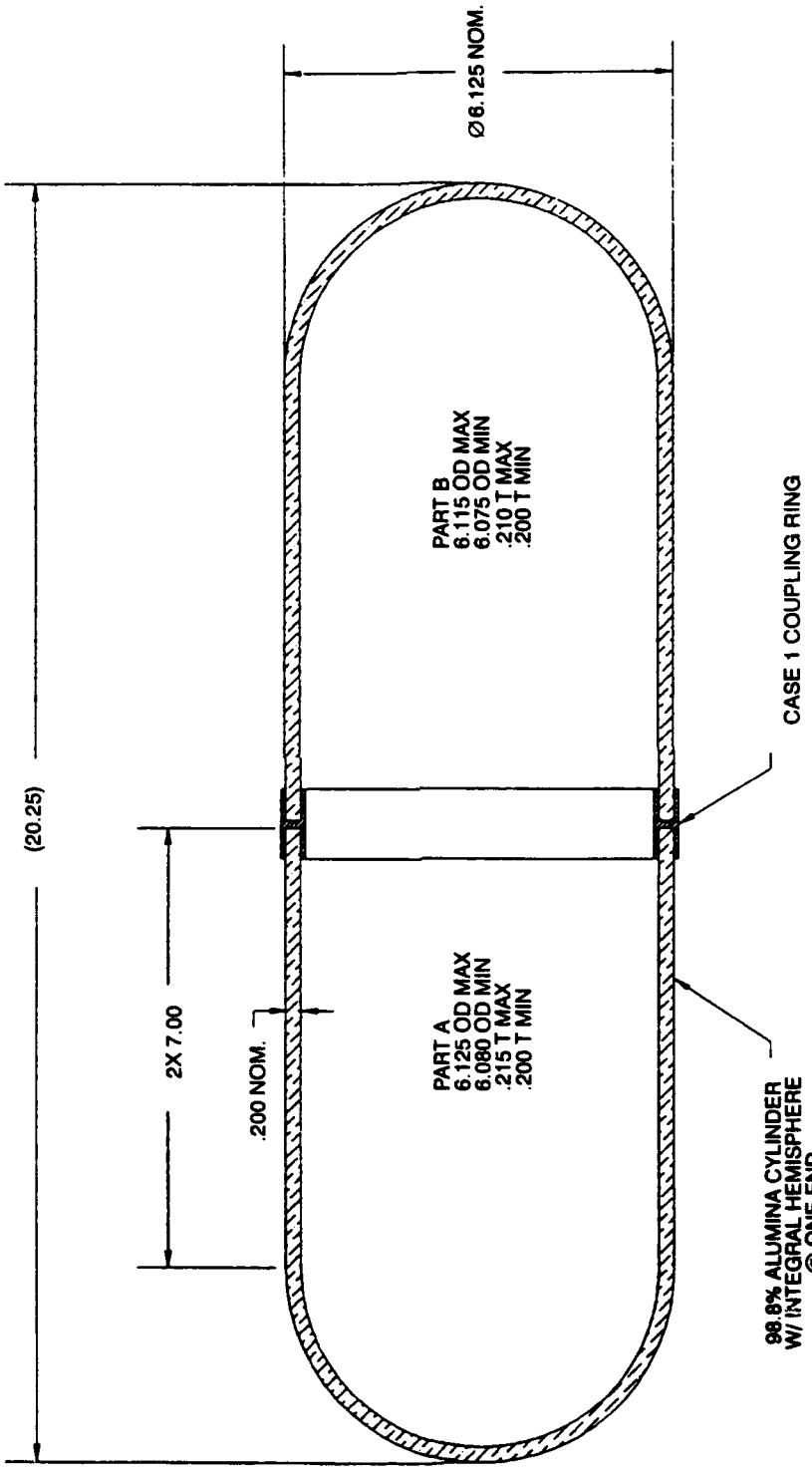

Figure 7. Case 1 ceramic hull component details.

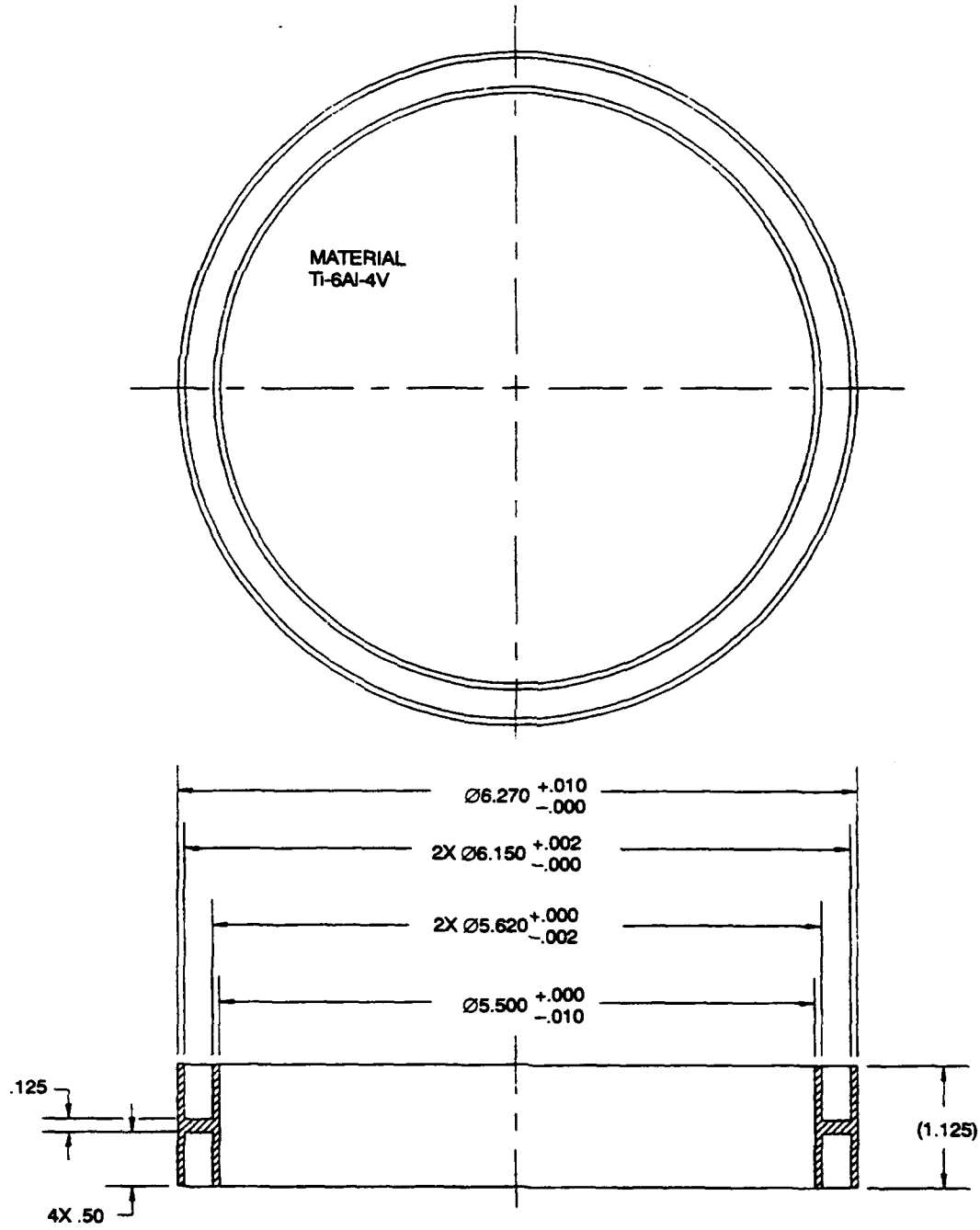

Figure 8. Case 1 coupling ring details.

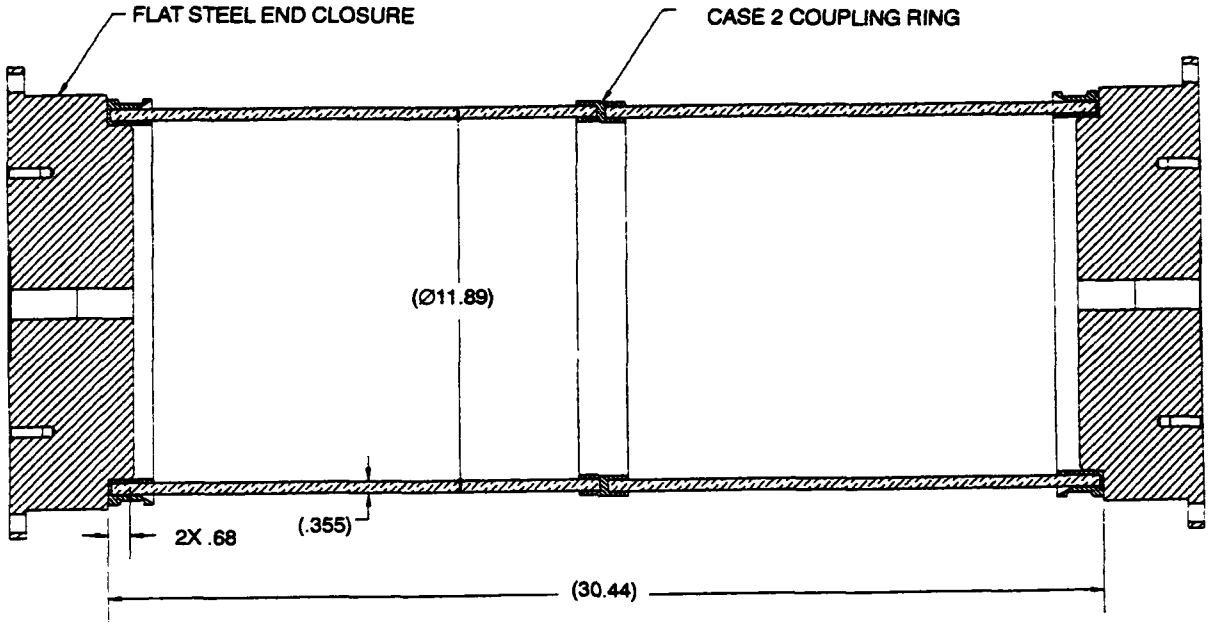

Figure 9. Case 2 test assembly for evaluation of coupling rings.

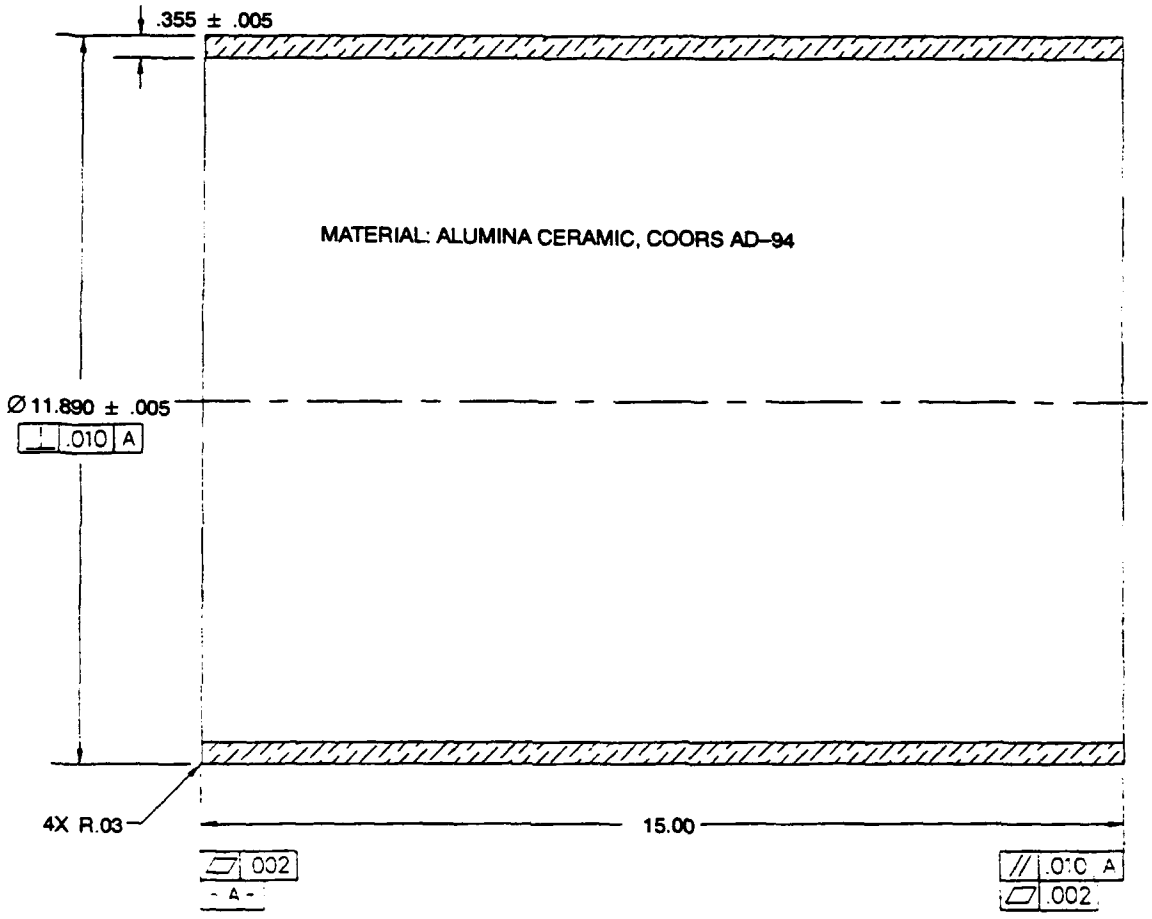

Figure 10. Case 2 and case 3 ceramic hull component details.

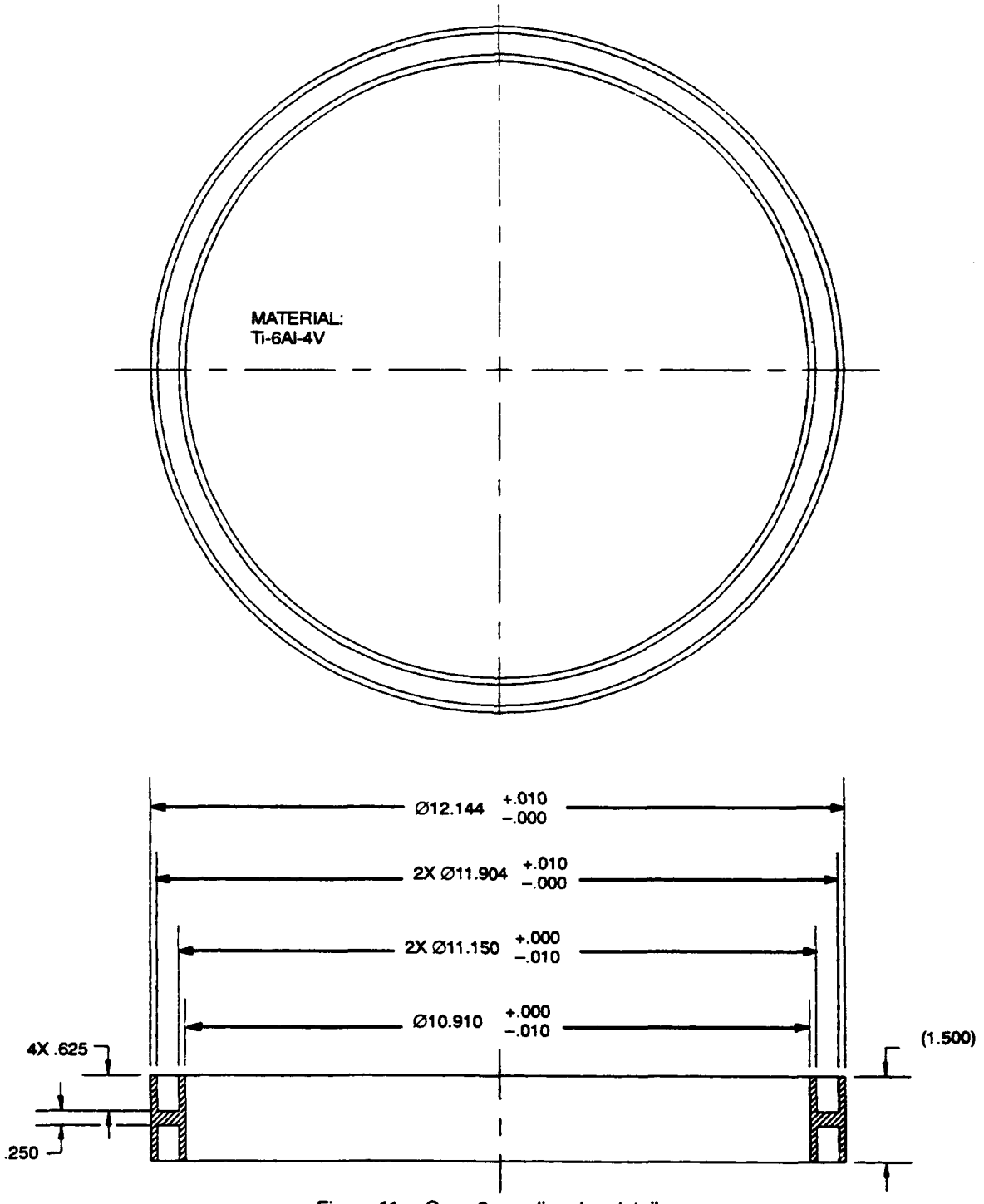

Figure 11. Case 2 coupling ring details.

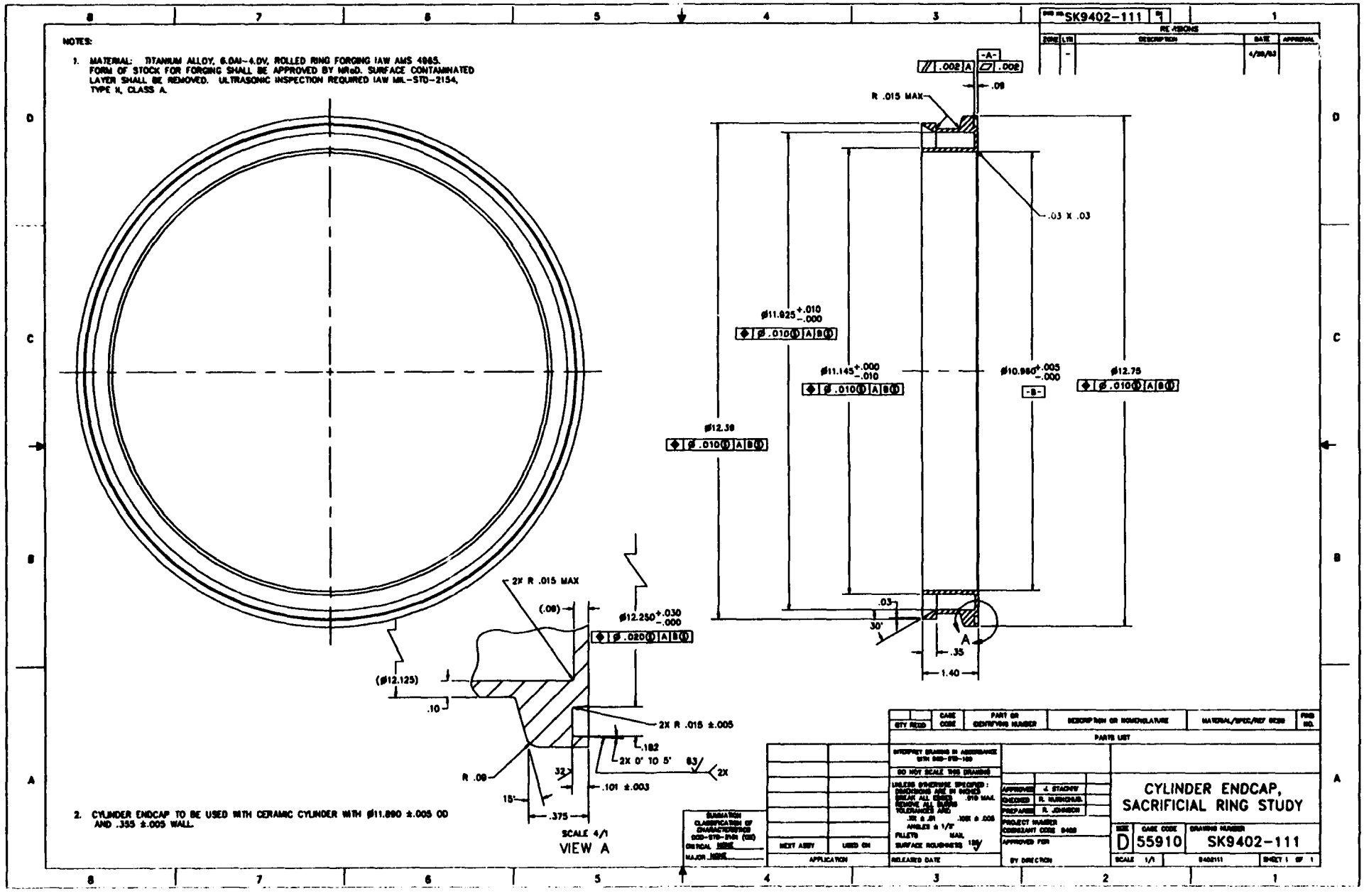

Figure 12. Case 2 and case 3 end cap joint ring details.

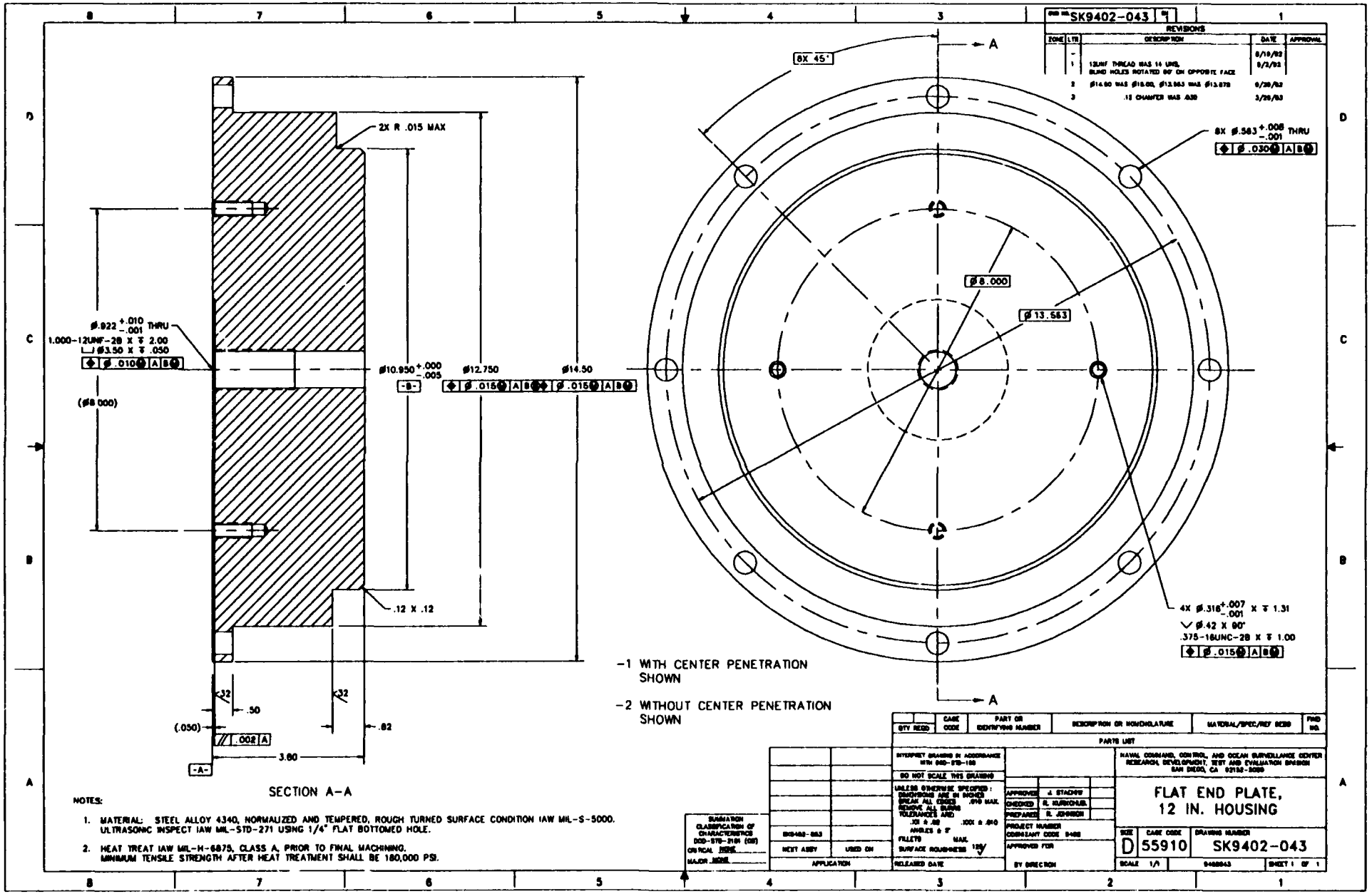

Figure 13. Case 2 flat steel end closure details.

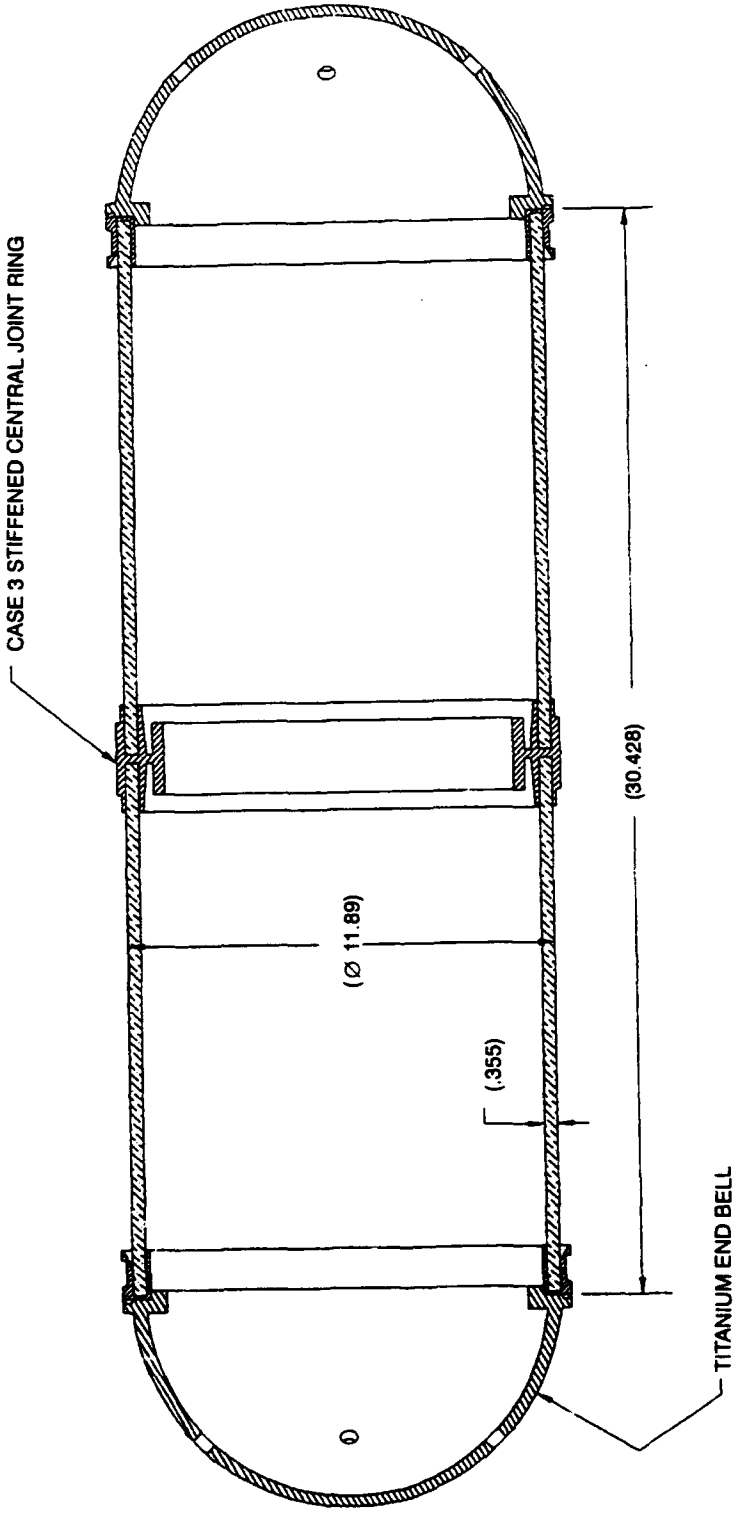

Figure 14. Case 3 test assembly for evaluation of central stiffened joint rings.

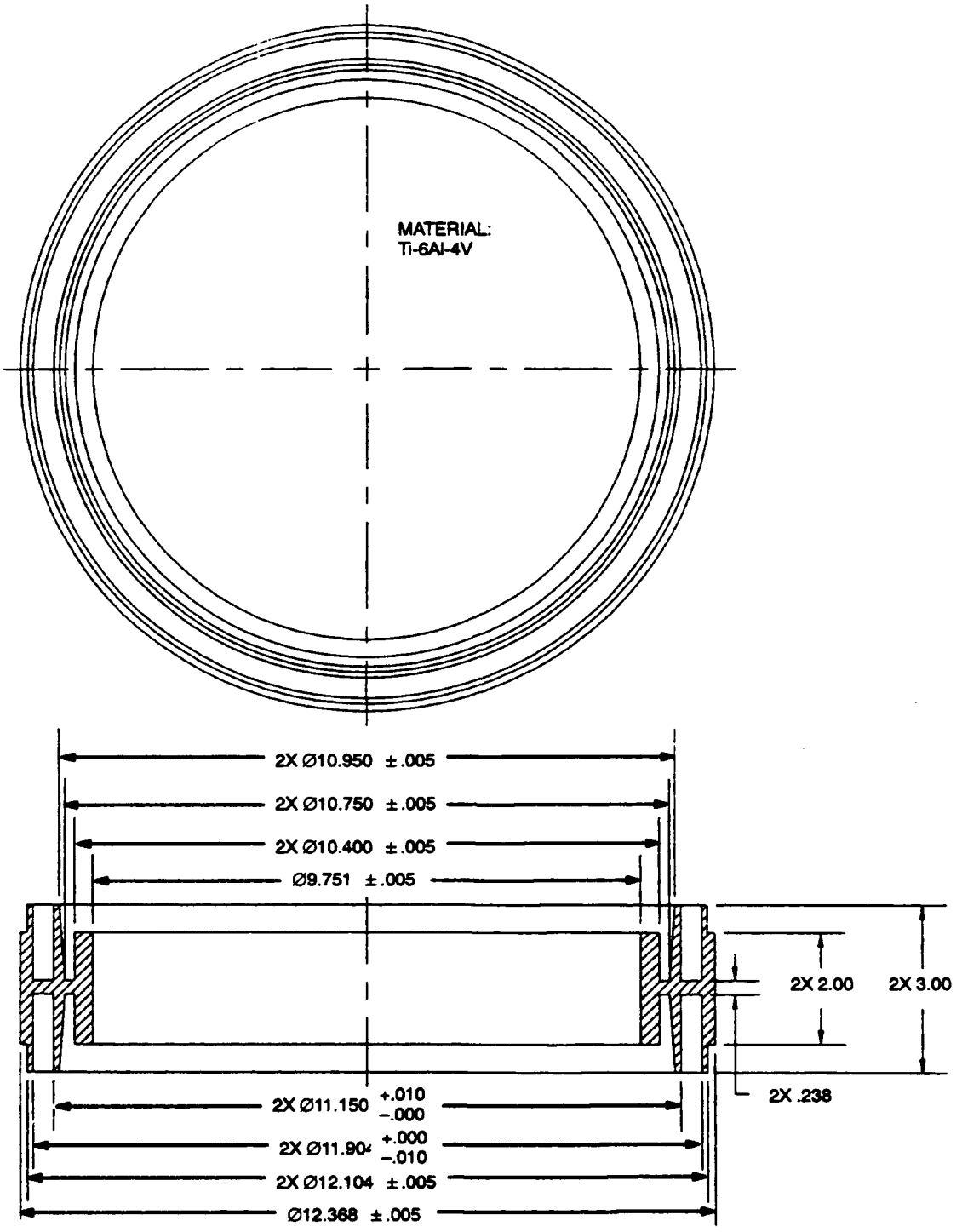

Figure 15. Case 3 central stiffened joint ring details.

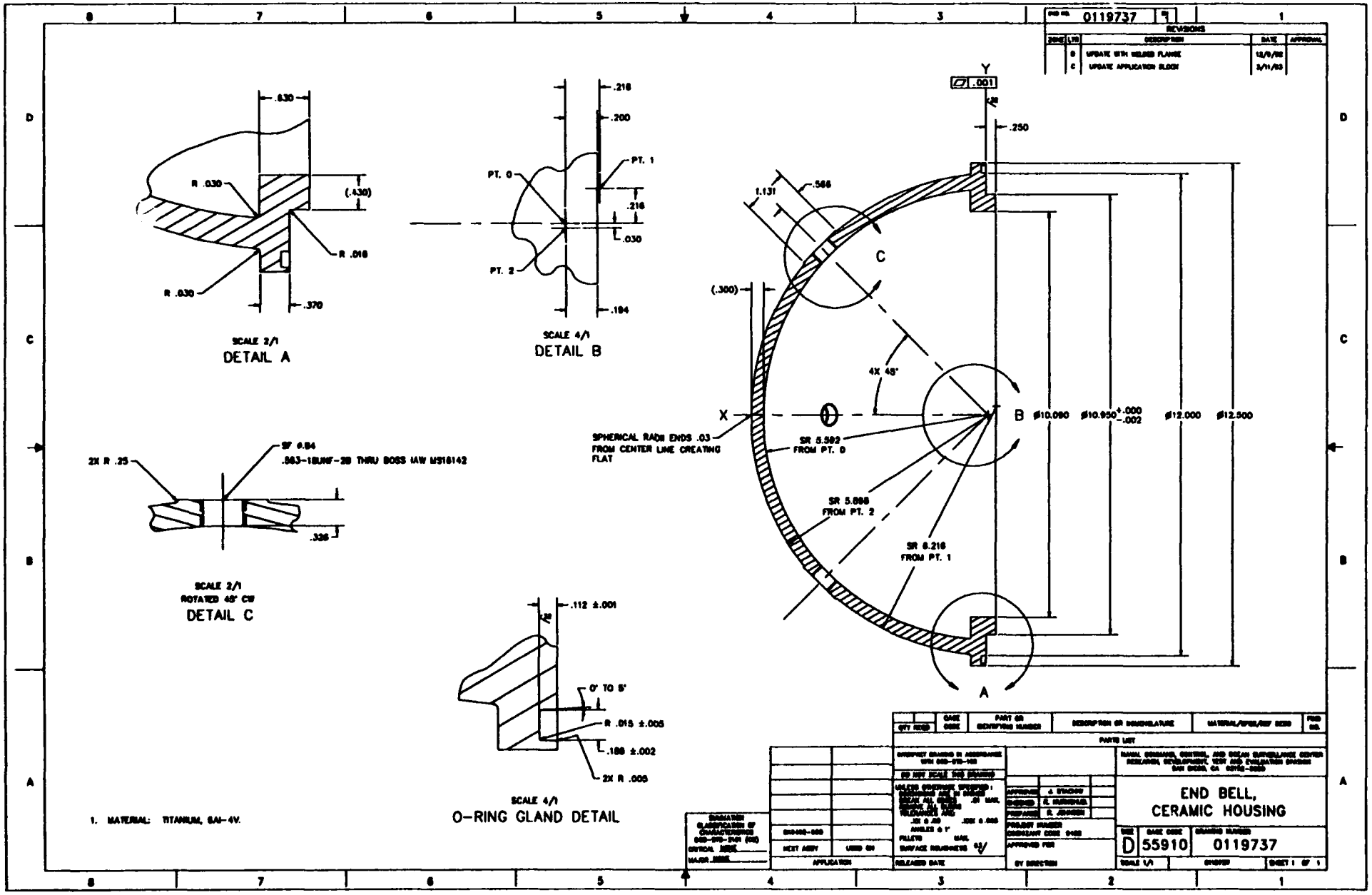

Figure 16. Case 3 hemispherical end closure details.

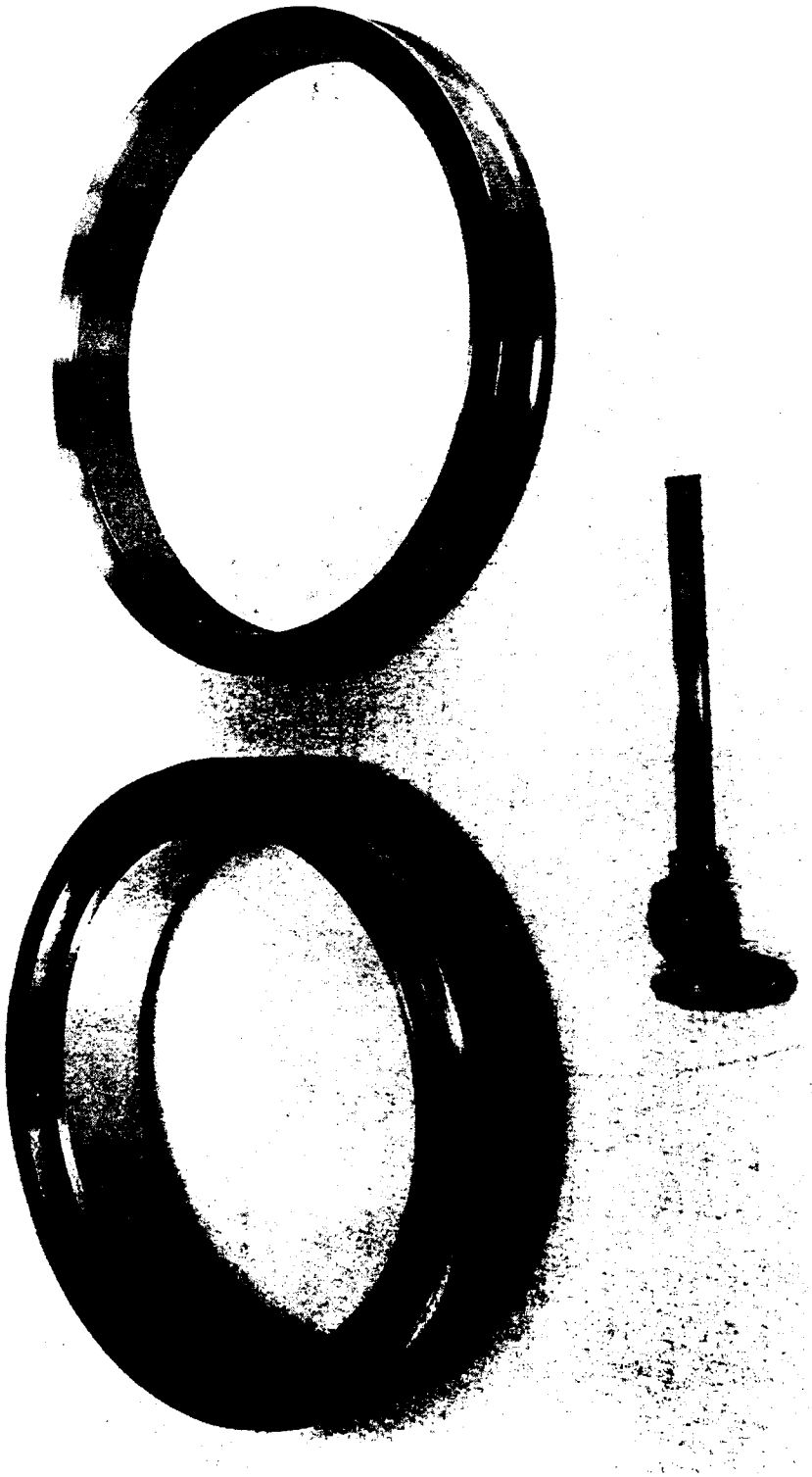

Figure 17. Case 3 joint ring components

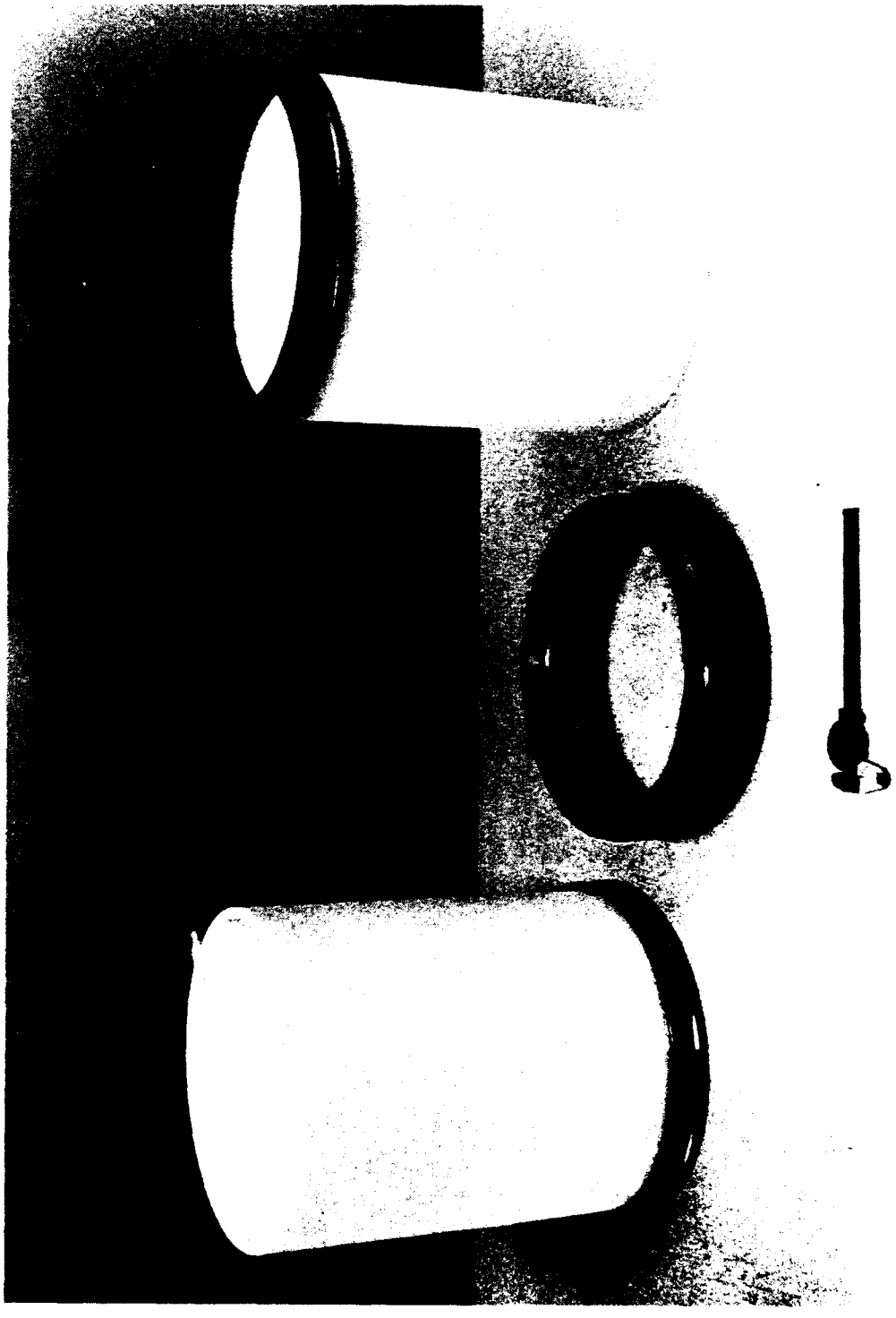

Figure 18. Case 3 ceramic hull components.

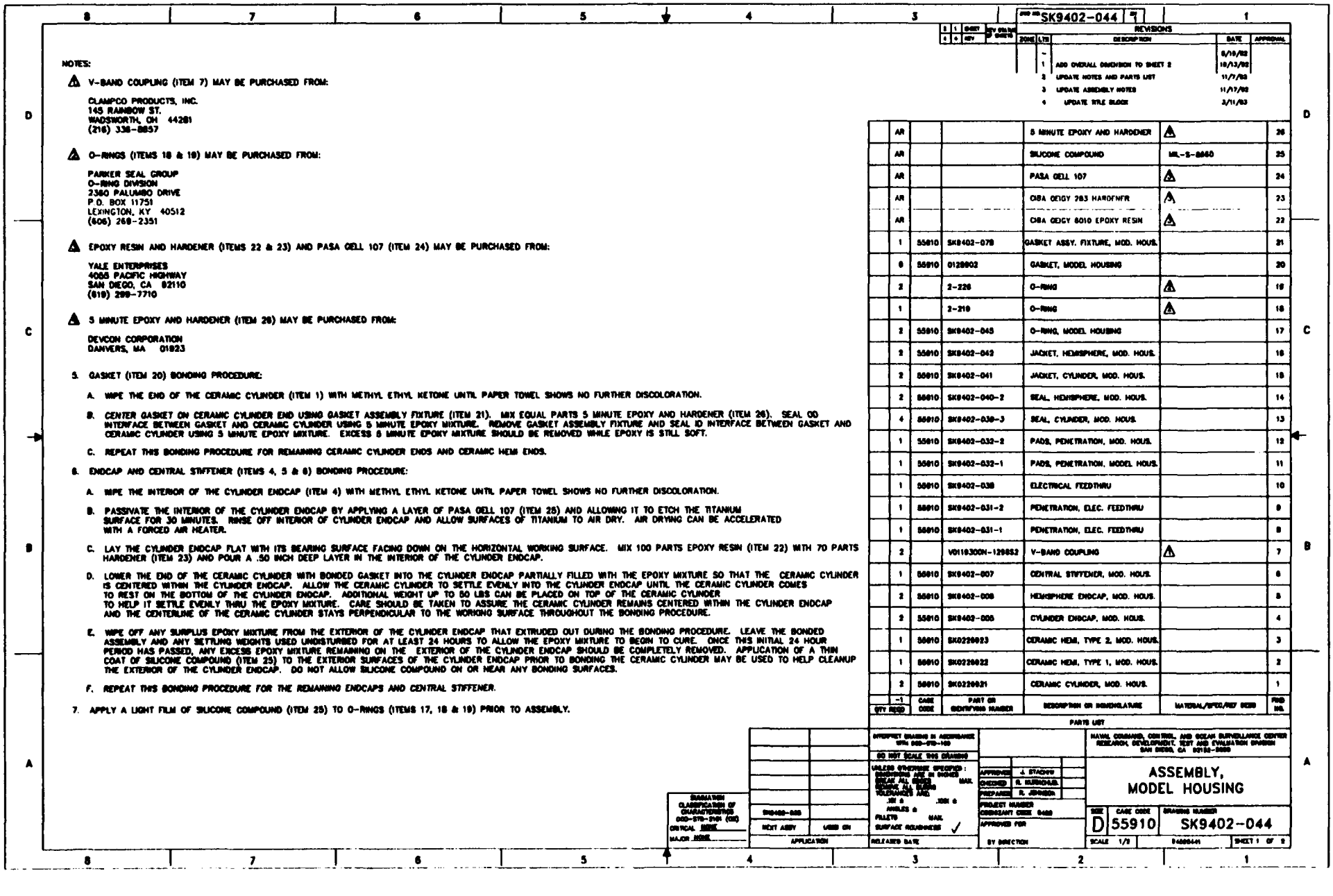

NOTES:

⚠ V-BAND COUPLING (ITEM 7) MAY BE PURCHASED FROM:

CLAMPCO PRODUCTS, INC.
145 RAINBOW ST.
WADSWORTH, OH 44281
(216) 336-8857

⚠ O-RINGS (ITEMS 18 & 19) MAY BE PURCHASED FROM:

PARKER SEAL GROUP
O-RING DIVISION
2360 PALUMBO DRIVE
P.O. BOX 11751
LEXINGTON, KY 40512
(606) 269-2351

⚠ EPOXY RESIN AND HARDENER (ITEMS 22 & 23) AND PASA GELL 107 (ITEM 24) MAY BE PURCHASED FROM:

YALE ENTERPRISES
4068 PACIFIC HIGHWAY
SAN DIEGO, CA 92110
(619) 299-7710

⚠ 5 MINUTE EPOXY AND HARDENER (ITEM 26) MAY BE PURCHASED FROM:

DEVCON CORPORATION
DANVERS, MA 01923

5. GASKET (ITEM 20) BONDING PROCEDURE:

A. WIPE THE END OF THE CERAMIC CYLINDER (ITEM 1) WITH METHYL ETHYL KETONE UNTIL PAPER TOWEL SHOWS NO FURTHER DISCOLORATION.

B. CENTER GASKET ON CERAMIC CYLINDER END USING GASKET ASSEMBLY FIXTURE (ITEM 21). MIX EQUAL PARTS 5 MINUTE EPOXY AND HARDENER (ITEM 26). SEAL OD INTERFACE BETWEEN GASKET AND CERAMIC CYLINDER USING 5 MINUTE EPOXY MIXTURE. REMOVE GASKET ASSEMBLY FIXTURE AND SEAL ID INTERFACE BETWEEN GASKET AND CERAMIC CYLINDER USING 5 MINUTE EPOXY MIXTURE. EXCESS 5 MINUTE EPOXY MIXTURE SHOULD BE REMOVED WHILE EPOXY IS STILL SOFT.

C. REPEAT THIS BONDING PROCEDURE FOR REMAINING CERAMIC CYLINDER ENDS AND CERAMIC HEMI ENDS.

6. ENDCAP AND CENTRAL STIFFENER (ITEMS 4, 5 & 6) BONDING PROCEDURE:

A. WIPE THE INTERIOR OF THE CYLINDER ENDCAP (ITEM 4) WITH METHYL ETHYL KETONE UNTIL PAPER TOWEL SHOWS NO FURTHER DISCOLORATION.

B. PASSIVATE THE INTERIOR OF THE CYLINDER ENDCAP BY APPLYING A LAYER OF PASA GELL 107 (ITEM 25) AND ALLOWING IT TO ETCH THE TITANIUM SURFACE FOR 30 MINUTES. RINSE OFF INTERIOR OF CYLINDER ENDCAP AND ALLOW SURFACES OF TITANIUM TO AIR DRY. AIR DRYING CAN BE ACCELERATED WITH A FORCED AIR HEATER.

C. LAY THE CYLINDER ENDCAP FLAT WITH ITS BEARING SURFACE FACING DOWN ON THE HORIZONTAL WORKING SURFACE. MIX 100 PARTS EPOXY RESIN (ITEM 22) WITH 70 PARTS HARDENER (ITEM 23) AND POUR A .50 INCH DEEP LAYER IN THE INTERIOR OF THE CYLINDER ENDCAP.

D. LOWER THE END OF THE CERAMIC CYLINDER WITH BONDED GASKET INTO THE CYLINDER ENDCAP PARTIALLY FILLED WITH THE EPOXY MIXTURE SO THAT THE CERAMIC CYLINDER IS CENTERED WITHIN THE CYLINDER ENDCAP. ALLOW THE CERAMIC CYLINDER TO SETTLE EVENLY INTO THE CYLINDER ENDCAP UNTIL THE CERAMIC CYLINDER COMES TO REST ON THE BOTTOM OF THE CYLINDER ENDCAP. ADDITIONAL WEIGHT UP TO 50 LBS CAN BE PLACED ON TOP OF THE CERAMIC CYLINDER TO HELP IT SETTLE EVENLY THRU THE EPOXY MIXTURE. CARE SHOULD BE TAKEN TO ASSURE THE CERAMIC CYLINDER REMAINS CENTERED WITHIN THE CYLINDER ENDCAP AND THE CENTERLINE OF THE CERAMIC CYLINDER STAYS PERPENDICULAR TO THE WORKING SURFACE THROUGHOUT THE BONDING PROCEDURE.

E. WIPE OFF ANY SURPLUS EPOXY MIXTURE FROM THE EXTERIOR OF THE CYLINDER ENDCAP THAT EXTRUDED OUT DURING THE BONDING PROCEDURE. LEAVE THE BONDED ASSEMBLY AND ANY SETTLING WEIGHTS USED UNDISTURBED FOR AT LEAST 24 HOURS TO ALLOW THE EPOXY MIXTURE TO BEGIN TO CURE. ONCE THIS INITIAL 24 HOUR PERIOD HAS PASSED, ANY EXCESS EPOXY MIXTURE REMAINING ON THE EXTERIOR OF THE CYLINDER ENDCAP SHOULD BE COMPLETELY REMOVED. APPLICATION OF A THIN COAT OF SILICONE COMPOUND (ITEM 25) TO THE EXTERIOR SURFACES OF THE CYLINDER ENDCAP PRIOR TO BONDING THE CERAMIC CYLINDER MAY BE USED TO HELP CLEANUP THE EXTERIOR OF THE CYLINDER ENDCAP. DO NOT ALLOW SILICONE COMPOUND ON OR NEAR ANY BONDING SURFACES.

F. REPEAT THIS BONDING PROCEDURE FOR THE REMAINING ENDCAPS AND CENTRAL STIFFENER.

7. APPLY A LIGHT FILM OF SILICONE COMPOUND (ITEM 25) TO O-RINGS (ITEMS 17, 18 & 19) PRIOR TO ASSEMBLY.

REVISIONS				
ZONE	LTR	DESCRIPTION	DATE	APPROVAL
	~		8/19/92	
	1	ADD OVERALL DIMENSION TO SHEET 2	10/13/92	
	2	UPDATE NOTES AND PARTS LIST	11/7/92	
	3	UPDATE ASSEMBLY NOTES	11/17/92	
	4	UPDATE TITLE BLOCK	3/11/93	

PARTS LIST

ITEM NO.	QTY REQD	CAGE CODE	PART OR IDENTIFYING NUMBER	DESCRIPTION OR NOMENCLATURE	MATERIAL/SPEC/REF DESIG
26	AR			5 MINUTE EPOXY AND HARDENER	⚠
25	AR			SILICONE COMPOUND	MIL-S-8660
24	AR			PASA GELL 107	⚠
23	AR			CIBA GEIGY 283 HARDENER	⚠
22	AR			CIBA GEIGY 8010 EPOXY RESIN	⚠
21	1	55910	SK9402-078	GASKET ASSY. FIXTURE, MOD. HOUS.	
20	8	55910	0128902	GASKET, MODEL HOUSING	
19	2		2-226	O-RING	⚠
18	1		2-219	O-RING	⚠
17	2	55910	SK9402-045	O-RING, MODEL HOUSING	
16	2	55910	SK9402-042	JACKET, HEMISPHERE, MOD. HOUS.	
15	2	55910	SK9402-041	JACKET, CYLINDER, MOD. HOUS.	
14	2	55910	SK9402-040-2	SEAL, HEMISPHERE, MOD. HOUS.	
13	4	55910	SK9402-038-3	SEAL, CYLINDER, MOD. HOUS.	
12	1	55910	SK9402-032-2	PADS, PENETRATION, MOD. HOUS.	
11	1	55910	SK9402-032-1	PADS, PENETRATION, MODEL HOUS.	
10	1	55910	SK9402-038	ELECTRICAL FEEDTHRU	
9	1	55910	SK9402-031-2	PENETRATION, ELEC. FEEDTHRU	
8	1	55910	SK9402-031-1	PENETRATION, ELEC. FEEDTHRU	
7	2		V0116300N-129853	V-BAND COUPLING	⚠
6	1	55910	SK9402-007	CENTRAL STIFFENER, MOD. HOUS.	
5	2	55910	SK9402-006	HEMISPHERE ENDCAP, MOD. HOUS.	
4	2	55910	SK9402-005	CYLINDER ENDCAP, MOD. HOUS.	
3	1	55910	SK0220923	CERAMIC HEMI, TYPE 2, MOD. HOUS.	
2	1	55910	SK0220922	CERAMIC HEMI, TYPE 1, MOD. HOUS.	
1	2	55910	SK0220921	CERAMIC CYLINDER, MOD. HOUS.	

DO NOT SCALE THIS DRAWING

NAVAL COMMAND, CONTROL, AND OCEAN SURVEILLANCE CENTER RESEARCH, DEVELOPMENT, TEST AND EVALUATION DIVISION SAN DIEGO, CA 92152-5000

ASSEMBLY, MODEL HOUSING

SIZE D | CAGE CODE 55910 | DRAWING NUMBER SK9402-044

SCALE 1/2 | SHEET 1 OF 2

38

Figure 19. Case 4 test assembly for evaluation of central stiffened joint rings, Sheet 1.

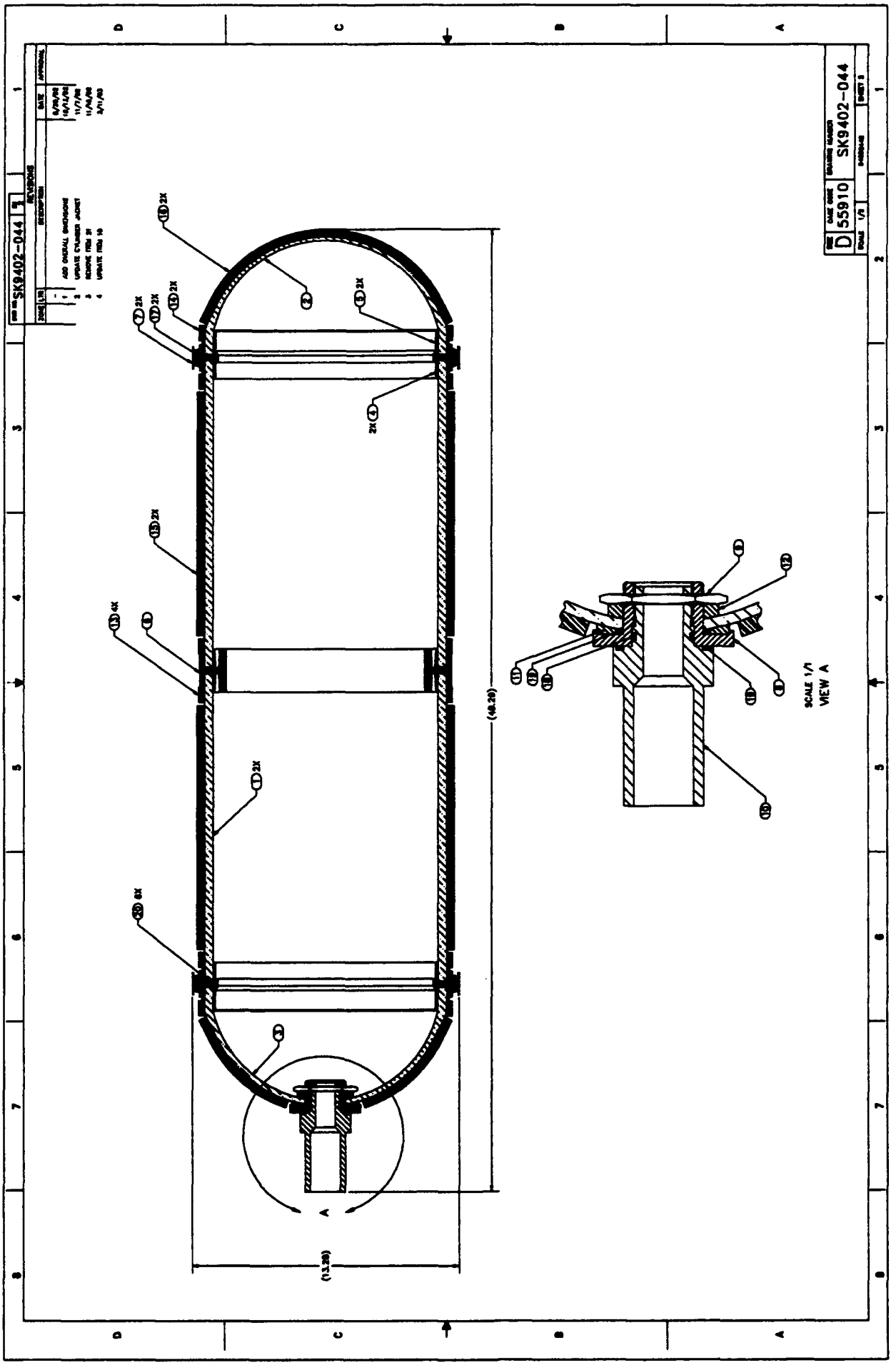

Figure 19. Case 4 test assembly for evaluation of central stiffened joint rings, Sheet 2.

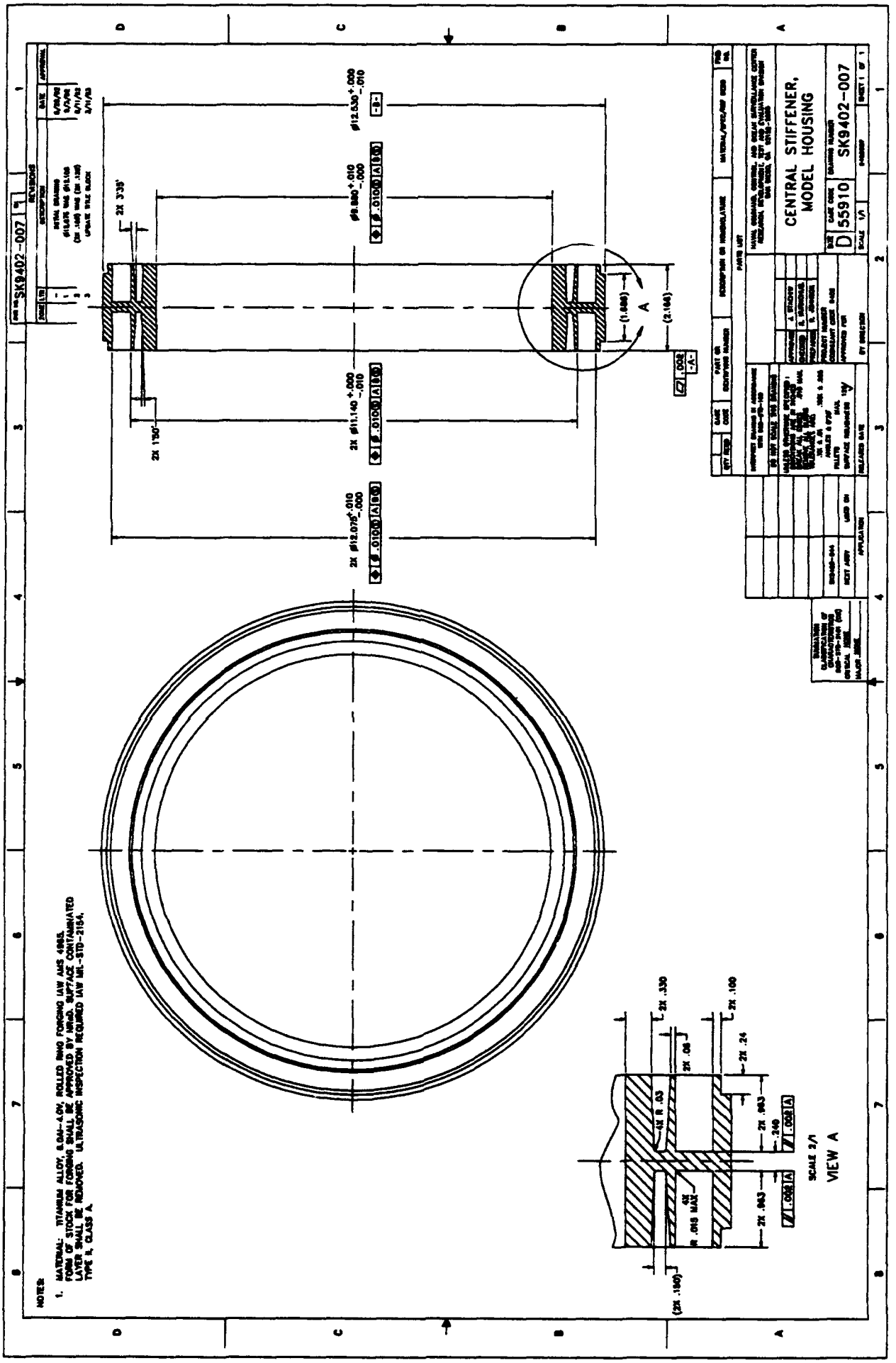

Figure 20. Case 4 central stiffened joint ring details.

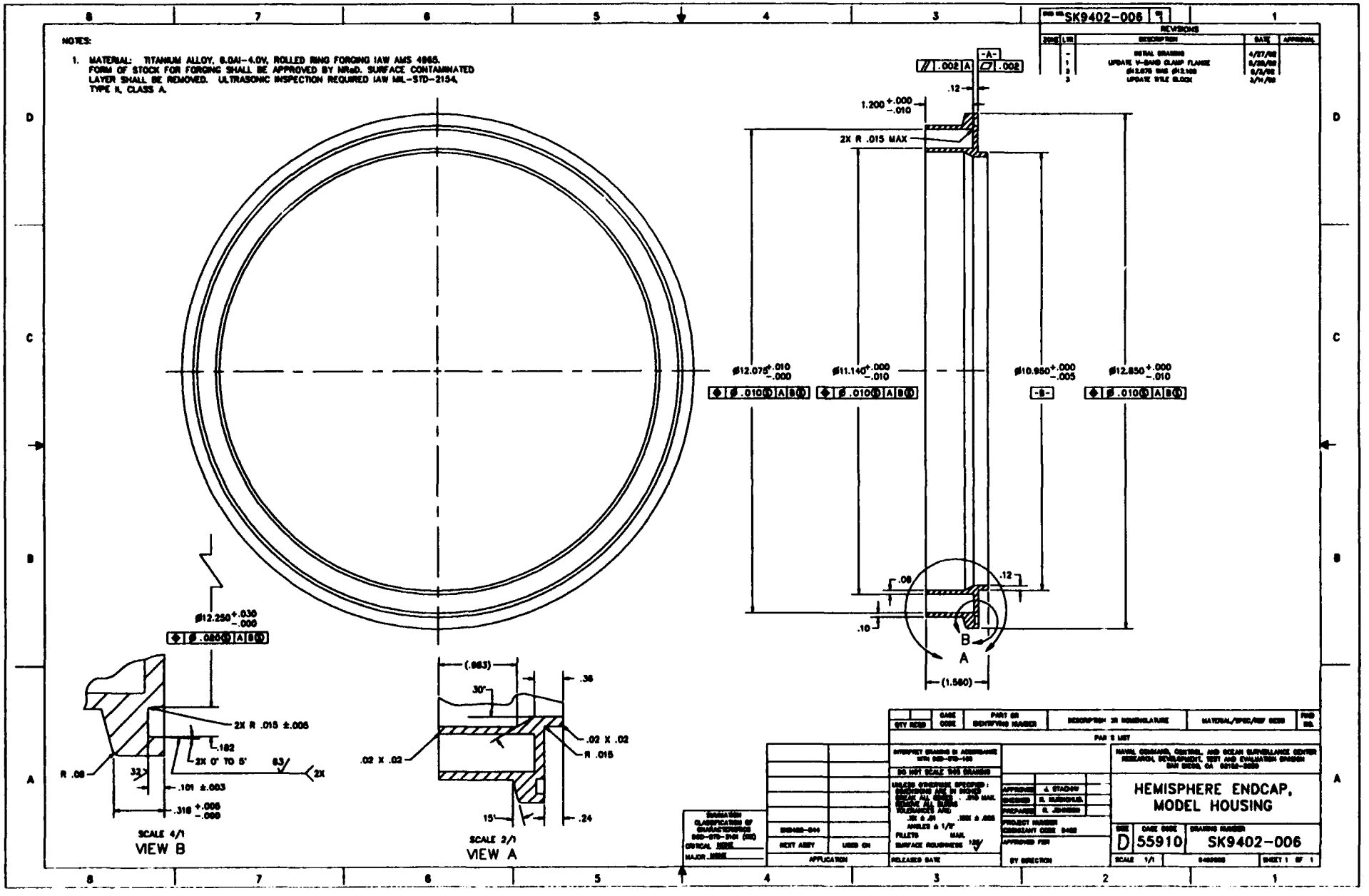

Figure 21. Case 4 hemisphere end cap joint ring details.

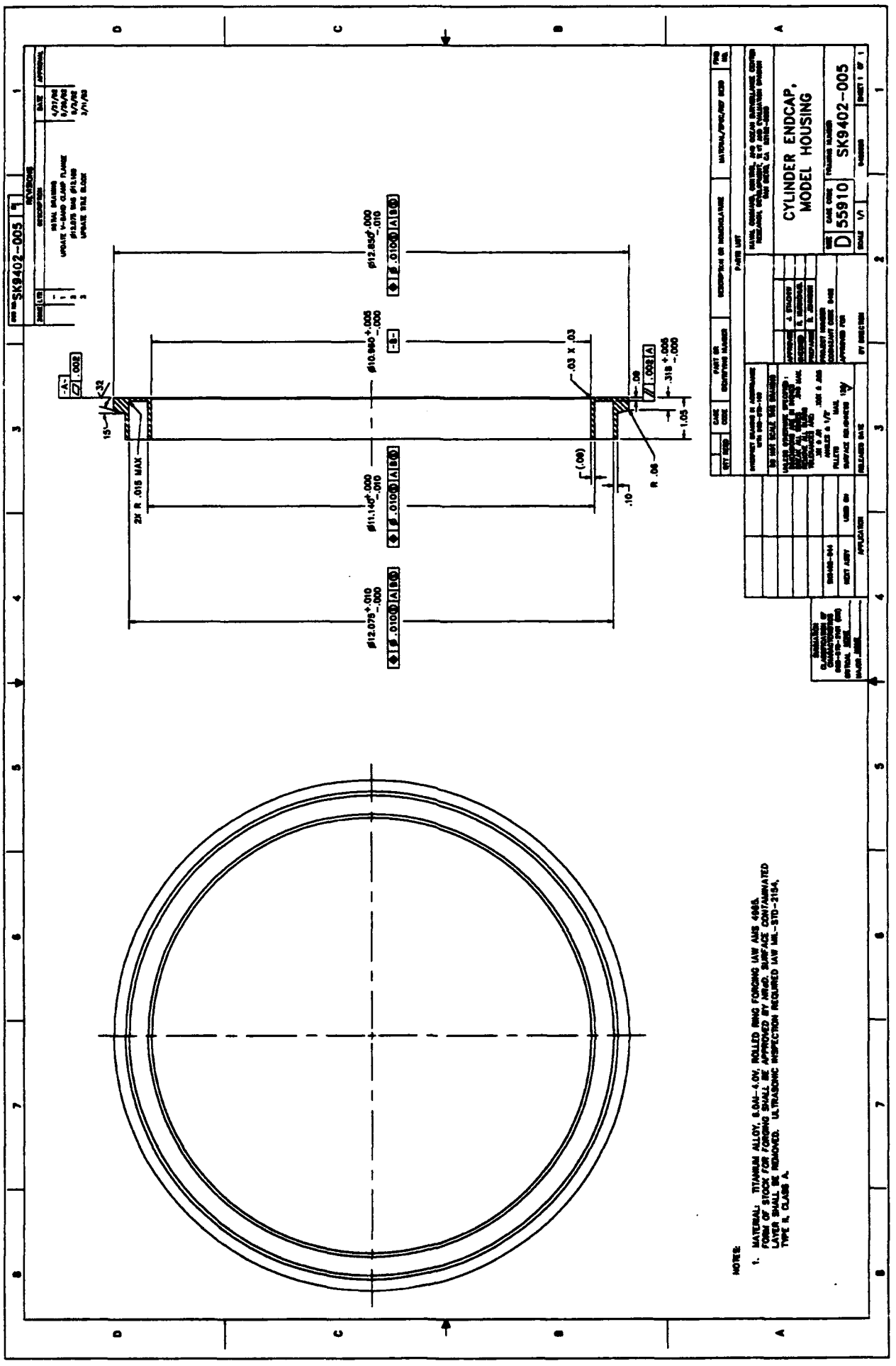

Figure 22. Case 4 cylinder end cap joint ring details.

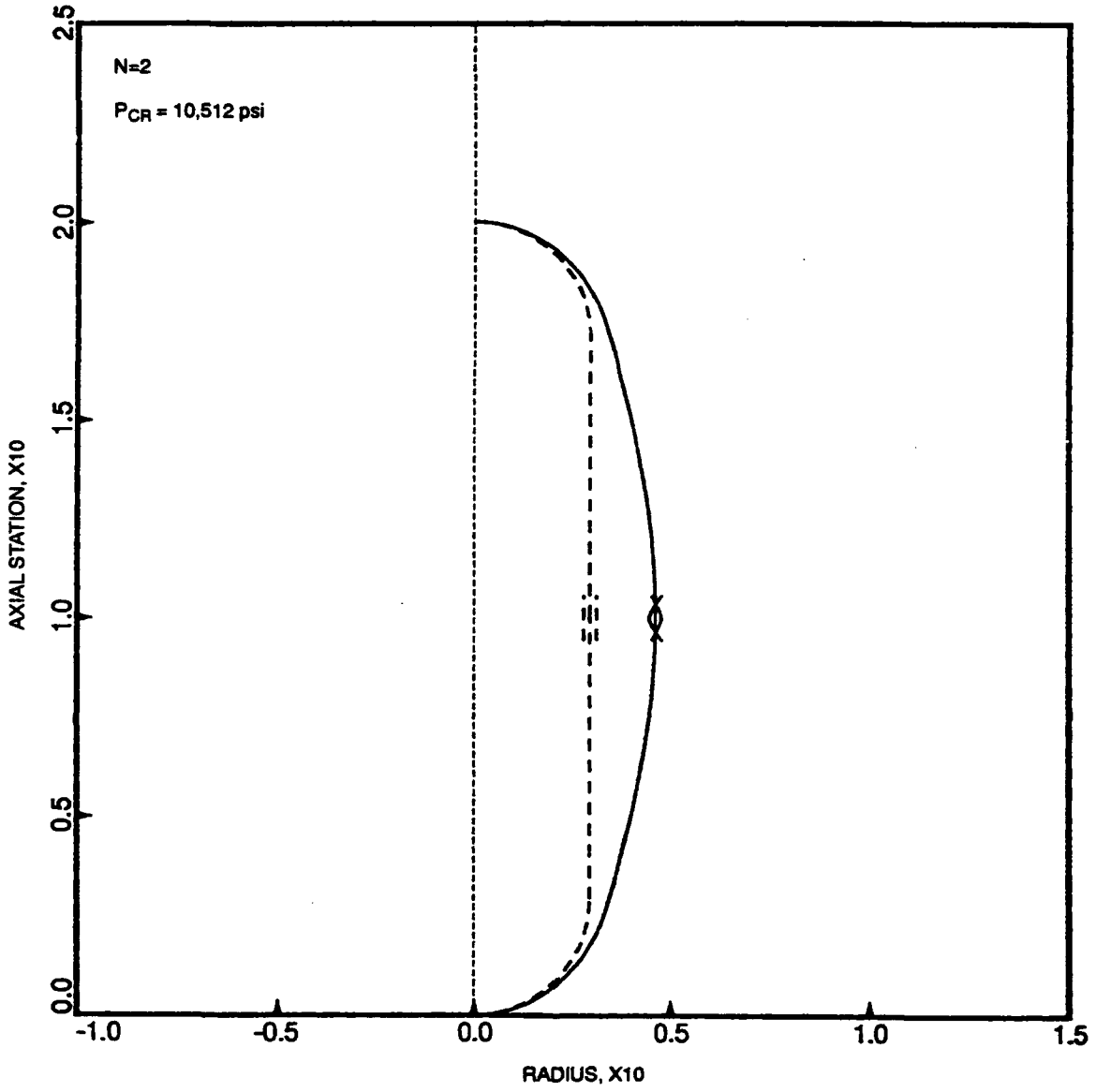

Figure 23. BOSOR4 predicted failure mode for case 1 test assembly.

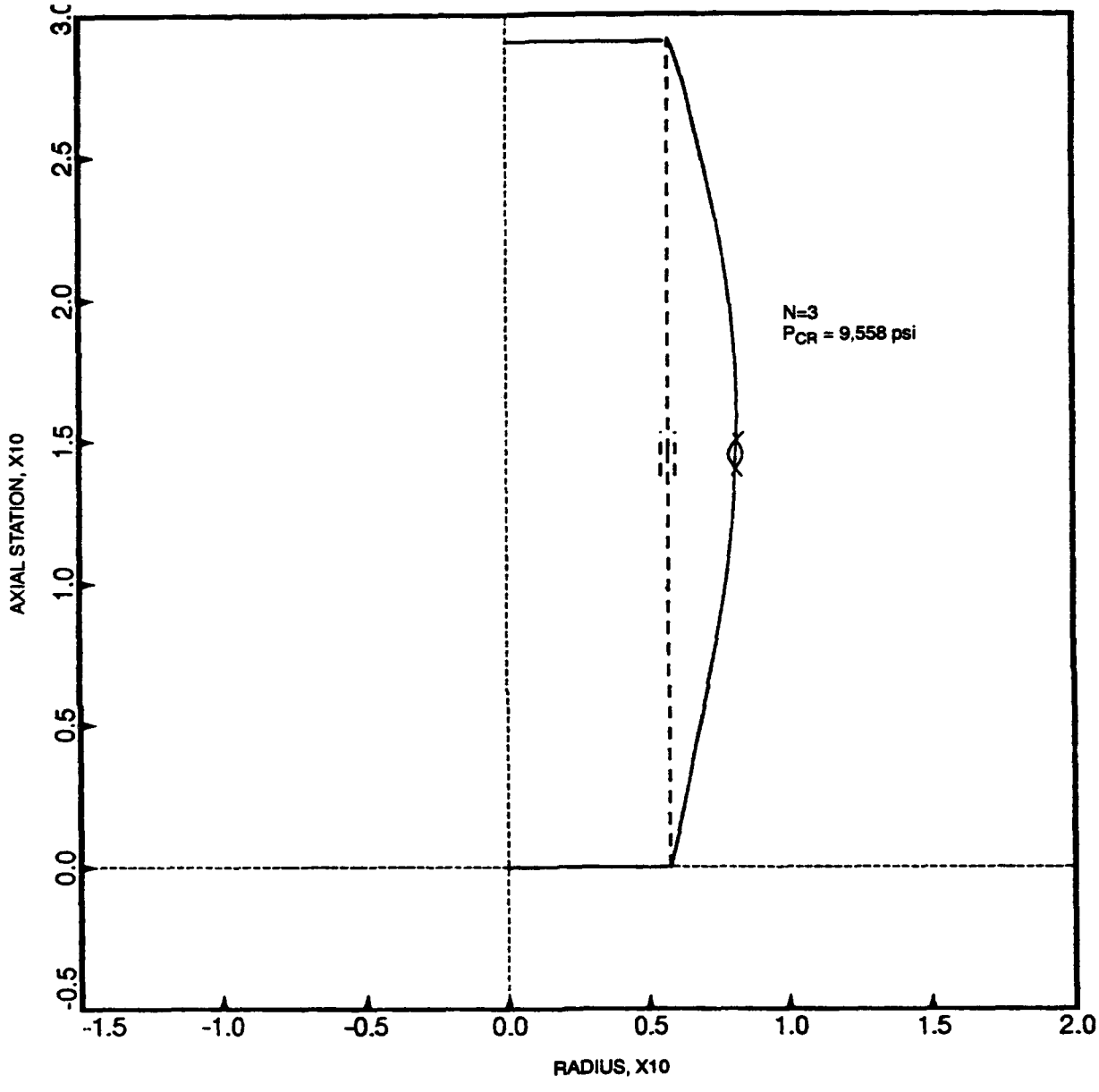

Figure 24. BOSOR4 predicted failure mode for case 2 test assembly.

Figure 25. Buckled case 2 coupling ring.

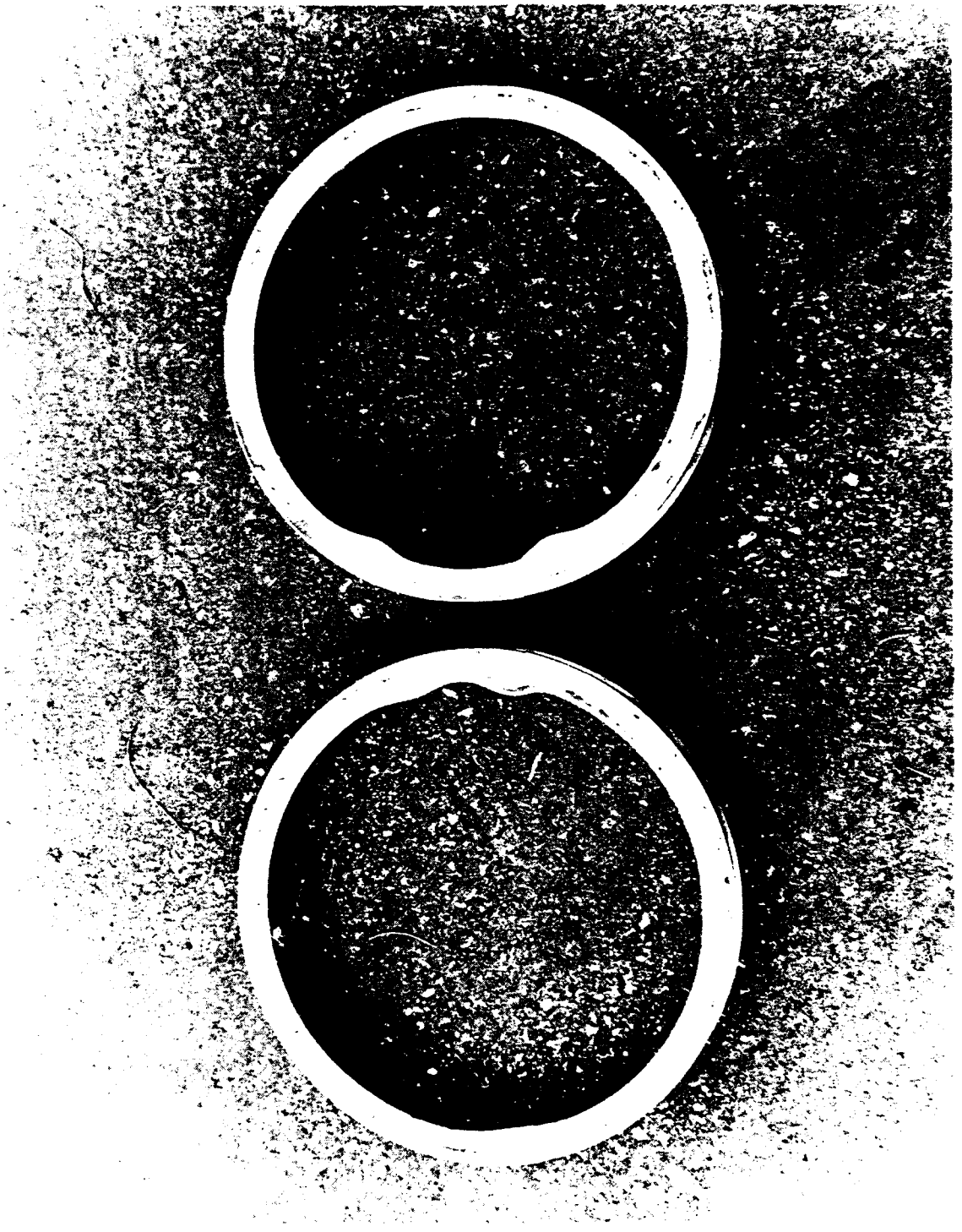

Figure 26. Buckled case 2 end cap joint rings.

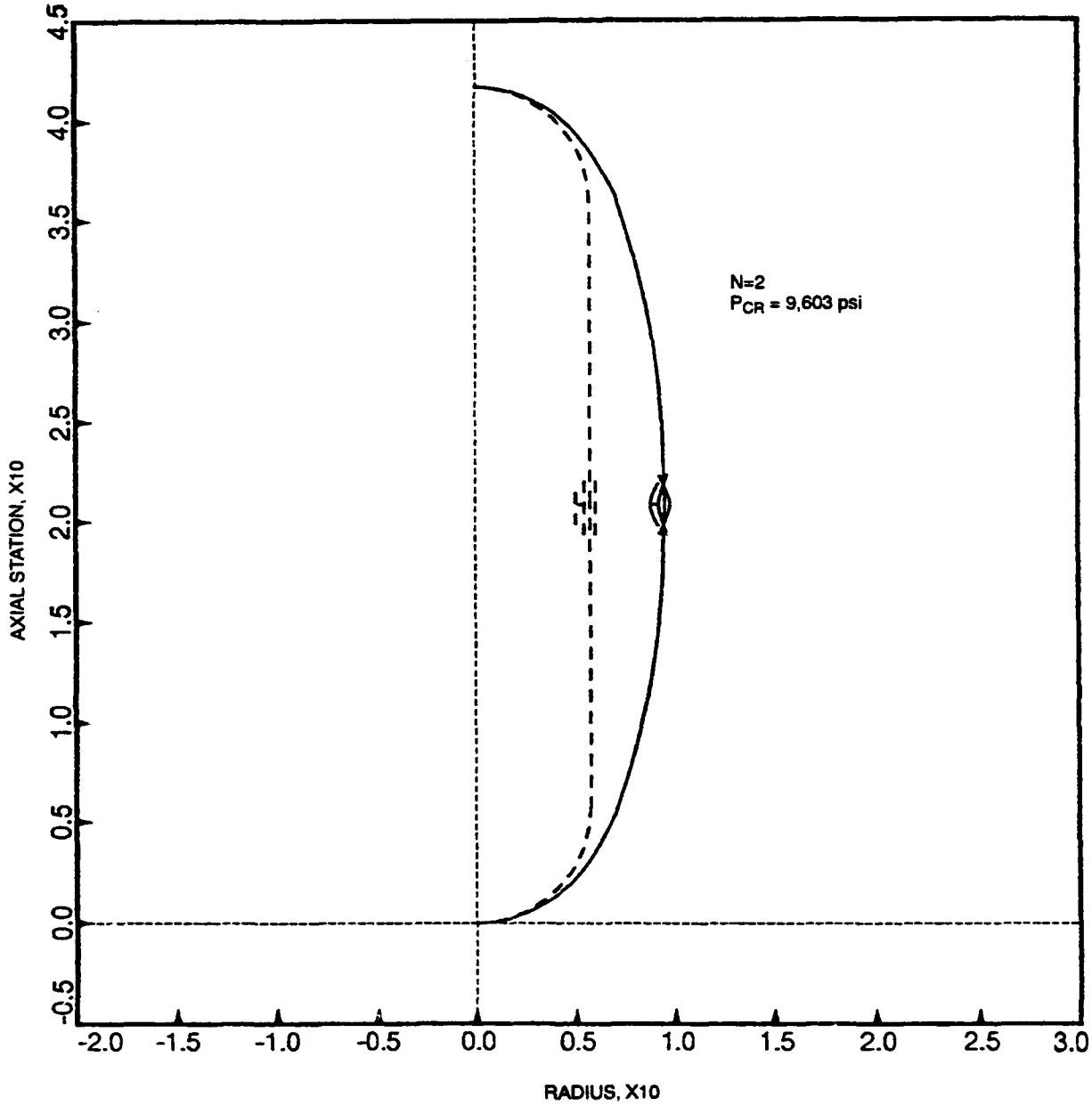

Figure 27. BOSOR4 predicted failure mode for case 3 test assembly.

Figure 28. Case 3 test assembly after failure by buckling.

Figure 29. Buckled case 3 central stiffened joint ring.

LOCATION OF STRAIN GAGES
ON
CENTRAL JOINT STIFFENER

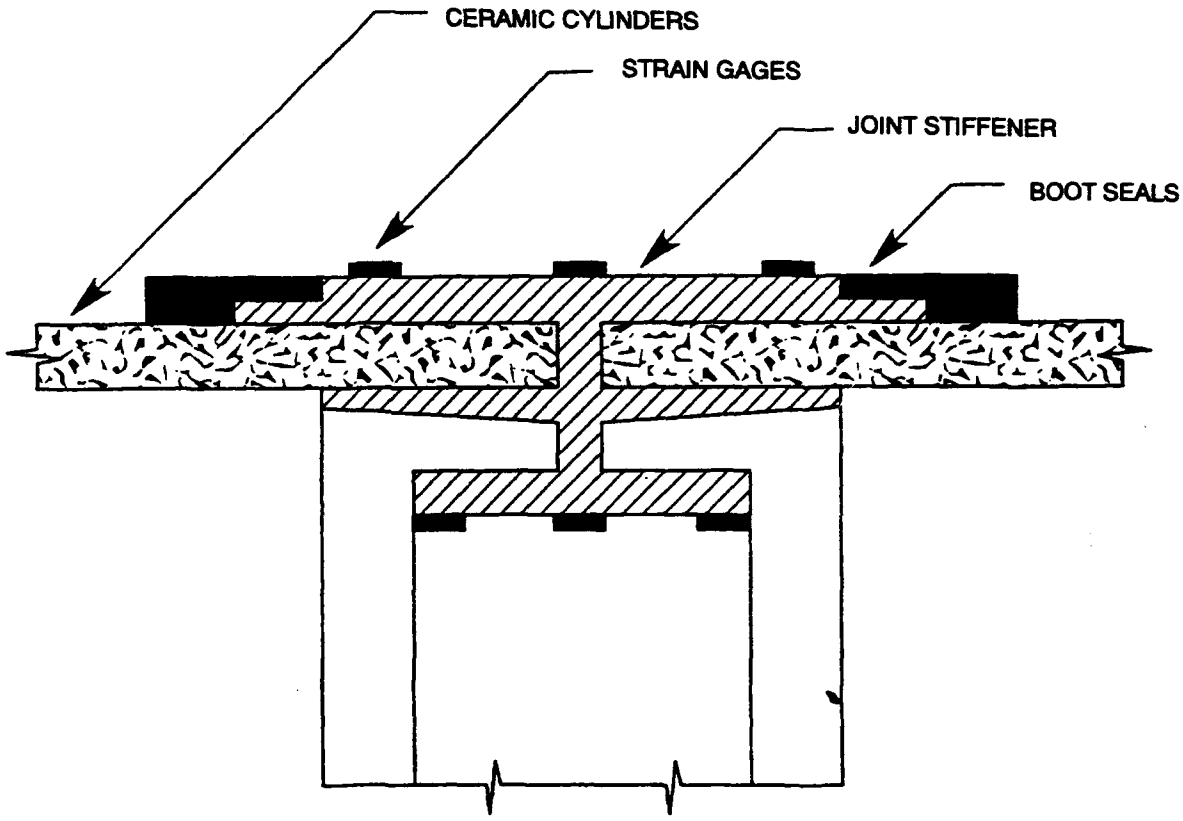

STRAIN GAGES: CEA–06–125WT–120

Figure 30. Location of strain gages on case 3 central stiffened joint ring.

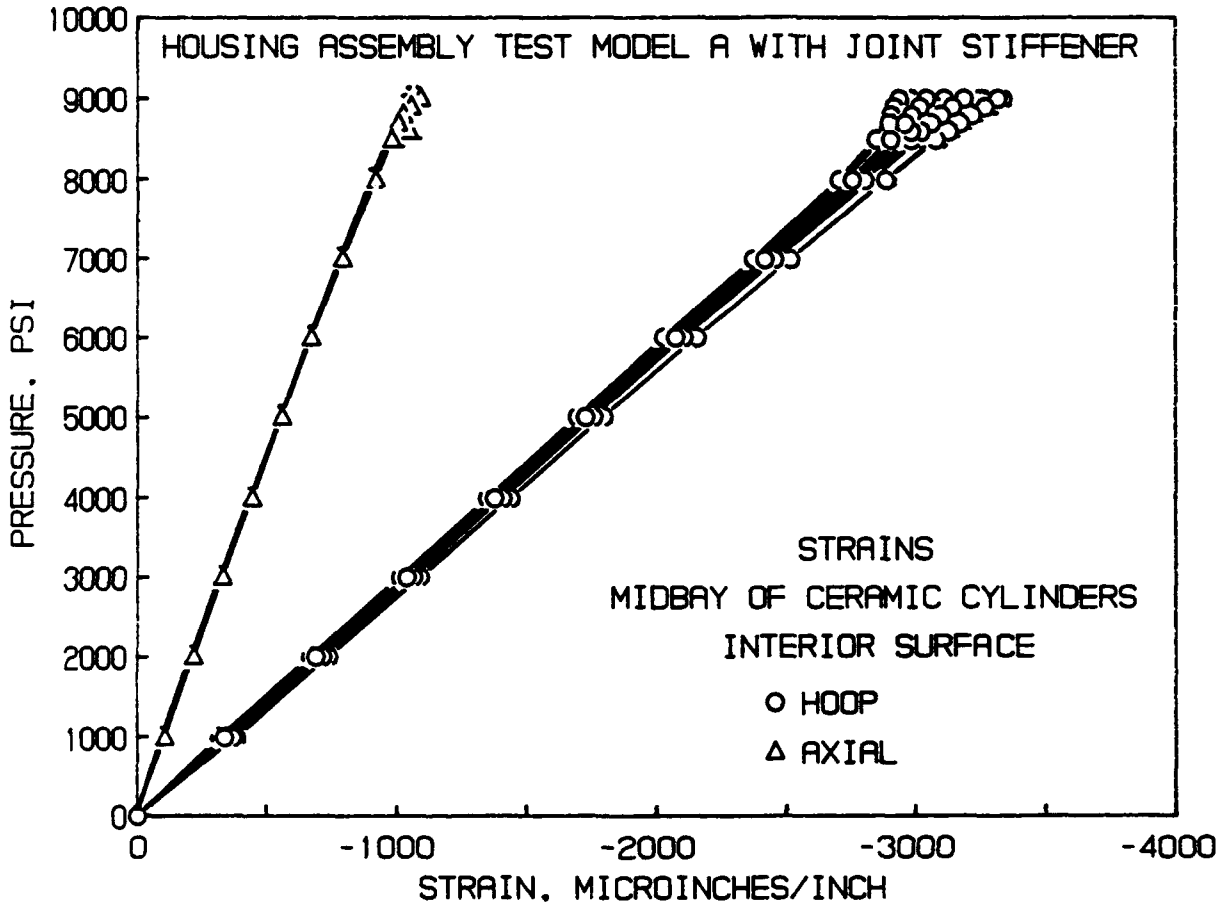

Figure 31. Plot of strains recorded on interior surface of case 3 ceramic cylinders at midbay.

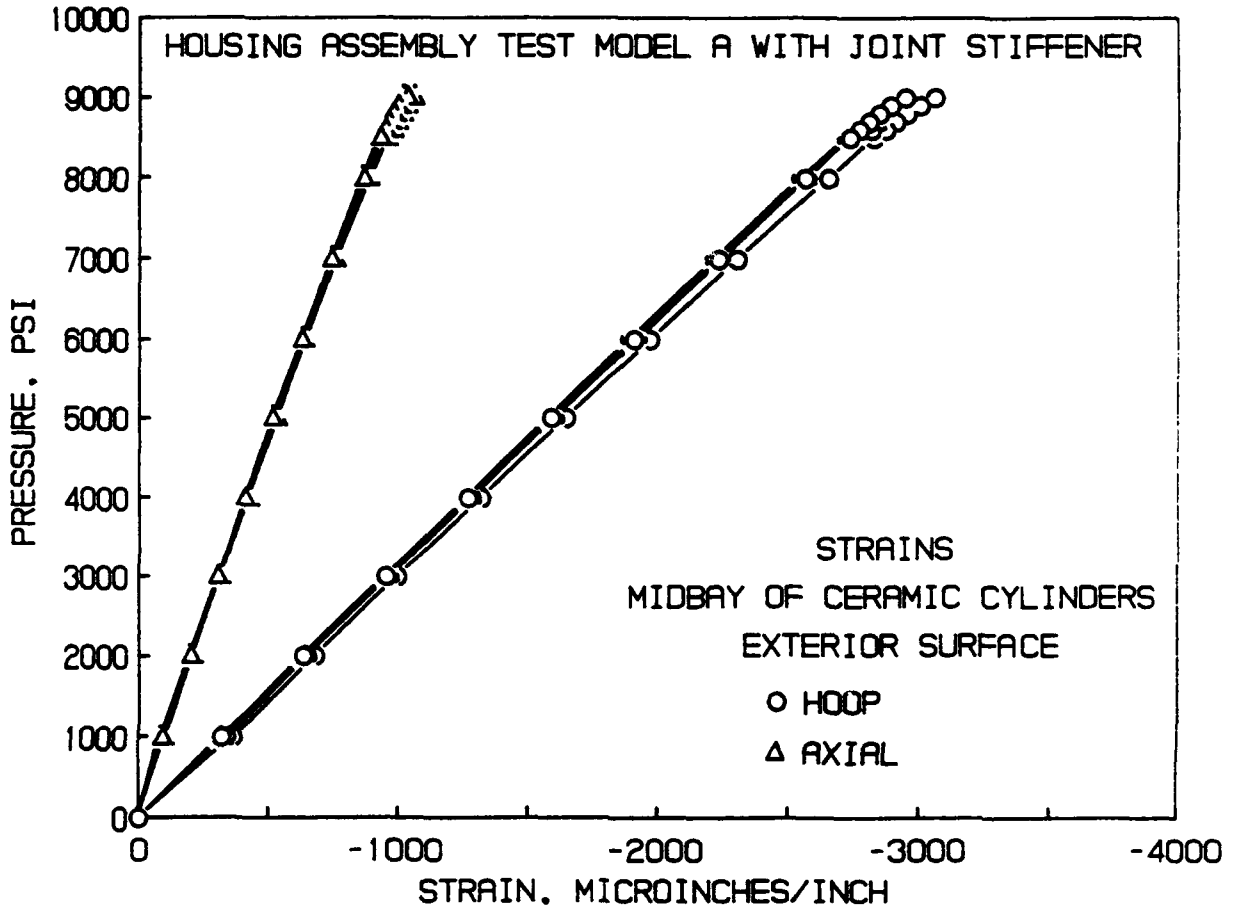

Figure 32. Plot of strains recorded on exterior surface of case 3 ceramic cylinders at midbay.

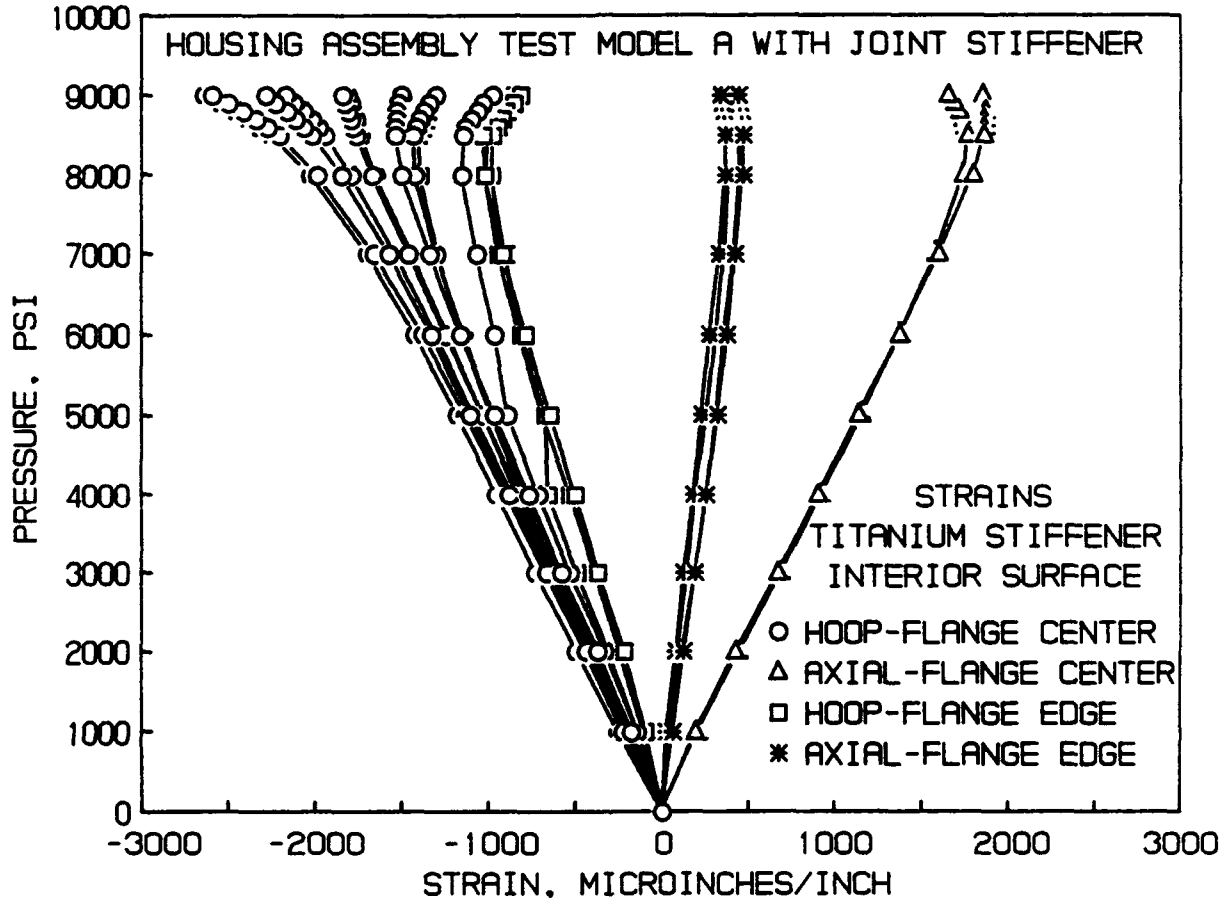

Figure 33. Plot of strains recorded on interior surfaces of case 3 central stiffened joint ring.

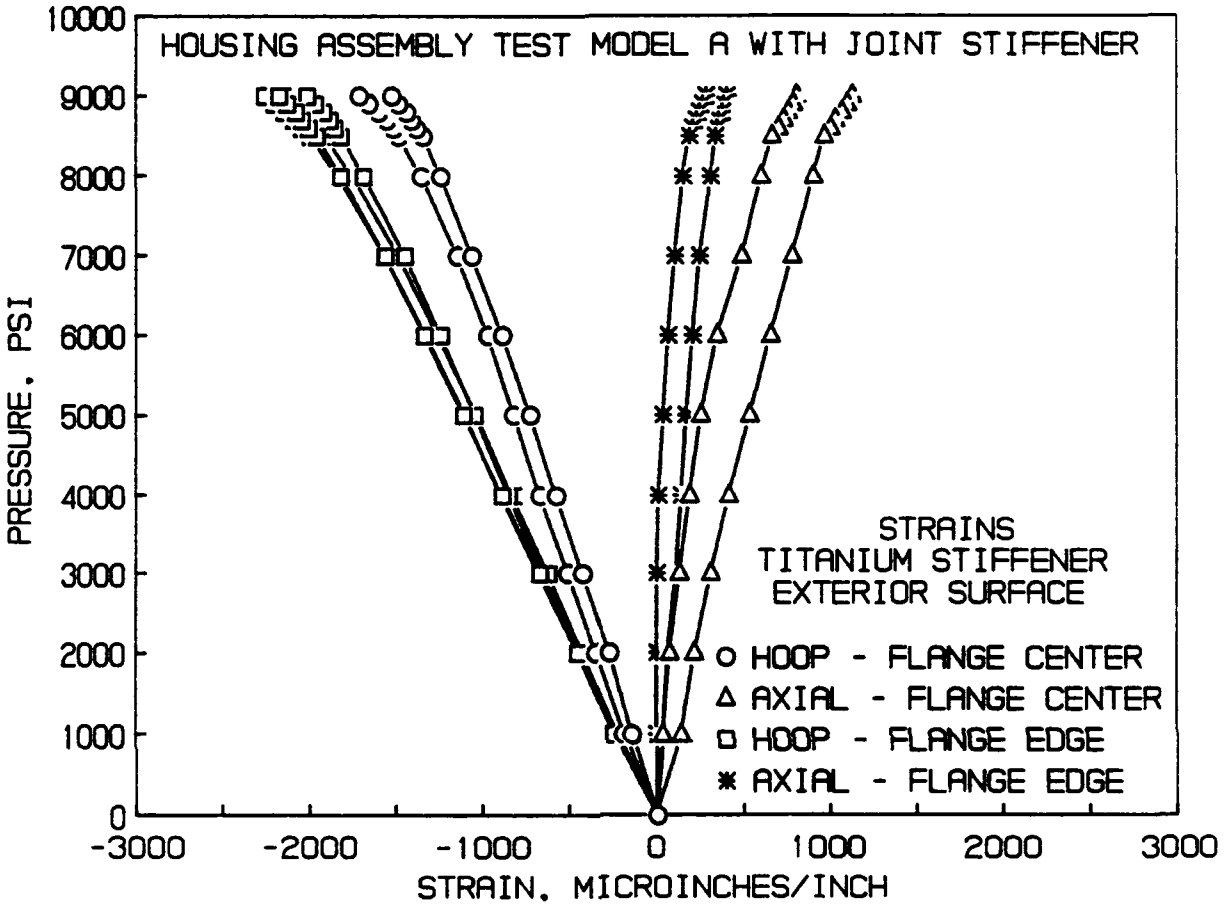

Figure 34. Plot of strains recorded on exterior surfaces of case 3 central stiffened joint ring.

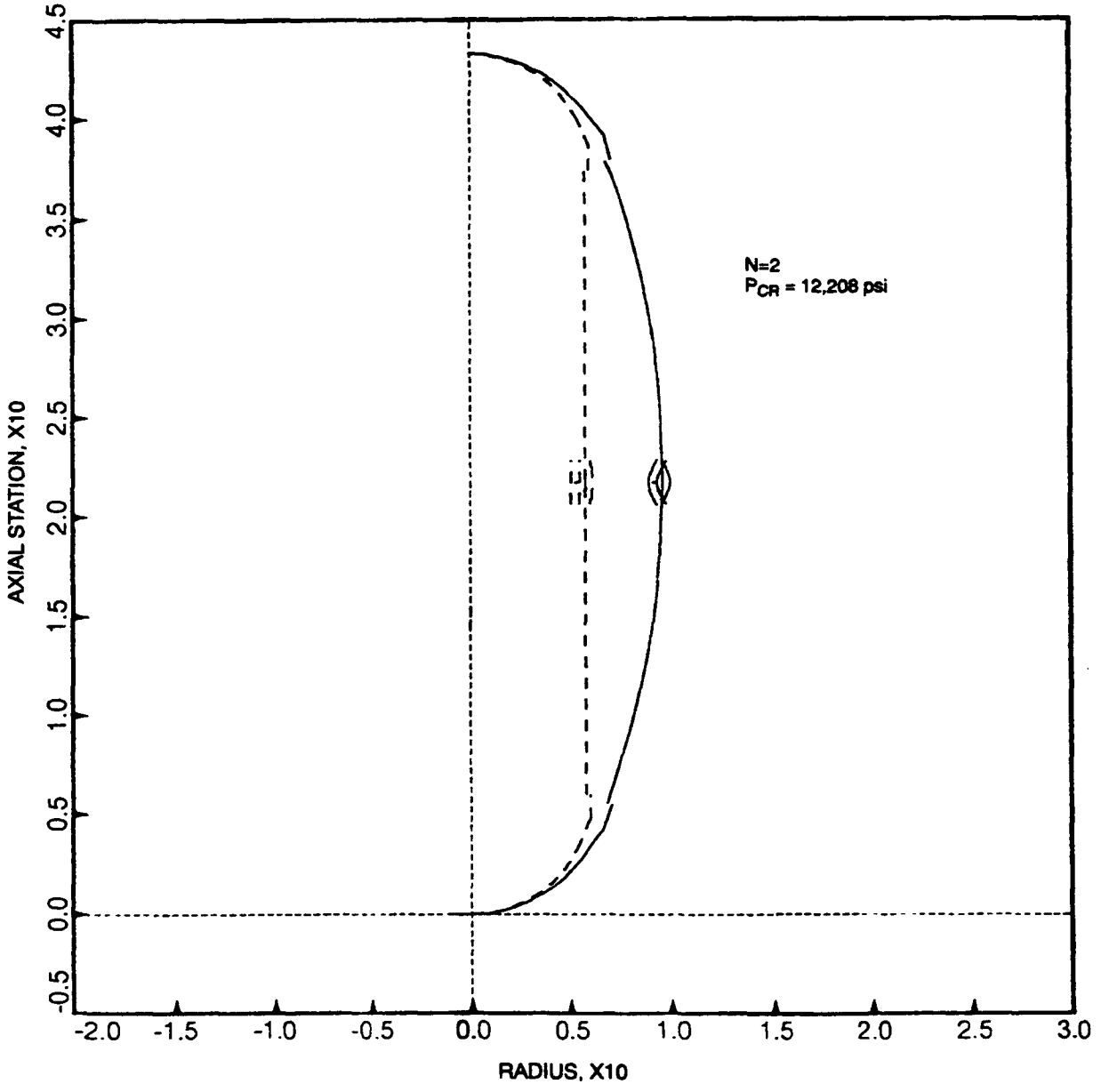

Figure 35. BOSOR4 predicted failure mode for case 4 test assembly.

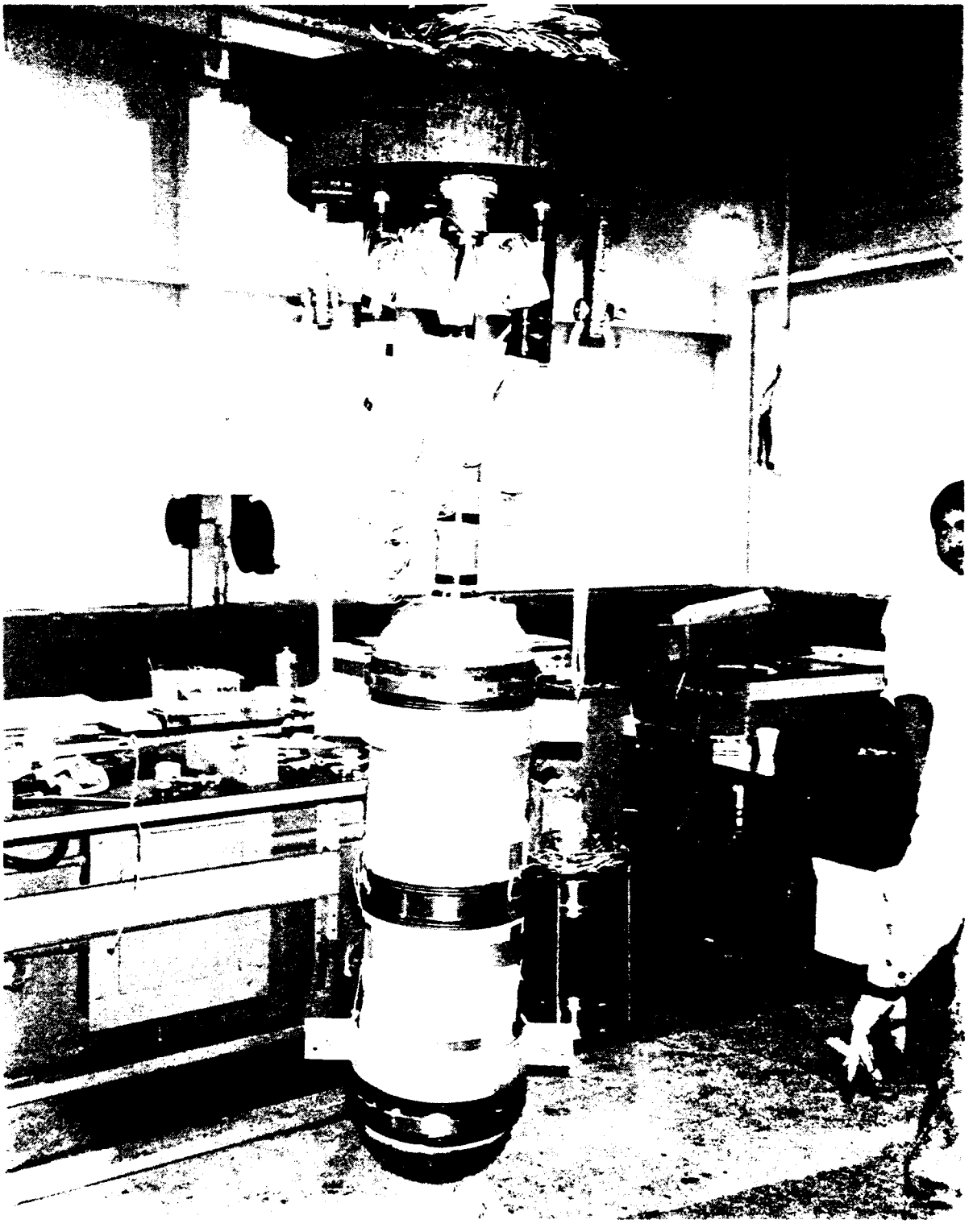

Figure 36. Case 4 test assembly.

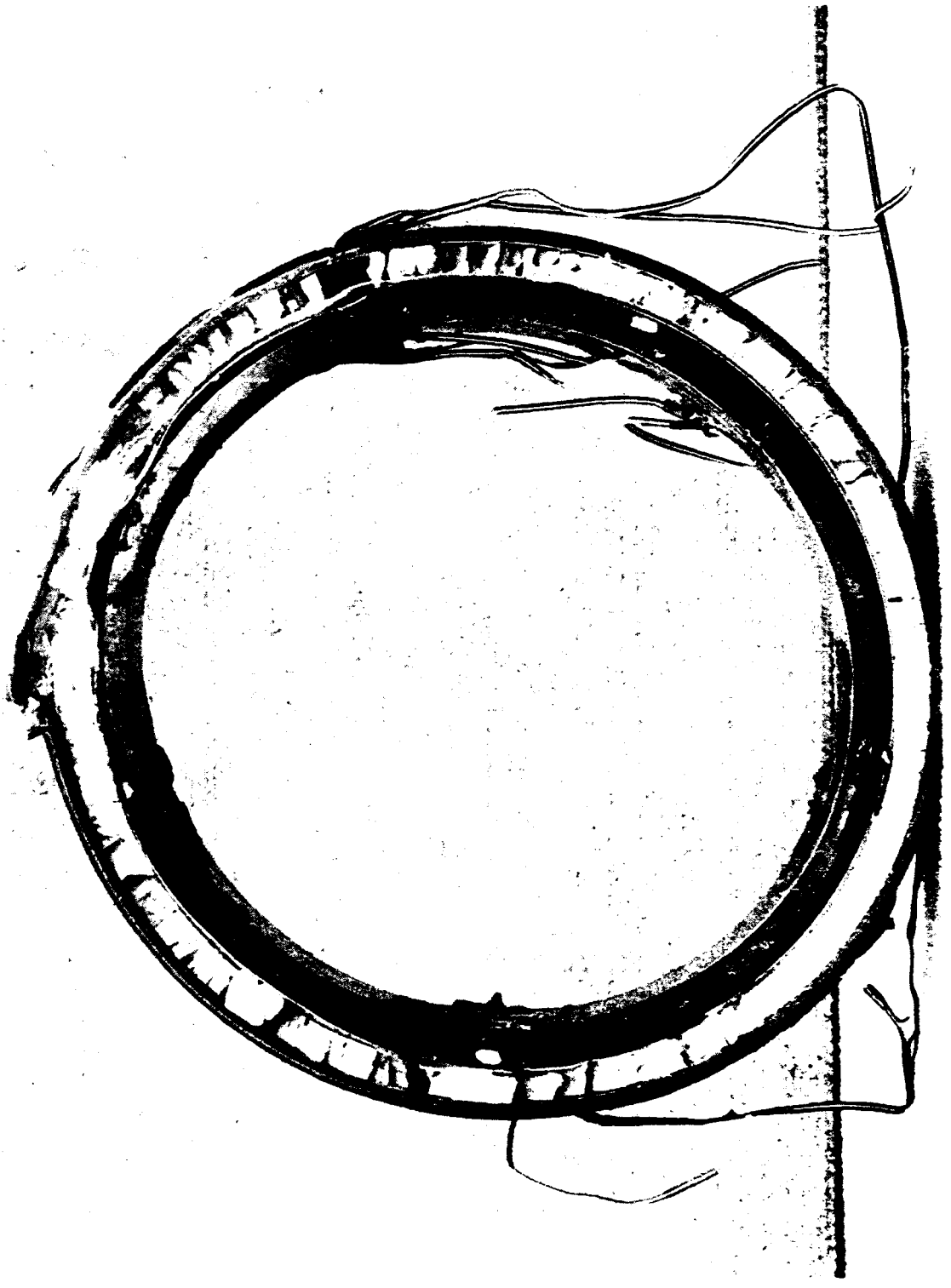

Figure 37. Buckle case 4 central stiffened joint ring.

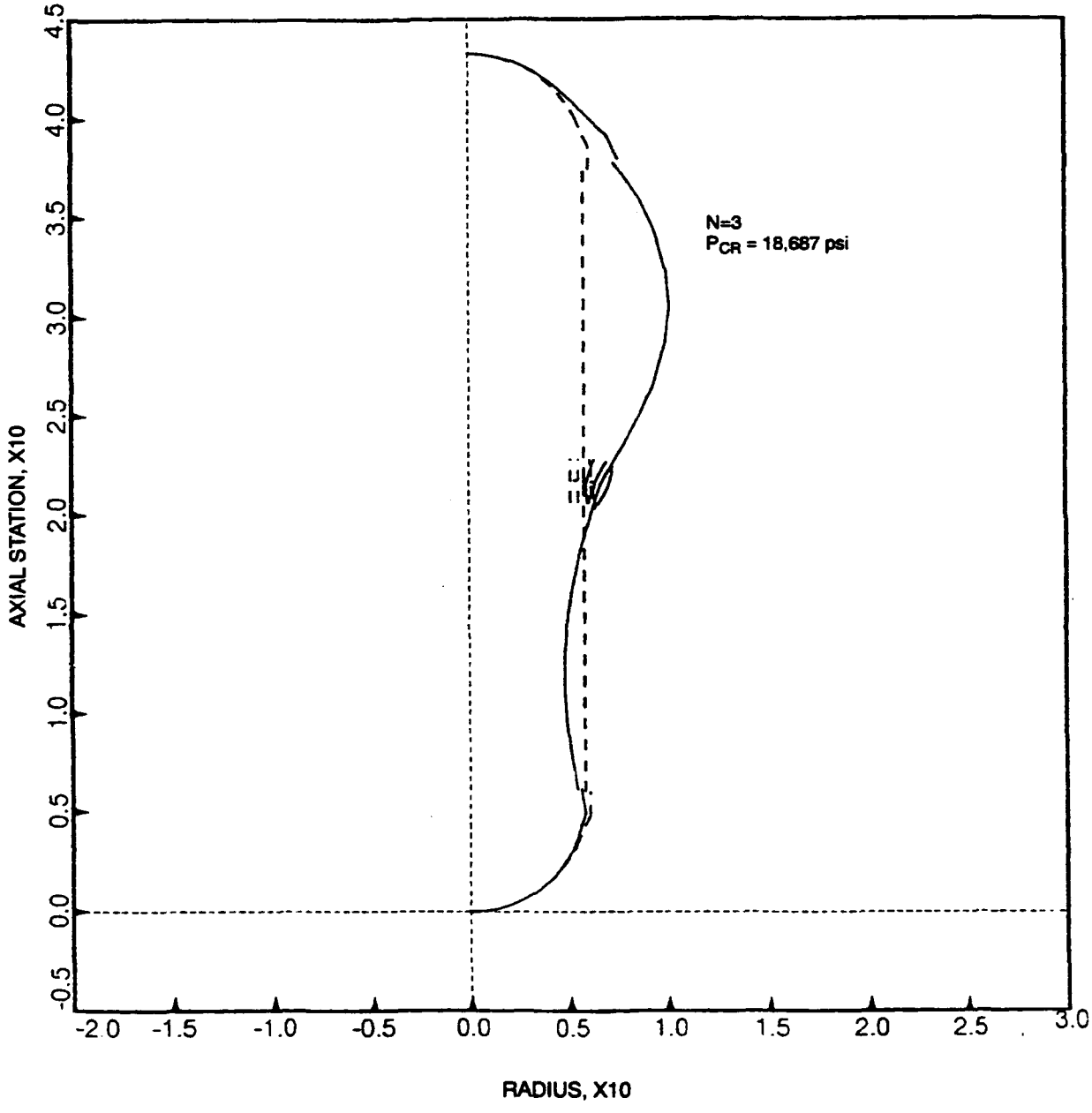

Figure 38. BOSOR4 N=3 failure mode for case 4 test assembly.

Table 1. Results of joint ring structural stability calculations.

	CASE 1 E=54E6 psi v=.22 L=16.16" D=6.1" t=.2"	CASE 2 E=44E6 psi v=.21 L=29.03" D=11.89" t=.355"	CASE 3 E=44E6 psi v=.21	CASE 4 E=44E6 psi v=.21
EQUATION 1	Pcrit (psi)	Pcrit (psi)		
N=2	11582	9274		
N=3	13253	8413		
N=4	22141	13680		
BOSOR4	Pcrit (psi)	Pcrit (psi)	Pcrit (psi)	Pcrit (psi)
N=2	10512	13083	9603	12208
N=3	13978	9558	11771	18687
N=4	24507	15245	15338	26919
TEST RESULTS	BUCKLED @ 9200 psi	BUCKLED @ 10,250 psi	BUCKLED @ 9550 psi	BUCKLED @ 11,930 psi

Table 2. Strains recorded during pressure testing of case 3 test assembly, Sheet 1.

	Cylinder No. 1 Midbay Interior										
Pressure	Hoop 12	Axial 13	Hoop 14	Hoop 15	Hoop 16	Hoop 17	Axial 18	Hoop 19	Hoop 20	Hoop 21	Hoop 22
0	0	0	0	0	0	0	0	0	0	0	0
1000	-350	-103	-351	-354	-3 :	-349	-106	-353	-354	-355	-354
2000	-692	-213	-695	-699	-696	-692	-219	-696	-699	-698	-694
3000	-1040	-326	-1046	-1051	-1045	-1041	-330	-1046	-1051	-1049	-1040
4000	-1380	-436	-1391	-1397	-1385	-1382	-439	-1389	-1396	-1393	-1380
5000	-1724	-550	-1742	-1748	-1731	-1727	-551	-1737	-1747	-1743	-1723
6000	-2064	-664	-2093	-2101	-2074	-2069	-664	-2083	-2099	-2091	-2063
7000	-2399	-781	-2447	-2458	-2414	-2404	-780	-2428	-2455	-2442	-2399
8000	-2721	-900	-2805	-2825	-2749	-2726	-899	-2771	-2821	-2797	-2722
8500	-2868	-963	-2986	-3017	-2909	-2868	-964	-2936	-3011	-2976	-2869
8600	-2897	-979	-3027	-3062	-2943	-2895	-979	-2971	-3056	-3016	-2897
8700	-2922	-993	-3064	-3105	-2973	-2917	-994	-3003	-3098	-3054	-2922
8800	-2946	-1008	-3106	-3151	-3004	-2940	-1010	-3038	-3142	-3094	-2946
8900	-2973	-1025	-3151	-3203	-3038	-2963	-1029	-3074	-3193	-3138	-2972
9000	-2995	-1042	-3193	-3253	-3069	-2981	-1047	-3106	-3242	-3180	-2993

NOTES: 1. The housing assembly consists of two 94 percent alumina ceramic cylinders with 11.89 OD x 11.18 ID x 15 L dimensions bonded to a simple titanium joint stiffener Type RJ1.

2. The ends of the ceramic cylinders were closed off with titanium hemispheres providing radial and axial support.

3. The assembly successfully withstood 11 pressure cycles to 9000 psi.

Table 2. Strains recorded during pressure testing of case 3 test assembly, Sheet 2.

	Cylinder No. 2 Midbay Interior										
Pressure	Hoop 23	Axial 24	Hoop 25	Hoop 26	Hoop 27	Hoop 28	Axial 29	Hoop 30	Hoop 31	Hoop 32	Hoop 33
0	0	0	0	0	0	0	0	0	0	0	0
1000	-339	-105	-368	-383	-344	-321	-93	-357	-386	-356	-330
2000	-684	-218	-711	-732	-689	-663	-205	-701	-733	-700	-673
3000	-1032	-331	-1062	-1087	-1042	-1009	-320	-1053	-1088	-1051	-1021
4000	-1376	-444	-1405	-1437	-1387	-1347	-434	-1396	-1437	-1394	-1362
5000	-1723	-558	-1755	-1793	-1737	-1690	-549	-1745	-1793	-1742	-1707
6000	-2068	-673	-2103	-2151	-2085	-2027	-667	-2090	-2151	-2088	-2049
7000	-2413	-793	-2452	-2514	-2432	-2371	-788	-2436	-2516	-2434	-2386
8000	-2750	-917	-2804	-2887	-2776	-2703	-918	-2779	-2893	-2779	-2710
8500	-2901	-976	-2982	-3081	-2941	-2846	-983	-2943	-3091	-2952	-2855
8600	-2984	-1045	-3021	-3127	-2976	-2925	-1052	-2977	-3138	-2991	-2883
8700	-2957	-1004	-3058	-3170	-3008	-2899	-1014	-3009	-3182	-3027	-2907
8800	-2985	-1021	-3098	-3216	-3040	-2901	-1032	-3041	-3229	-3064	-2931
8900	-3014	-1055	-3142	-3267	-3076	-2918	-1054	-3078	-3283	-3106	-2957
9000	-3043	-1089	-3184	-3317	-3108	-2935	-1076	-3109	-3335	-3146	-2977

Table 2. Strains recorded during pressure testing of case 3 test assembly, Sheet 3.

	<---------- Cylinder No. 1 & 2 Midbay Exterior ---------->							
Pressure	Hoop 34	Axial 35	Hoop 36	Axial 37	Hoop 38	Axial 39	Hoop 40	Axial 41
0	0	0	0	0	0	0	0	0
1000	-322	-93	-319	-99	-337	-102	-361	-83
2000	-634	-198	-630	-204	-646	-205	-675	-193
3000	-953	-305	-947	-308	-966	-314	-999	-305
4000	-1265	-410	-1258	-413	-1280	-421	-1317	-414
5000	-1585	-517	-1573	-517	-1600	-531	-1642	-527
6000	-1905	-627	-1890	-625	-1918	-642	-1968	-642
7000	-2230	-742	-2213	-738	-2240	-757	-2301	-760
8000	-2562	-866	-2548	-861	-2570	-877	-2649	-889
8500	-2732	-926	-2718	-923	-2730	-937	-2826	-960
8600	-2772	-946	-2813	-939	-2814	-950	-2866	-979
8700	-2809	-958	-2839	-956	-2874	-968	-2909	-996
8800	-2848	-976	-2841	-974	-2844	-985	-2954	-1015
8900	-2893	-998	-2891	-994	-2887	-1005	-3006	-1037
9000	-2945	-1033	-2941	-1014	-2930	-1025	-3058	-1059

Table 2. Strains recorded during pressure testing of case 3 test assembly, Sheet 4.

		<---------- Joint Stiffener, Internal Flange Center ----------									
Pressure	Hoop 1	Axial 2	Hoop 3	Hoop 4	Hoop 5	Hoop 6	Axial 7	Hoop 8	Hoop 9	Hoop 10	Hoop 11
0	0	0	0	0	0	0	0	0	0	0	0
1000	-176	201	-224	-226	-174	-143	204	-197	-255	-215	-170
2000	-369	431	-436	-443	-384	-330	447	-409	-486	-426	-372
3000	-570	674	-658	-670	-604	-524	698	-625	-720	-644	-579
4000	-765	908	-875	-897	-815	-708	935	-830	-946	-859	-775
5000	-962	1146	-1097	-1131	-1024	-886	1162	-1027	-1171	-1081	-964
6000	-1154	1380	-1323	-1377	-1239	-891	1383	-1232	-1416	-1302	-1139
7000	-1339	1610	-1568	-1655	-1460	-1060	1591	-1441	-1691	-1531	-1302
8000	-1493	1807	-1846	-1986	-1668	-1149	1752	-1644	-2026	-1788	-1421
8500	-1536	1873	-2014	-2203	-1757	-1141	1776	-1733	-2248	-1938	-1426
8600	-1532	1876	-2059	-2267	-1775	-1124	1763	-1746	-2312	-1977	-1410
8700	-1527	1876	-2104	-2332	-1791	-1093	1748	-1760	-2377	-2017	-1392
8800	-1521	1876	-2155	-2405	-1806	-1057	1728	-1775	-2452	-2061	-1368
8900	-1510	1871	-2217	-2493	-1820	-1026	1700	-1791	-2543	-2114	-1335
9000	-1495	1862	-2278	-2584	-1830	-969	1665	-1805	-2637	-2167	-1295

Table 2. Strains recorded during pressure testing of case 3 test assembly, Sheet 5.

	|<---------- Joint Stiffener, Internal Flange Edges ---------->							
Pressure	Hoop 42	Axial 43	Hoop 44	Axial 45	Hoop 46	Axial 47	Hoop 48	Axial 49
0	0	0	0	0	0	0	0	0
1000	-211	66	-90	32	-142	55	-101	36
2000	-415	134	-220	80	-312	125	-242	90
3000	-610	200	-363	134	-486	194	-387	147
4000	-795	263	-500	184	-649	260	-529	202
5000	-975	326	-638	236	-668	317	-682	262
6000	-1144	385	-776	286	-807	371	-822	317
7000	-1291	437	-911	337	-902	422	-945	365
8000	-1393	476	-1014	374	-980	458	-1017	395
8500	-1401	482	-1029	380	-967	456	-1001	392
8600	-1384	478	-1021	378	-941	448	-984	386
8700	-1367	473	-1012	374	-916	441	-963	379
8800	-1348	468	-999	370	-889	431	-936	371
8900	-1323	461	-980	363	-850	418	-901	359
9000	-1294	453	-956	354	-807	404	-858	344

Table 2. Strains recorded during pressure testing of case 3 test assembly, Sheet 6.

Joint Stiffener, External Flange

	<---------- Center ---------->				<---------- Edges ---------->							
Pressure	Hoop 50	Axial 51	Hoop 52	Axial 53	Hoop 54	Axial 55	Hoop 56	Axial 57	Hoop 58	Axial 59	Hoop 60	Axial 61
0	0	0	0	0	0	0	0	0	0	0	0	0
1000	-139	38	-188	138	-241	-1	-236	0	-238	-9	-224	34
2000	-277	73	-347	221	-454	-1	-439	0	-454	-10	-419	70
3000	-425	130	-512	310	-671	0	-645	0	-675	-5	-622	109
4000	-571	185	-668	414	-887	1	-842	0	-890	5	-824	143
5000	-727	255	-815	539	-1111	3	-1042	0	-1105	34	-1038	170
6000	-888	352	-972	659	-1333	6	-1243	0	-1326	66	-1257	205
7000	-1058	485	-1144	780	-1563	10	-1450	0	-1565	107	-1490	249
8000	-1242	602	-1351	903	-1813	16	-1683	0	-1834	154	-1751	307
8500	-1349	669	-1483	973	-1958	21	-1817	0	-1997	190	-1910	342
8600	-1381	704	-1517	1008	-2000	23	-1851	0	-2044	209	-1957	351
8700	-1410	735	-1555	1039	-2040	25	-1884	0	-2089	226	-2001	362
8800	-1443	762	-1599	1070	-2081	27	-1920	0	-2140	243	-2050	375
8900	-1482	788	-1652	1101	-2128	28	-1965	0	-2198	262	-2108	390
9000	-1519	810	-1708	1128	-2175	30	-2008	0	-2257	280	-2167	405

APPENDIX A: NRaD EPOXY BONDING PROCEDURES FOR METALLIC JOINT RINGS USED IN CERAMIC UNDERWATER PRESSURE HOUSINGS

FIGURE

A-1. Axial clearance spacer for epoxy bonding.

APPENDIX A: NRaD EPOXY BONDING PROCEDURES FOR METALLIC JOINT RINGS USED IN CERAMIC UNDERWATER PRESSURE HOUSINGS

1. Wipe bond surfaces of the ceramic hull component with a clean cloth using methyl ethyl ketone (MEK) until cloth shows no further discoloration.
2. Wipe the interior surfaces of the metallic joint ring with a clean cloth using MEK until cloth shows no further discoloration.
3. For titanium joint rings: Passivate the interior surfaces of the joint ring by applying a layer of PASA JELL 107 and allowing it to etch the titanium surfaces for 30 minutes. Thoroughly rinse off interior of the metallic end cap and allow surfaces of titanium to air dry. Air drying can be accelerated with a forced-air heater.
4. Mix 100 parts CIBA Geigy 6010 epoxy resin with 70 parts CIBA Geigy 283 hardener. Use a vacuum chamber to remove air bubbles introduced to epoxy during mixing.
5. Pour a .12-inch-thick layer of the epoxy mixture into the interior of the cylinder end cap. Place axial clearance spacer on top of the epoxy layer and press it down through the epoxy mixture to the bottom of the joint ring using a clean tool. A typical NRaD spacer giving an axial clearance of .010 of an inch for a 12-inch OD ceramic cylinder (.412-inch-thick wall) or hemisphere is shown in figure A-1.
6. Pour additional epoxy mixture into the bottom of the joint ring until the epoxy fills at least half the depth of the interior of the joint ring.
7. Lower the end of the ceramic hull component into the joint ring interior (partially filled with the epoxy mixture) keeping the ceramic hull centered within the joint ring. Allow the hull to settle evenly into the joint ring interior until the hull comes to rest on the spacer at the bottom of the joint ring interior. Additional weight can be placed on top of ceramic hull component to help it settle evenly through the epoxy mixture. Care should be taken to assure the hull remains centered with the joint ring and the center line of the hull remains perpendicular to the working surface throughout the bonding procedure.
8. Leave the bonded assembly and any settling weight used undisturbed for at least 24 hours to allow the epoxy mixture to begin to cure. Once this initial 24-hour period has passed, completely remove any excess epoxy mixture remaining on the exterior surface of the joint ring that extruded out during assembly. Application of a thin coat of silicone-based mold release to the exterior surfaces of the joint ring prior to bonding the hull may be used to aid in the subsequent cleanup. Care should be taken to not allow mold release on or near any bonding surfaces on the hull or joint ring.
9. After the epoxy has cured, apply a bead of RTV or other suitable sealant to externally exposed portions of the epoxy bond between the metallic joint ring and outer surface of the ceramic hull component.

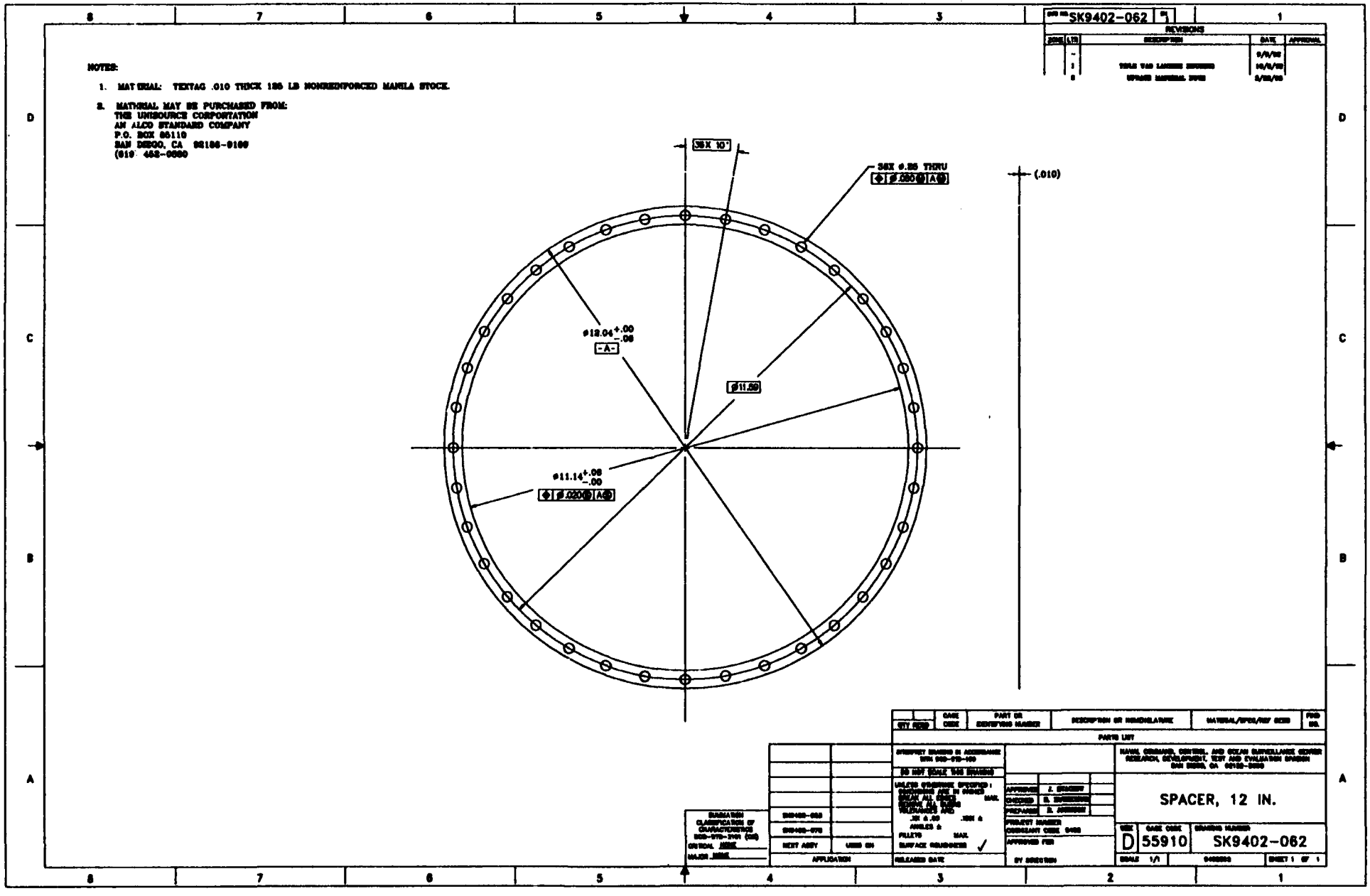

Figure A-1. Axial clearance spacer for epoxy bonding.

APPENDIX B: BOSOR4 BUCKLING ANALYSIS INPUT FILE FOR CASE 4 TEST ASSEMBLY

FIGURES

```
CASE 4:  SCALE MODEL HOUSING
         1       $ INDIC = analysis type indicator
         1       $ NPRT = output options (1=minimum, 2=medium, 3=maximum)
         0       $ ISTRES= output control (0=resultants, 1=sigma, 2=epsilon)
        15       $ NSEG  = number of shell segments (less than 95)
       H         $
       H         $ SEGMENT NUMBER    1    1    1    1    1    1    1    1
       H         $ NODAL POINT DISTRIBUTION FOLLOWS...
        10       $ NMESH = number of node points (5 = min.; 98 = max.)( 1)
         3       $ NTYPEH= control integer (1 or 3) for nodal point spacing
       H         $ REFERENCE SURFACE GEOMETRY FOLLOWS...
         2       $ NSHAPE= indicator (1,2 or 4) for geometry of meridian
        0.       $ R1      = radius at beginning of segment (see p. 66)
        0.       $ Z1      = global axial coordinate at beginning of segment
  5.353000       $ R2      = radius at end of segment
  3.306000       $ Z2      = global axial coordinate at end of segment
        0.       $ RC      = radius from axis of rev. to center of curvature
  5.988000       $ ZC      = axial coordinate of center of curvature
        -1       $ SROT=indicator for direction of increasing arc (-1. or +1.)
       H         $ IMPERFECTION SHAPE FOLLOWS...
         0       $ IMP   = indicator for imperfection (0=none, 1=some)
       H         $ REFERENCE SURFACE LOCATION RELATIVE TO WALL
         3       $ NTYPEZ= control (1 or 3) for reference surface location
  0.2710000      $ ZVAL  = distance from leftmost surf. to reference surf.
       N         $ Do you want to print out r(s), r'(s), etc. for this segment?
       H         $ DISCRETE RING INPUT FOLLOWS...
         0       $ NRINGS= number (max=20) of discrete rings in this segment
         0       $ K=elastic foundation modulus (e.g. lb/in**3)in this seg.
       H         $ LINE LOAD INPUT FOLLOWS...
         0       $ LINTYP= indicator (0, 1, 2 or 3) for type of line loads
       H         $ DISTRIBUTED LOAD INPUT FOLLOWS...
         1       $ IDISAB= indicator (0, 1, 2 or 3) for load set A and B
       H         $ SURFACE LOAD INPUT FOR LOAD SET "A" FOLLOWS
         1       $ NLTYPE=control (0,1,2,3) for type of surface loading
         2       $ NPSTAT= number of meridional callouts for surface loading
         0       $ NLOAD(1)=indicator for meridional traction (0=none, 1=some)
         0       $ NLOAD(2)=indicator for circumferential traction
         1       $ NLOAD(3)=indicator for normal pressure     (0=none, 1=some)
        -1       $ PN(i)   = normal pressure (p.74) at ith callout, PN( 1)
        -1       $ PN(i)   = normal pressure (p.74) at ith callout, PN( 2)
         2       $ NTYPE = control for meaning of loading callout (2=z, 3=r)
        0.       $ Z(I)  = axial coordinate of Ith loading callout, z( 1)
  3.306000       $ Z(I)  = axial coordinate of Ith loading callout, z( 2)
       H         $ SHELL WALL CONSTRUCTION FOLLOWS...
         2       $ NWALL=index (1, 2, 4, 5, 6, 7, 8) for wall construction
0.4400000E+08    $ E     = Young's modulus for skin
  0.2100000      $ U     = Poisson's ratio for skin
        0.       $ SM =mass density of skin (e.g. alum.=.00025 lb-sec**2/in**4)
        0.       $ ALPHA = coefficient of thermal expansion
         0       $ NRS   = control (0 or 1) for addition of smeared stiffeners
         1       $ NSUR    = control for thickness input (0 or 1 or -1)
       N         $ Do you want to print out the C(i,j) at meridional stations?
       N         $ Do you want to print out distributed loads along meridian?
       H         $
       H         $ SEGMENT NUMBER    2    2    2    2    2    2    2    2
       H         $ NODAL POINT DISTRIBUTION FOLLOWS...
         5       $ NMESH = number of node points (5 = min.; 98 = max.)( 2)
         3       $ NTYPEH= control integer (1 or 3) for nodal point spacing
       H         $ REFERENCE SURFACE GEOMETRY FOLLOWS...
         1       $ NSHAPE= indicator (1,2 or 4) for geometry of meridian
  5.353000       $ R1      = radius at beginning of segment (see p. 66)
  3.306000       $ Z1      = global axial coordinate at beginning of segment
  6.024000       $ R2      = radius at end of segment
  4.783000       $ Z2      = global axial coordinate at end of segment
       H         $ IMPERFECTION SHAPE FOLLOWS...
         0       $ IMP   = indicator for imperfection (0=none, 1=some)
```

B-1. Scale model housing data for case 4, Sheet 1.

```
     H          $ REFERENCE SURFACE LOCATION RELATIVE TO WALL
        1       $ NTYPEZ= control (1 or 3) for reference surface location
        2       $ NZVALU= number of meridional callouts for ref. surf.
        2       $ NTYPE = control for meaning of callout (2=z, 3=r)
 3.306000       $ Z(I)  = axial coordinate of Ith callout, z( 1)
 4.783000       $ Z(I)  = axial coordinate of Ith callout, z( 2)
0.2710000       $ ZVAL  = distance from leftmost surf. to ref. surf.,ZVAL( 1)
0.4340000       $ ZVAL  = distance from leftmost surf. to ref. surf.,ZVAL( 2)
     N          $ Do you want to print out r(s), r'(s), etc. for this segment?
     H          $ DISCRETE RING INPUT FOLLOWS...
        0       $ NRINGS= number (max=20) of discrete rings in this segment
        0       $ K=elastic foundation modulus (e.g. lb/in**3)in this seg.
     H          $ LINE LOAD INPUT FOLLOWS...
        0       $ LINTYP= indicator (0, 1, 2 or 3) for type of line loads
     H          $ DISTRIBUTED LOAD INPUT FOLLOWS...
        1       $ IDISAB= indicator (0, 1, 2 or 3) for load set A and B
     H          $ SURFACE LOAD INPUT FOR LOAD SET "A" FOLLOWS
        1       $ NLTYPE=control (0,1,2,3) for type of surface loading
        2       $ NPSTAT= number of meridional callouts for surface loading
        0       $ NLOAD(1)=indicator for meridional traction (0=none, 1=some)
        0       $ NLOAD(2)=indicator for circumferential traction
        1       $ NLOAD(3)=indicator for normal pressure     (0=none, 1=some)
       -1       $ PN(i)   = normal pressure (p.74) at ith callout, PN( 1)
       -1       $ PN(i)   = normal pressure (p.74) at ith callout, PN( 2)
        2       $ NTYPE = control for meaning of loading callout (2=z, 3=r)
 3.306000       $ Z(I)  = axial coordinate of Ith loading callout, z( 1)
 4.783000       $ Z(I)  = axial coordinate of Ith loading callout, z( 2)
     H          $ SHELL WALL CONSTRUCTION FOLLOWS...
        2       $ NWALL=index (1, 2, 4, 5, 6, 7, 8) for wall construction
0.4400000E+08   $ E     = Young's modulus for skin
0.2100000       $ U     = Poisson's ratio for skin
        0.      $ SM =mass density of skin (e.g. alum.=.00025 lb-sec**2/in**4)
        0.      $ ALPHA = coefficient of thermal expansion
        0       $ NRS   = control (0 or 1) for addition of smeared stiffeners
        1       $ NSUR    = control for thickness input (0 or 1 or -1)
     N          $ Do you want to print out the C(i,j) at meridional stations?
     N          $ Do you want to print out distributed loads along meridian?
     H          $
     H          $ SEGMENT NUMBER    3    3    3    3    3    3    3    3
     H          $ NODAL POINT DISTRIBUTION FOLLOWS...
        5       $ NMESH = number of node points (5 = min.; 98 = max.)( 3)
        3       $ NTYPEH= control integer (1 or 3) for nodal point spacing
     H          $ REFERENCE SURFACE GEOMETRY FOLLOWS...
        1       $ NSHAPE= indicator (1,2 or 4) for geometry of meridian
 6.024000       $ R1      = radius at beginning of segment (see p. 66)
 4.783000       $ Z1      = global axial coordinate at beginning of segment
 6.024000       $ R2      = radius at end of segment
 5.988000       $ Z2      = global axial coordinate at end of segment
     H          $ IMPERFECTION SHAPE FOLLOWS...
        0       $ IMP   = indicator for imperfection (0=none, 1=some)
     H          $ REFERENCE SURFACE LOCATION RELATIVE TO WALL
        3       $ NTYPEZ= control (1 or 3) for reference surface location
0.4340000       $ ZVAL  = distance from leftmost surf. to reference surf.
     N          $ Do you want to print out r(s), r'(s), etc. for this segment?
     H          $ DISCRETE RING INPUT FOLLOWS...
        0       $ NRINGS= number (max=20) of discrete rings in this segment
        0       $ K=elastic foundation modulus (e.g. lb/in**3)in this seg.
     H          $ LINE LOAD INPUT FOLLOWS...
        0       $ LINTYP= indicator (0, 1, 2 or 3) for type of line loads
     H          $ DISTRIBUTED LOAD INPUT FOLLOWS...
        1       $ IDISAB= indicator (0, 1, 2 or 3) for load set A and B
     H          $ SURFACE LOAD INPUT FOR LOAD SET "A" FOLLOWS
        1       $ NLTYPE=control (0,1,2,3) for type of surface loading
        2       $ NPSTAT= number of meridional callouts for surface loading
        0       $ NLOAD(1)=indicator for meridional traction (0=none, 1=some)
        0       $ NLOAD(2)=indicator for circumferential traction
```

B-1. Scale model housing data for case 4, Sheet 2.

```
      1       $ NLOAD(3)=indicator for normal pressure     (0=none, 1=some)
     -1       $ PN(i)   = normal pressure (p.74) at ith callout, PN( 1)
     -1       $ PN(i)   = normal pressure (p.74) at ith callout, PN( 2)
      2       $ NTYPE = control for meaning of loading callout (2=z, 3=r)
 4.783000     $ Z(I)  = axial coordinate of Ith loading callout, z( 1)
 5.988000     $ Z(I)  = axial coordinate of Ith loading callout, z( 2)
    H         $ SHELL WALL CONSTRUCTION FOLLOWS...
      2       $ NWALL=index (1, 2, 4, 5, 6, 7, 8) for wall construction
0.4400000E+08 $ E     = Young's modulus for skin
0.2100000     $ U     = Poisson's ratio for skin
      0.      $ SM =mass density of skin (e.g. alum.=.00025 lb-sec**2/in**4)
      0.      $ ALPHA = coefficient of thermal expansion
      0       $ NRS  = control (0 or 1) for addition of smeared stiffeners
      1       $ NSUR   = control for thickness input (0 or 1 or -1)
    N         $ Do you want to print out the C(i,j) at meridional stations?
    N         $ Do you want to print out distributed loads along meridian?
    H         $
    H         $ SEGMENT NUMBER    4    4    4    4    4    4    4    4
    H         $ NODAL POINT DISTRIBUTION FOLLOWS...
     10       $ NMESH = number of node points (5 = min.; 98 = max.)( 4)
      3       $ NTYPEH= control integer (1 or 3) for nodal point spacing
    H         $ REFERENCE SURFACE GEOMETRY FOLLOWS...
      1       $ NSHAPE= indicator (1,2 or 4) for geometry of meridian
 5.807000     $ R1      = radius at beginning of segment (see p. 66)
 5.988000     $ Z1      = global axial coordinate at beginning of segment
 5.807000     $ R2      = radius at end of segment
 21.57300     $ Z2      = global axial coordinate at end of segment
    H         $ IMPERFECTION SHAPE FOLLOWS...
      0       $ IMP   = indicator for imperfection (0=none, 1=some)
    H         $ REFERENCE SURFACE LOCATION RELATIVE TO WALL
      3       $ NTYPEZ= control (1 or 3) for reference surface location
0.2170000     $ ZVAL  = distance from leftmost surf. to reference surf.
    N         $ Do you want to print out r(s), r'(s), etc. for this segment?
    H         $ DISCRETE RING INPUT FOLLOWS...
      0       $ NRINGS= number (max=20) of discrete rings in this segment
      0       $ K=elastic foundation modulus (e.g. lb/in**3)in this seg.
    H         $ LINE LOAD INPUT FOLLOWS...
      0       $ LINTYP= indicator (0, 1, 2 or 3) for type of line loads
    H         $ DISTRIBUTED LOAD INPUT FOLLOWS...
      1       $ IDISAB= indicator (0, 1, 2 or 3) for load set A and B
    H         $ SURFACE LOAD INPUT FOR LOAD SET "A" FOLLOWS
      1       $ NLTYPE=control (0,1,2,3) for type of surface loading
      2       $ NPSTAT= number of meridional callouts for surface loading
      0       $ NLOAD(1)=indicator for meridional traction (0=none, 1=some)
      0       $ NLOAD(2)=indicator for circumferential traction
      1       $ NLOAD(3)=indicator for normal pressure     (0=none, 1=some)
     -1       $ PN(i)   = normal pressure (p.74) at ith callout, PN( 1)
     -1       $ PN(i)   = normal pressure (p.74) at ith callout, PN( 2)
      2       $ NTYPE = control for meaning of loading callout (2=z, 3=r)
 5.988000     $ Z(I)  = axial coordinate of Ith loading callout, z( 1)
 21.57300     $ Z(I)  = axial coordinate of Ith loading callout, z( 2)
    H         $ SHELL WALL CONSTRUCTION FOLLOWS...
      2       $ NWALL=index (1, 2, 4, 5, 6, 7, 8) for wall construction
0.4400000E+08 $ E     = Young's modulus for skin
0.2100000     $ U     = Poisson's ratio for skin
      0.      $ SM =mass density of skin (e.g. alum.=.00025 lb-sec**2/in**4)
      0.      $ ALPHA = coefficient of thermal expansion
      0       $ NRS  = control (0 or 1) for addition of smeared stiffeners
      0       $ NSUR   = control for thickness input (0 or 1 or -1)
    Y         $ Do you want to print out ref. surf. location and thickness?
    N         $ Do you want to print out the C(i,j) at meridional stations?
    N         $ Do you want to print out distributed loads along meridian?
    H         $
    H         $
    H         $ SEGMENT NUMBER    5    5    5    5    5    5    5    5
    H         $ NODAL POINT DISTRIBUTION FOLLOWS...
```

B-1. Scale model housing data for case 4, Sheet 3.

```
      13        $ NMESH = number of node points (5 = min.; 98 = max.)( 5)
       3        $ NTYPEH= control integer (1 or 3) for nodal point spacing
       H        $ REFERENCE SURFACE GEOMETRY FOLLOWS...
       1        $ NSHAPE= indicator (1,2 or 4) for geometry of meridian
 5.804000       $ R1     = radius at beginning of segment (see p. 66)
 21.57300       $ Z1     = global axial coordinate at beginning of segment
 5.804000       $ R2     = radius at end of segment
 21.81300       $ Z2     = global axial coordinate at end of segment
       H        $ IMPERFECTION SHAPE FOLLOWS...
       0        $ IMP    = indicator for imperfection (0=none, 1=some)
       H        $ REFERENCE SURFACE LOCATION RELATIVE TO WALL
       3        $ NTYPEZ= control (1 or 3) for reference surface location
0.2340000       $ ZVAL   = distance from leftmost surf. to reference surf.
       N        $ Do you want to print out r(s), r'(s), etc. for this segment?
       H        $ DISCRETE RING INPUT FOLLOWS...
       0        $ NRINGS= number (max=20) of discrete rings in this segment
       0        $ K=elastic foundation modulus (e.g. lb/in**3) in this seg.
       H        $ LINE LOAD INPUT FOLLOWS...
       0        $ LINTYP= indicator (0, 1, 2 or 3) for type of line loads
       H        $ DISTRIBUTED LOAD INPUT FOLLOWS...
       1        $ IDISAB= indicator (0, 1, 2 or 3) for load set A and B
       H        $ SURFACE LOAD INPUT FOR LOAD SET "A" FOLLOWS
       1        $ NLTYPE=control (0,1,2,3) for type of surface loading
       2        $ NPSTAT= number of meridional callouts for surface loading
       0        $ NLOAD(1)=indicator for meridional traction (0=none, 1=some)
       0        $ NLOAD(2)=indicator for circumferential traction
       1        $ NLOAD(3)=indicator for normal pressure     (0=none, 1=some)
      -1        $ PN(i)   = normal pressure (p.74) at ith callout, PN( 1)
      -1        $ PN(i)   = normal pressure (p.74) at ith callout, PN( 2)
       2        $ NTYPE = control for meaning of loading callout (2=z, 3=r)
 21.57300       $ Z(I)   = axial coordinate of Ith loading callout, z( 1)
 21.81300       $ Z(I)   = axial coordinate of Ith loading callout, z( 2)
       H        $ SHELL WALL CONSTRUCTION FOLLOWS...
       2        $ NWALL=index (1, 2, 4, 5, 6, 7, 8) for wall construction
0.1640000E+08   $ E      = Young's modulus for skin
0.3100000       $ U      = Poisson's ratio for skin
       0.       $ SM =mass density of skin (e.g. alum.=.00025 lb-sec**2/in**4)
       0.       $ ALPHA = coefficient of thermal expansion
       0        $ NRS   = control (0 or 1) for addition of smeared stiffeners
       0        $ NSUR   = control for thickness input (0 or 1 or -1)
       Y        $ Do you want to print out ref. surf. location and thickness?
       N        $ Do you want to print out the C(i,j) at meridional stations?
       N        $ Do you want to print out distributed loads along meridian?
       H        $
       H        $ SEGMENT NUMBER    6    6    6    6    6    6    6    6
       H        $ NODAL POINT DISTRIBUTION FOLLOWS...
      13        $ NMESH = number of node points (5 = min.; 98 = max.)( 6)
       3        $ NTYPEH= control integer (1 or 3) for nodal point spacing
       H        $ REFERENCE SURFACE GEOMETRY FOLLOWS...
       1        $ NSHAPE= indicator (1,2 or 4) for geometry of meridian
 5.510000       $ R1     = radius at beginning of segment (see p. 66)
 20.61000       $ Z1     = global axial coordinate at beginning of segment
 5.510000       $ R2     = radius at end of segment
 22.77600       $ Z2     = global axial coordinate at end of segment
       H        $ IMPERFECTION SHAPE FOLLOWS...
       0        $ IMP    = indicator for imperfection (0=none, 1=some)
       H        $ REFERENCE SURFACE LOCATION RELATIVE TO WALL
       1        $ NTYPEZ= control (1 or 3) for reference surface location
       4        $ NZVALU= number of meridional callouts for ref. surf.
       2        $ NTYPE = control for meaning of callout (2=z, 3=r)
 20.61000       $ Z(I)   = axial coordinate of Ith callout, z( 1)
 21.57300       $ Z(I)   = axial coordinate of Ith callout, z( 2)
 21.81300       $ Z(I)   = axial coordinate of Ith callout, z( 3)
 22.77600       $ Z(I)   = axial coordinate of Ith callout, z( 4)
       0.       $ ZVAL   = distance from leftmost surf. to ref. surf.,ZVAL( 1)
0.6000000E-01   $ ZVAL   = distance from leftmost surf. to ref. surf.,ZVAL( 2)
```

B-1. Scale model housing data for case 4, Sheet 4.

```
0.6000000E-01 $ ZVAL  = distance from leftmost surf. to ref. surf.,ZVAL( 3)
       0.     $ ZVAL  = distance from leftmost surf. to ref. surf.,ZVAL( 4)
    N         $ Do you want to print out r(s), r'(s), etc. for this segment?
    H         $ DISCRETE RING INPUT FOLLOWS...
       0      $ NRINGS= number (max=20) of discrete rings in this segment
       0      $ K=elastic foundation modulus (e.g. lb/in**3)in this seg.
    H         $ LINE LOAD INPUT FOLLOWS...
       0      $ LINTYP= indicator (0, 1, 2 or 3) for type of line loads
    H         $ DISTRIBUTED LOAD INPUT FOLLOWS...
       0      $ IDISAB= indicator (0, 1, 2 or 3) for load set A and B
    H         $ SHELL WALL CONSTRUCTION FOLLOWS...
       2      $ NWALL=index (1, 2, 4, 5, 6, 7, 8) for wall construction
0.1640000E+08 $ E     = Young's modulus for skin
0.3100000     $ U     = Poisson's ratio for skin
       0.     $ SM =mass density of skin (e.g. alum.=.00025 lb-sec**2/in**4)
       0.     $ ALPHA = coefficient of thermal expansion
       0      $ NRS  = control (0 or 1) for addition of smeared stiffeners
      -1      $ NSUR   = control for thickness input (0 or 1 or -1)
       1      $ NTYPET= index (1 or 3) for type of input for thickness
       4      $ NTVALU= number of callouts along segment for thickness
       2      $ NTYPE = control for meaning of thickness callout (2=z, 3=r)
 20.61000     $ Z(I)  = axial coordinate of Ith thickness callout, z( 1)
 21.57300     $ Z(I)  = axial coordinate of Ith thickness callout, z( 2)
 21.81300     $ Z(I)  = axial coordinate of Ith thickness callout, z( 3)
 22.77600     $ Z(I)  = axial coordinate of Ith thickness callout, z( 4)
0.6000000E-01 $ TVAL(i) = thickness at Ith callout, TVAL( 1)
0.1200000     $ TVAL(i) = thickness at Ith callout, TVAL( 2)
0.1200000     $ TVAL(i) = thickness at Ith callout, TVAL( 3)
0.6000000E-01 $ TVAL(i) = thickness at Ith callout, TVAL( 4)
    Y         $ Do you want to print out ref. surf. location and thickness?
    N         $ Do you want to print out the C(i,j) at meridional stations?
    N         $ Do you want to print out distributed loads along meridian?
    H         $
    H         $ SEGMENT NUMBER    7    7    7    7    7    7    7    7
    H         $ NODAL POINT DISTRIBUTION FOLLOWS...
       9      $ NMESH = number of node points (5 = min.; 98 = max.)( 7)
       3      $ NTYPEH= control integer (1 or 3) for nodal point spacing
    H         $ REFERENCE SURFACE GEOMETRY FOLLOWS...
       1      $ NSHAPE= indicator (1,2 or 4) for geometry of meridian
 5.450000     $ R1    = radius at beginning of segment (see p. 66)
 21.69300     $ Z1    = global axial coordinate at beginning of segment
 5.300000     $ R2    = radius at end of segment
 21.69300     $ Z2    = global axial coordinate at end of segment
    H         $ IMPERFECTION SHAPE FOLLOWS...
       0      $ IMP   = indicator for imperfection (0=none, 1=some)
    H         $ REFERENCE SURFACE LOCATION RELATIVE TO WALL
       3      $ NTYPEZ= control (1 or 3) for reference surface location
0.1200000     $ ZVAL  = distance from leftmost surf. to reference surf.
    N         $ Do you want to print out r(s), r'(s), etc. for this segment?
    H         $ DISCRETE RING INPUT FOLLOWS...
       0      $ NRINGS= number (max=20) of discrete rings in this segment
       0      $ K=elastic foundation modulus (e.g. lb/in**3)in this seg.
    H         $ LINE LOAD INPUT FOLLOWS...
       0      $ LINTYP= indicator (0, 1, 2 or 3) for type of line loads
    H         $ DISTRIBUTED LOAD INPUT FOLLOWS...
       0      $ IDISAB= indicator (0, 1, 2 or 3) for load set A and B
    H         $ SHELL WALL CONSTRUCTION FOLLOWS...
       2      $ NWALL=index (1, 2, 4, 5, 6, 7, 8) for wall construction
0.1640000E+08 $ E     = Young's modulus for skin
0.3100000     $ U     = Poisson's ratio for skin
       0.     $ SM =mass density of skin (e.g. alum.=.00025 lb-sec**2/in**4)
       0.     $ ALPHA = coefficient of thermal expansion
       0      $ NRS  = control (0 or 1) for addition of smeared stiffeners
       0      $ NSUR   = control for thickness input (0 or 1 or -1)
    Y         $ Do you want to print out ref. surf. location and thickness?
    N         $ Do you want to print out the C(i,j) at meridional stations?
```

B-1. Scale model housing data for case 4, Sheet 5.

```
    N          $ Do you want to print out distributed loads along meridian?
    H          $
    H          $ SEGMENT NUMBER    8    8    8    8    8    8    8    8
    H          $ NODAL POINT DISTRIBUTION FOLLOWS...
   13          $ NMESH = number of node points (5 = min.; 98 = max.)( 8)
    3          $ NTYPEH= control integer (1 or 3) for nodal point spacing
    H          $ REFERENCE SURFACE GEOMETRY FOLLOWS...
    1          $ NSHAPE= indicator (1,2 or 4) for geometry of meridian
 5.105000      $ R1     = radius at beginning of segment (see p. 66)
 20.61000      $ Z1     = global axial coordinate at beginning of segment
 5.105000      $ R2     = radius at end of segment
 22.77600      $ Z2     = global axial coordinate at end of segment
    H          $ IMPERFECTION SHAPE FOLLOWS...
    0          $ IMP    = indicator for imperfection (0=none, 1=some)
    H          $ REFERENCE SURFACE LOCATION RELATIVE TO WALL
    3          $ NTYPEZ= control (1 or 3) for reference surface location
0.1650000      $ ZVAL   = distance from leftmost surf. to reference surf.
    N          $ Do you want to print out r(s), r'(s), etc. for this segment?
    H          $ DISCRETE RING INPUT FOLLOWS...
    0          $ NRINGS= number (max=20) of discrete rings in this segment
    0          $ K=elastic foundation modulus (e.g. lb/in**3)in this seg.
    H          $ LINE LOAD INPUT FOLLOWS...
    0          $ LINTYP= indicator (0, 1, 2 or 3) for type of line loads
    H          $ DISTRIBUTED LOAD INPUT FOLLOWS...
    0          $ IDISAB= indicator (0, 1, 2 or 3) for load set A and B
    H          $ SHELL WALL CONSTRUCTION FOLLOWS...
    2          $ NWALL=index (1, 2, 4, 5, 6, 7, 8) for wall construction
0.1640000E+08  $ E      = Young's modulus for skin
0.3100000      $ U      = Poisson's ratio for skin
    0.         $ SM =mass density of skin (e.g. alum.=.00025 lb-sec**2/in**4)
    0.         $ ALPHA = coefficient of thermal expansion
    0          $ NRS    = control (0 or 1) for addition of smeared stiffeners
   -1          $ NSUR   = control for thickness input (0 or 1 or -1)
    1          $ NTYPET= index (1 or 3) for type of input for thickness
    4          $ NTVALU= number of callouts along segment for thickness
    2          $ NTYPE = control for meaning of thickness callout (2=z, 3=r)
 20.61000      $ Z(I)   = axial coordinate of Ith thickness callout, z( 1)
 21.57300      $ Z(I)   = axial coordinate of Ith thickness callout, z( 2)
 21.81300      $ Z(I)   = axial coordinate of Ith thickness callout, z( 3)
 22.77600      $ Z(I)   = axial coordinate of Ith thickness callout, z( 4)
0.3300000      $ TVAL(i) = thickness at Ith callout, TVAL( 1)
0.3600000      $ TVAL(i) = thickness at Ith callout, TVAL( 2)
0.3600000      $ TVAL(i) = thickness at Ith callout, TVAL( 3)
0.3300000      $ TVAL(i) = thickness at Ith callout, TVAL( 4)
    Y          $ Do you want to print out ref. surf. location and thickness?
    N          $ Do you want to print out the C(i,j) at meridional stations?
    N          $ Do you want to print out distributed loads along meridian?
    H          $
    H          $ SEGMENT NUMBER    9    9    9    9    9    9    9    9
    H          $ NODAL POINT DISTRIBUTION FOLLOWS...
    5          $ NMESH = number of node points (5 = min.; 98 = max.)( 9)
    3          $ NTYPEH= control integer (1 or 3) for nodal point spacing
    H          $ REFERENCE SURFACE GEOMETRY FOLLOWS...
    1          $ NSHAPE= indicator (1,2 or 4) for geometry of meridian
 6.088000      $ R1     = radius at beginning of segment (see p. 66)
 20.61000      $ Z1     = global axial coordinate at beginning of segment
 6.088000      $ R2     = radius at end of segment
 20.85000      $ Z2     = global axial coordinate at end of segment
    H          $ IMPERFECTION SHAPE FOLLOWS...
    0          $ IMP    = indicator for imperfection (0=none, 1=some)
    H          $ REFERENCE SURFACE LOCATION RELATIVE TO WALL
    3          $ NTYPEZ= control (1 or 3) for reference surface location
0.5000000E-01  $ ZVAL   = distance from leftmost surf. to reference surf.
    N          $ Do you want to print out r(s), r'(s), etc. for this segment?
    H          $ DISCRETE RING INPUT FOLLOWS...
    0          $ NRINGS= number (max=20) of discrete rings in this segment
```

B-1. Scale model housing data for case 4, Sheet 6.

```
       0        $ K=elastic foundation modulus (e.g. lb/in**3)in this seg.
    H           $ LINE LOAD INPUT FOLLOWS...
       0        $ LINTYP= indicator (0, 1, 2 or 3) for type of line loads
    H           $ DISTRIBUTED LOAD INPUT FOLLOWS...
       0        $ IDISAB= indicator (0, 1, 2 or 3) for load set A and B
    H           $ SHELL WALL CONSTRUCTION FOLLOWS...
       2        $ NWALL=index (1, 2, 4, 5, 6, 7, 8) for wall construction
0.1640000E+08   $ E      = Young's modulus for skin
0.3100000       $ U      = Poisson's ratio for skin
       0.       $ SM =mass density of skin (e.g. alum.=.00025 lb-sec**2/in**4)
       0.       $ ALPHA = coefficient of thermal expansion
       0        $ NRS  = control (0 or 1) for addition of smeared stiffeners
       0        $ NSUR   = control for thickness input (0 or 1 or -1)
    Y           $ Do you want to print out ref. surf. location and thickness?
    N           $ Do you want to print out the C(i,j) at meridional stations?
    N           $ Do you want to print out distributed loads along meridian?
    H           $
    H           $ SEGMENT NUMBER   10   10   10   10   10   10   10   10
    H           $ NODAL POINT DISTRIBUTION FOLLOWS...
      13        $ NMESH = number of node points (5 = min.; 98 = max.)(10)
       3        $ NTYPEH= control integer (1 or 3) for nodal point spacing
    H           $ REFERENCE SURFACE GEOMETRY FOLLOWS...
       1        $ NSHAPE= indicator (1,2 or 4) for geometry of meridian
 6.151000       $ R1     = radius at beginning of segment (see p. 66)
 20.85000       $ Z1     = global axial coordinate at beginning of segment
 6.151000       $ R2     = radius at end of segment
 22.53600       $ Z2     = global axial coordinate at end of segment
    H           $ IMPERFECTION SHAPE FOLLOWS...
       0        $ IMP    = indicator for imperfection (0=none, 1=some)
    H           $ REFERENCE SURFACE LOCATION RELATIVE TO WALL
       3        $ NTYPEZ= control (1 or 3) for reference surface location
0.1140000       $ ZVAL   = distance from leftmost surf. to reference surf.
    N           $ Do you want to print out r(s), r'(s), etc. for this segment?
    H           $ DISCRETE RING INPUT FOLLOWS...
       0        $ NRINGS= number (max=20) of discrete rings in this segment
       0        $ K=elastic foundation modulus (e.g. lb/in**3)in this seg.
    H           $ LINE LOAD INPUT FOLLOWS...
       0        $ LINTYP= indicator (0, 1, 2 or 3) for type of line loads
    H           $ DISTRIBUTED LOAD INPUT FOLLOWS...
       0        $ IDISAB= indicator (0, 1, 2 or 3) for load set A and B
    H           $ SHELL WALL CONSTRUCTION FOLLOWS...
       2        $ NWALL=index (1, 2, 4, 5, 6, 7, 8) for wall construction
0.1640000E+08   $ E      = Young's modulus for skin
0.3100000       $ U      = Poisson's ratio for skin
       0.       $ SM =mass density of skin (e.g. alum.=.00025 lb-sec**2/in**4)
       0.       $ ALPHA = coefficient of thermal expansion
       0        $ NRS  = control (0 or 1) for addition of smeared stiffeners
       0        $ NSUR   = control for thickness input (0 or 1 or -1)
    Y           $ Do you want to print out ref. surf. location and thickness?
    N           $ Do you want to print out the C(i,j) at meridional stations?
    N           $ Do you want to print out distributed loads along meridian?
    H           $
    H           $ SEGMENT NUMBER   11   11   11   11   11   11   11   11
    H           $ NODAL POINT DISTRIBUTION FOLLOWS...
       5        $ NMESH = number of node points (5 = min.; 98 = max.)(11)
       3        $ NTYPEH= control integer (1 or 3) for nodal point spacing
    H           $ REFERENCE SURFACE GEOMETRY FOLLOWS...
       1        $ NSHAPE= indicator (1,2 or 4) for geometry of meridian
 6.088000       $ R1     = radius at beginning of segment (see p. 66)
 22.53600       $ Z1     = global axial coordinate at beginning of segment
 6.088000       $ R2     = radius at end of segment
 22.77600       $ Z2     = global axial coordinate at end of segment
    H           $ IMPERFECTION SHAPE FOLLOWS...
       0        $ IMP    = indicator for imperfection (0=none, 1=some)
    H           $ REFERENCE SURFACE LOCATION RELATIVE TO WALL
       3        $ NTYPEZ= control (1 or 3) for reference surface location
```

B-1. Scale model housing data for case 4, Sheet 7.

```
0.5000000E-01 $ ZVAL  = distance from leftmost surf. to reference surf.
    N         $ Do you want to print out r(s), r'(s), etc. for this segment?
    H         $ DISCRETE RING INPUT FOLLOWS...
      0       $ NRINGS= number (max=20) of discrete rings in this segment
      0       $ K=elastic foundation modulus (e.g. lb/in**3)in this seg.
    H         $ LINE LOAD INPUT FOLLOWS...
      0       $ LINTYP= indicator (0, 1, 2 or 3) for type of line loads
    H         $ DISTRIBUTED LOAD INPUT FOLLOWS...
      0       $ IDISAB= indicator (0, 1, 2 or 3) for load set A and B
    H         $ SHELL WALL CONSTRUCTION FOLLOWS...
      2       $ NWALL=index (1, 2, 4, 5, 6, 7, 8) for wall construction
0.1640000E+08 $ E     = Young's modulus for skin
0.3100000     $ U     = Poisson's ratio for skin
      0.      $ SM =mass density of skin (e.g. alum.=.00025 lb-sec**2/in**4)
      0.      $ ALPHA = coefficient of thermal expansion
      0       $ NRS  = control (0 or 1) for addition of smeared stiffeners
      0       $ NSUR   = control for thickness input (0 or 1 or -1)
    Y         $ Do you want to print out ref. surf. location and thickness?
    N         $ Do you want to print out the C(i,j) at meridional stations?
    N         $ Do you want to print out distributed loads along meridian?
    H         $ SEGMENT NUMBER   12   12   12   12   12   12   12   12
    H         $ NODAL POINT DISTRIBUTION FOLLOWS...
     10       $ NMESH = number of node points (5 = min.; 98 = max.)(12)
      3       $ NTYPEH= control integer (1 or 3) for nodal point spacing
    H         $ REFERENCE SURFACE GEOMETRY FOLLOWS...
      1       $ NSHAPE= indicator (1,2 or 4) for geometry of meridian
 5.807000     $ R1     = radius at beginning of segment (see p. 66)
 21.81300     $ Z1     = global axial coordinate at beginning of segment
 5.807000     $ R2     = radius at end of segment
 37.39800     $ Z2     = global axial coordinate at end of segment
    H         $ IMPERFECTION SHAPE FOLLOWS...
      0       $ IMP   = indicator for imperfection (0=none, 1=some)
    H         $ REFERENCE SURFACE LOCATION RELATIVE TO WALL
      3       $ NTYPEZ= control (1 or 3) for reference surface location
0.2170000     $ ZVAL  = distance from leftmost surf. to reference surf.
    N         $ Do you want to print out r(s), r'(s), etc. for this segment?
    H         $ DISCRETE RING INPUT FOLLOWS...
      0       $ NRINGS= number (max=20) of discrete rings in this segment
      0       $ K=elastic foundation modulus (e.g. lb/in**3)in this seg.
    H         $ LINE LOAD INPUT FOLLOWS...
      0       $ LINTYP= indicator (0, 1, 2 or 3) for type of line loads
    H         $ DISTRIBUTED LOAD INPUT FOLLOWS...
      1       $ IDISAB= indicator (0, 1, 2 or 3) for load set A and B
    H         $ SURFACE LOAD INPUT FOR LOAD SET "A" FOLLOWS
      1       $ NLTYPE=control (0,1,2,3) for type of surface loading
      2       $ NPSTAT= number of meridional callouts for surface loading
      0       $ NLOAD(1)=indicator for meridional traction (0=none, 1=some)
      0       $ NLOAD(2)=indicator for circumferential traction
      1       $ NLOAD(3)=indicator for normal pressure     (0=none, 1=some)
     -1       $ PN(i)   = normal pressure (p.74) at ith callout, PN( 1)
     -1       $ PN(i)   = normal pressure (p.74) at ith callout, PN( 2)
      2       $ NTYPE = control for meaning of loading callout (2=z, 3=r)
 21.81300     $ Z(I)  = axial coordinate of Ith loading callout, z( 1)
 37.39800     $ Z(I)  = axial coordinate of Ith loading callout, z( 2)
    H         $ SHELL WALL CONSTRUCTION FOLLOWS...
      2       $ NWALL=index (1, 2, 4, 5, 6, 7, 8) for wall construction
0.4400000E+08 $ E     = Young's modulus for skin
0.2100000     $ U     = Poisson's ratio for skin
      0.      $ SM =mass density of skin (e.g. alum.=.00025 lb-sec**2/in**4)
      0.      $ ALPHA = coefficient of thermal expansion
      0       $ NRS  = control (0 or 1) for addition of smeared stiffeners
      0       $ NSUR   = control for thickness input (0 or 1 or -1)
    Y         $ Do you want to print out ref. surf. location and thickness?
    N         $ Do you want to print out the C(i,j) at meridional stations?
    N         $ Do you want to print out distributed loads along meridian?
    H         $
```

B-1. Scale model housing data for case 4, Sheet 8.

```
     H          $ SEGMENT NUMBER   13   13   13   13   13   13   13   13
     H          $ NODAL POINT DISTRIBUTION FOLLOWS...
        5       $ NMESH = number of node points (5 = min.; 98 = max.)(13)
        3       $ NTYPEH= control integer (1 or 3) for nodal point spacing
     H          $ REFERENCE SURFACE GEOMETRY FOLLOWS...
        1       $ NSHAPE= indicator (1,2 or 4) for geometry of meridian
 6.024000       $ R1      = radius at beginning of segment (see p. 66)
 37.39800       $ Z1      = global axial coordinate at beginning of segment
 6.024000       $ R2      = radius at end of segment
 38.60300       $ Z2      = global axial coordinate at end of segment
     H          $ IMPERFECTION SHAPE FOLLOWS...
        0       $ IMP     = indicator for imperfection (0=none, 1=some)
     H          $ REFERENCE SURFACE LOCATION RELATIVE TO WALL
        3       $ NTYPEZ= control (1 or 3) for reference surface location
0.4340000       $ ZVAL  = distance from leftmost surf. to reference surf.
     N          $ Do you want to print out r(s), r'(s), etc. for this segment?
     H          $ DISCRETE RING INPUT FOLLOWS...
        0       $ NRINGS= number (max=20) of discrete rings in this segment
        0       $ K=elastic foundation modulus (e.g. lb/in**3)in this seg.
     H          $ LINE LOAD INPUT FOLLOWS...
        0       $ LINTYP= indicator (0, 1, 2 or 3) for type of line loads
     H          $ DISTRIBUTED LOAD INPUT FOLLOWS...
        1       $ IDISAB= indicator (0, 1, 2 or 3) for load set A and B
     H          $ SURFACE LOAD INPUT FOR LOAD SET "A" FOLLOWS
        1       $ NLTYPE=control (0,1,2,3) for type of surface loading
        2       $ NPSTAT= number of meridional callouts for surface loading
        0       $ NLOAD(1)=indicator for meridional traction (0=none, 1=some)
        0       $ NLOAD(2)=indicator for circumferential traction
        1       $ NLOAD(3)=indicator for normal pressure     (0=none, 1=some)
       -1       $ PN(i)   = normal pressure (p.74) at ith callout, PN( 1)
       -1       $ PN(i)   = normal pressure (p.74) at ith callout, PN( 2)
        2       $ NTYPE = control for meaning of loading callout (2=z, 3=r)
 37.39800       $ Z(I)  = axial coordinate of Ith loading callout, z( 1)
 38.60300       $ Z(I)  = axial coordinate of Ith loading callout, z( 2)
     H          $ SHELL WALL CONSTRUCTION FOLLOWS...
        2       $ NWALL=index (1, 2, 4, 5, 6, 7, 8) for wall construction
0.4400000E+08   $ E     = Young's modulus for skin
0.2100000       $ U     = Poisson's ratio for skin
        0.      $ SM =mass density of skin (e.g. alum.=.00025 lb-sec**2/in**4)
        0.      $ ALPHA = coefficient of thermal expansion
        0       $ NRS   = control (0 or 1) for addition of smeared stiffeners
        1       $ NSUR    = control for thickness input (0 or 1 or -1)
     N          $ Do you want to print out the C(i,j) at meridional stations?
     N          $ Do you want to print out distributed loads along meridian?
     H          $
     H          $ SEGMENT NUMBER   14   14   14   14   14   14   14   14
     H          $ NODAL POINT DISTRIBUTION FOLLOWS...
        5       $ NMESH = number of node points (5 = min.; 98 = max.)(14)
        3       $ NTYPEH= control integer (1 or 3) for nodal point spacing
     H          $ REFERENCE SURFACE GEOMETRY FOLLOWS...
        1       $ NSHAPE= indicator (1,2 or 4) for geometry of meridian
 6.024000       $ R1      = radius at beginning of segment (see p. 66)
 38.60300       $ Z1      = global axial coordinate at beginning of segment
 5.427000       $ R2      = radius at end of segment
 39.93700       $ Z2      = global axial coordinate at end of segment
     H          $ IMPERFECTION SHAPE FOLLOWS...
        0       $ IMP     = indicator for imperfection (0=none, 1=some)
     H          $ REFERENCE SURFACE LOCATION RELATIVE TO WALL
        1       $ NTYPEZ= control (1 or 3) for reference surface location
        2       $ NZVALU= number of meridional callouts for ref. surf.
        2       $ NTYPE = control for meaning of callout (2=z, 3=r)
 38.60300       $ Z(I)  = axial coordinate of Ith callout, z( 1)
 39.93700       $ Z(I)  = axial coordinate of Ith callout, z( 2)
0.4340000       $ ZVAL  = distance from leftmost surf. to ref. surf.,ZVAL( 1)
0.2750000       $ ZVAL  = distance from leftmost surf. to ref. surf.,ZVAL( 2)
     N          $ Do you want to print out r(s), r'(s), etc. for this segment?
```

B-1. Scale model housing data for case 4, Sheet 9.

```
     H          $ DISCRETE RING INPUT FOLLOWS...
     0          $ NRINGS= number (max=20) of discrete rings in this segment
     0          $ K=elastic foundation modulus (e.g. lb/in**3)in this seg.
     H          $ LINE LOAD INPUT FOLLOWS...
     0          $ LINTYP= indicator (0, 1, 2 or 3) for type of line loads
     H          $ DISTRIBUTED LOAD INPUT FOLLOWS...
     1          $ IDISAB= indicator (0, 1, 2 or 3) for load set A and B
     H          $ SURFACE LOAD INPUT FOR LOAD SET "A" FOLLOWS
     1          $ NLTYPE=control (0,1,2,3) for type of surface loading
     2          $ NPSTAT= number of meridional callouts for surface loading
     0          $ NLOAD(1)=indicator for meridional traction (0=none, 1=some)
     0          $ NLOAD(2)=indicator for circumferential traction
     1          $ NLOAD(3)=indicator for normal pressure     (0=none, 1=some)
    -1          $ PN(i)   = normal pressure (p.74) at ith callout, PN( 1)
    -1          $ PN(i)   = normal pressure (p.74) at ith callout, PN( 2)
     2          $ NTYPE = control for meaning of loading callout (2=z, 3=r)
 38.60300       $ Z(I)  = axial coordinate of Ith loading callout, z( 1)
 39.93700       $ Z(I)  = axial coordinate of Ith loading callout, z( 2)
     H          $ SHELL WALL CONSTRUCTION FOLLOWS...
     2          $ NWALL=index (1, 2, 4, 5, 6, 7, 8) for wall construction
0.4400000E+08   $ E     = Young's modulus for skin
0.2100000       $ U     = Poisson's ratio for skin
     0.         $ SM =mass density of skin (e.g. alum.=.00025 lb-sec**2/in**4)
     0.         $ ALPHA = coefficient of thermal expansion
     0          $ NRS   = control (0 or 1) for addition of smeared stiffeners
     1          $ NSUR  = control for thickness input (0 or 1 or -1)
     N          $ Do you want to print out the C(i,j) at meridional stations?
     N          $ Do you want to print out distributed loads along meridian?
     H          $
     H          $ SEGMENT NUMBER   15   15   15   15   15   15   15   15
     H          $ NODAL POINT DISTRIBUTION FOLLOWS...
    10          $ NMESH = number of node points (5 = min.; 98 = max.)(15)
     3          $ NTYPEH= control integer (1 or 3) for nodal point spacing
     H          $ REFERENCE SURFACE GEOMETRY FOLLOWS...
     2          $ NSHAPE= indicator (1,2 or 4) for geometry of meridian
 5.427000       $ R1      = radius at beginning of segment (see p. 66)
 39.93700       $ Z1      = global axial coordinate at beginning of segment
     0.         $ R2      = radius at end of segment
 43.29500       $ Z2      = global axial coordinate at end of segment
     0.         $ RC      = radius from axis of rev. to center of curvature
 37.23000       $ ZC      = axial coordinate of center of curvature
    -1          $ SROT=indicator for direction of increasing arc (-1. or +1.)
     H          $ IMPERFECTION SHAPE FOLLOWS...
     0          $ IMP   = indicator for imperfection (0=none, 1=some)
     H          $ REFERENCE SURFACE LOCATION RELATIVE TO WALL
     1          $ NTYPEZ= control (1 or 3) for reference surface location
     2          $ NZVALU= number of meridional callouts for ref. surf.
     2          $ NTYPE = control for meaning of callout (2=z, 3=r)
 39.93700       $ Z(I)  = axial coordinate of Ith callout, z( 1)
 43.29500       $ Z(I)  = axial coordinate of Ith callout, z( 2)
0.2750000       $ ZVAL  = distance from leftmost surf. to ref. surf.,ZVAL( 1)
0.1810000       $ ZVAL  = distance from leftmost surf. to ref. surf.,ZVAL( 2)
     N          $ Do you want to print out r(s), r'(s), etc. for this segment?
     H          $ DISCRETE RING INPUT FOLLOWS...
     0          $ NRINGS= number (max=20) of discrete rings in this segment
     0          $ K=elastic foundation modulus (e.g. lb/in**3)in this seg.
     H          $ LINE LOAD INPUT FOLLOWS...
     0          $ LINTYP= indicator (0, 1, 2 or 3) for type of line loads
     H          $ DISTRIBUTED LOAD INPUT FOLLOWS...
     1          $ IDISAB= indicator (0, 1, 2 or 3) for load set A and B
     H          $ SURFACE LOAD INPUT FOR LOAD SET "A" FOLLOWS
     1          $ NLTYPE=control (0,1,2,3) for type of surface loading
     2          $ NPSTAT= number of meridional callouts for surface loading
     0          $ NLOAD(1)=indicator for meridional traction (0=none, 1=some)
     0          $ NLOAD(2)=indicator for circumferential traction
     1          $ NLOAD(3)=indicator for normal pressure     (0=none, 1=some)
```

B-1. Scale model housing data for case 4, Sheet 10.

```
      -1      $ PN(i)   = normal pressure (p.74) at ith callout, PN( 1)
      -1      $ PN(i)   = normal pressure (p.74) at ith callout, PN( 2)
       2      $ NTYPE = control for meaning of loading callout (2=z, 3=r)
 39.93700     $ Z(I)  = axial coordinate of Ith loading callout, z( 1)
 43.29500     $ Z(I)  = axial coordinate of Ith loading callout, z( 2)
    H         $ SHELL WALL CONSTRUCTION FOLLOWS...
       2      $ NWALL=index (1, 2, 4, 5, 6, 7, 8) for wall construction
0.4400000E+08 $ E     = Young's modulus for skin
0.2100000     $ U     = Poisson's ratio for skin
       0.     $ SM =mass density of skin (e.g. alum.=.00025 lb-sec**2/in**4)
       0.     $ ALPHA = coefficient of thermal expansion
       0      $ NRS  = control (0 or 1) for addition of smeared stiffeners
       1      $ NSUR   = control for thickness input (0 or 1 or -1)
    N         $ Do you want to print out the C(i,j) at meridional stations?
    N         $ Do you want to print out distributed loads along meridian?
    H         $
    H         $
    H         $ GLOBAL DATA BEGINS...
       0      $ NLAST = plot options  (-1=none, 0=geometry, 1=u,v,w)
    N         $ Are there any regions for which you want expanded plots?
       2      $ NOB   = starting number of circ. waves (buckling analysis)
       2      $ NMINB = minimum number of circ. waves  (buckling analysis)
      10      $ NMAXB = maximum number of circ. waves  (buckling analysis)
       1      $ INCRB = increment in number of circ. waves (buckling)
       1      $ NVEC  = number of eigenvalues for each wave number
       0      $ P      = pressure or surface traction multiplier
       1      $ DP     = pressure or surface traction multiplier increment
       0      $ TEMP   = temperature rise multiplier
       0      $ DTEMP  = temperature rise multiplier increment
       0      $ OMEGA  = angular vel. about axis of revolution (rad/sec)
       0      $ DOMEGA = angular velocity increment (rad/sec)
    H         $ CONSTRAINT CONDITIONS FOLLOW....
      15      $ How many segments in the structure?
    H         $
    H         $ CONSTRAINT CONDITIONS FOR SEGMENT NO.    1    1    1    1
    H         $ POLES INPUT FOLLOWS...
       1      $ Number of poles (places where r=0) in SEGMENT
       1      $ IPOLE = nodal point number of pole, IPOLE( 1)
    H         $ INPUT FOR CONSTRAINTS TO GROUND FOLLOWS...
       0      $ At how many stations is this segment constrained to ground?
    H         $ JUNCTION CONDITION INPUT FOLLOWS...
    N         $ Is this segment joined to any lower-numbered segments?
    H         $
    H         $ CONSTRAINT CONDITIONS FOR SEGMENT NO.    2    2    2    2
    H         $ POLES INPUT FOLLOWS...
       0      $ Number of poles (places where r=0) in SEGMENT
    H         $ INPUT FOR CONSTRAINTS TO GROUND FOLLOWS...
       0      $ At how many stations is this segment constrained to ground?
    H         $ JUNCTION CONDITION INPUT FOLLOWS...
    Y         $ Is this segment joined to any lower-numbered segments?
       1      $ At how may stations is this segment joined to previous segs.?
       1      $ INODE = node in current segment (ISEG) of junction, INODE( 1)
       1      $ JSEG  = segment no. of lowest segment involved in junction
      10      $ JNODE = node in lowest segmnt (JSEG) of junction
       1      $ IUSTAR= axial displacement (0=not slaved, 1=slaved)
       1      $ IVSTAR= circumferential displacement (0=not slaved, 1=slaved)
       1      $ IWSTAR= radial displacement (0=not slaved, 1=slaved)
       1      $ ICHI  = meridional rotation (0=not slaved, 1=slaved)
       0.     $ D1    = radial component of juncture gap
       0.     $ D2    = axial component of juncture gap
    Y         $ Is this constraint the same for both prebuckling and buckling?
    H         $
    H         $ CONSTRAINT CONDITIONS FOR SEGMENT NO.    3    3    3    3
    H         $ POLES INPUT FOLLOWS...
       0      $ Number of poles (places where r=0) in SEGMENT
    H         $ INPUT FOR CONSTRAINTS TO GROUND FOLLOWS...
```

B-1. Scale model housing data for case 4, Sheet 11.

```
         0      $ At how many stations is this segment constrained to ground?
         H      $ JUNCTION CONDITION INPUT FOLLOWS...
         Y      $ Is this segment joined to any lower-numbered segments?
         1      $ At how may stations is this segment joined to previous segs.?
         1      $ INODE = node in current segment (ISEG) of junction, INODE( 1)
         2      $ JSEG  = segment no. of lowest segment involved in junction
         5      $ JNODE = node in lowest segmnt (JSEG) of junction
         1      $ IUSTAR= axial displacement (0=not slaved, 1=slaved)
         1      $ IVSTAR= circumferential displacement (0=not slaved, 1=slaved)
         1      $ IWSTAR= radial displacement (0=not slaved, 1=slaved)
         1      $ ICHI  = meridional rotation (0=not slaved, 1=slaved)
         0.     $ D1    = radial component of juncture gap
         0.     $ D2    = axial component of juncture gap
         Y      $ Is this constraint the same for both prebuckling and buckling?
         H      $
         H      $ CONSTRAINT CONDITIONS FOR SEGMENT NO.    4    4    4    4
         H      $ POLES INPUT FOLLOWS...
         0      $ Number of poles (places where r=0) in SEGMENT
         H      $ INPUT FOR CONSTRAINTS TO GROUND FOLLOWS...
         0      $ At how many stations is this segment constrained to ground?
         H      $ JUNCTION CONDITION INPUT FOLLOWS...
         Y      $ Is this segment joined to any lower-numbered segments?
         1      $ At how may stations is this segment joined to previous segs.?
         1      $ INODE = node in current segment (ISEG) of junction, INODE( 1)
         3      $ JSEG  = segment no. of lowest segment involved in junction
         5      $ JNODE = node in lowest segmnt (JSEG) of junction
         1      $ IUSTAR= axial displacement (0=not slaved, 1=slaved)
         1      $ IVSTAR= circumferential displacement (0=not slaved, 1=slaved)
         1      $ IWSTAR= radial displacement (0=not slaved, 1=slaved)
         0      $ ICHI  = meridional rotation (0=not slaved, 1=slaved)
-0.2170000      $ D1    = radial component of juncture gap
         0.     $ D2    = axial component of juncture gap
         Y      $ Is this constraint the same for both prebuckling and buckling?
         H      $
         H      $ CONSTRAINT CONDITIONS FOR SEGMENT NO.    5    5    5    5
         H      $ POLES INPUT FOLLOWS...
         0      $ Number of poles (places where r=0) in SEGMENT
         H      $ INPUT FOR CONSTRAINTS TO GROUND FOLLOWS...
         0      $ At how many stations is this segment constrained to ground?
         H      $ JUNCTION CONDITION INPUT FOLLOWS...
         Y      $ Is this segment joined to any lower-numbered segments?
         1      $ At how may stations is this segment joined to previous segs.?
         1      $ INODE = node in current segment (ISEG) of junction, INODE( 1)
         4      $ JSEG  = segment no. of lowest segment involved in junction
        10      $ JNODE = node in lowest segmnt (JSEG) of junction
         1      $ IUSTAR= axial displacement (0=not slaved, 1=slaved)
         1      $ IVSTAR= circumferential displacement (0=not slaved, 1=slaved)
         1      $ IWSTAR= radial displacement (0=not slaved, 1=slaved)
         1      $ ICHI  = meridional rotation (0=not slaved, 1=slaved)
-0.3000000E-02  $ D1    = radial component of juncture gap
         0.     $ D2    = axial component of juncture gap
         Y      $ Is this constraint the same for both prebuckling and buckling?
         H      $
         H      $ CONSTRAINT CONDITIONS FOR SEGMENT NO.    6    6    6    6
         H      $ POLES INPUT FOLLOWS...
         0      $ Number of poles (places where r=0) in SEGMENT
         H      $ INPUT FOR CONSTRAINTS TO GROUND FOLLOWS...
         0      $ At how many stations is this segment constrained to ground?
         H      $ JUNCTION CONDITION INPUT FOLLOWS...
         Y      $ Is this segment joined to any lower-numbered segments?
         1      $ At how may stations is this segment joined to previous segs.?
         7      $ INODE = node in current segment (ISEG) of junction, INODE( 1)
         5      $ JSEG  = segment no. of lowest segment involved in junction
         7      $ JNODE = node in lowest segmnt (JSEG) of junction
         1      $ IUSTAR= axial displacement (0=not slaved, 1=slaved)
         1      $ IVSTAR= circumferential displacement (0=not slaved, 1=slaved)
```

B-1. Scale model housing data for case 4, Sheet 12.

```
         1      $ IWSTAR= radial displacement (0=not slaved, 1=slaved)
         1      $ ICHI  = meridional rotation (0=not slaved, 1=slaved)
-0.2940000      $ D1    = radial component of juncture gap
        0.      $ D2    = axial component of juncture gap
     Y          $ Is this constraint the same for both prebuckling and buckling?
     H          $
     H          $ CONSTRAINT CONDITIONS FOR SEGMENT NO.    7    7    7    7
     H          $ POLES INPUT FOLLOWS...
        0       $ Number of poles (places where r=0) in SEGMENT
     H          $ INPUT FOR CONSTRAINTS TO GROUND FOLLOWS...
        0       $ At how many stations is this segment constrained to ground?
     H          $ JUNCTION CONDITION INPUT FOLLOWS...
     Y          $ Is this segment joined to any lower-numbered segments?
        1       $ At how may stations is this segment joined to previous segs.?
        1       $ INODE = node in current segment (ISEG) of junction, INODE( 1)
        6       $ JSEG  = segment no. of lowest segment involved in junction
        7       $ JNODE = node in lowest segmnt (JSEG) of junction
        1       $ IUSTAR= axial displacement (0=not slaved, 1=slaved)
        1       $ IVSTAR= circumferential displacement (0=not slaved, 1=slaved)
        1       $ IWSTAR= radial displacement (0=not slaved, 1=slaved)
        1       $ ICHI  = meridional rotation (0=not slaved, 1=slaved)
-0.6000000E-01  $ D1    = radial component of juncture gap
        0.      $ D2    = axial component of juncture gap
     Y          $ Is this constraint the same for both prebuckling and buckling?
     H          $
     H          $ CONSTRAINT CONDITIONS FOR SEGMENT NO.    8    8    8    8
     H          $ POLES INPUT FOLLOWS...
        0       $ Number of poles (places where r=0) in SEGMENT
     H          $ INPUT FOR CONSTRAINTS TO GROUND FOLLOWS...
        0       $ At how many stations is this segment constrained to ground?
     H          $ JUNCTION CONDITION INPUT FOLLOWS...
     Y          $ Is this segment joined to any lower-numbered segments?
        1       $ At how may stations is this segment joined to previous segs.?
        7       $ INODE = node in current segment (ISEG) of junction, INODE( 1)
        7       $ JSEG  = segment no. of lowest segment involved in junction
        9       $ JNODE = node in lowest segmnt (JSEG) of junction
        1       $ IUSTAR= axial displacement (0=not slaved, 1=slaved)
        1       $ IVSTAR= circumferential displacement (0=not slaved, 1=slaved)
        1       $ IWSTAR= radial displacement (0=not slaved, 1=slaved)
        1       $ ICHI  = meridional rotation (0=not slaved, 1=slaved)
-0.1950000      $ D1    = radial component of juncture gap
        0.      $ D2    = axial component of juncture gap
     Y          $ Is this constraint the same for both prebuckling and buckling?
     H          $
     H          $ CONSTRAINT CONDITIONS FOR SEGMENT NO.    9    9    9    9
     H          $ POLES INPUT FOLLOWS...
        0       $ Number of poles (places where r=0) in SEGMENT
     H          $ INPUT FOR CONSTRAINTS TO GROUND FOLLOWS...
        0       $ At how many stations is this segment constrained to ground?
     H          $ JUNCTION CONDITION INPUT FOLLOWS...
     N          $ Is this segment joined to any lower-numbered segments?
     H          $
     H          $ CONSTRAINT CONDITIONS FOR SEGMENT NO.   10   10   10   10
     H          $ POLES INPUT FOLLOWS...
        0       $ Number of poles (places where r=0) in SEGMENT
     H          $ INPUT FOR CONSTRAINTS TO GROUND FOLLOWS...
        0       $ At how many stations is this segment constrained to ground?
     H          $ JUNCTION CONDITION INPUT FOLLOWS...
     Y          $ Is this segment joined to any lower-numbered segments?
        2       $ At how may stations is this segment joined to previous segs.?
        1       $ INODE = node in current segment (ISEG) of junction, INODE( 1)
        9       $ JSEG  = segment no. of lowest segment involved in junction
        5       $ JNODE = node in lowest segmnt (JSEG) of junction
        1       $ IUSTAR= axial displacement (0=not slaved, 1=slaved)
        1       $ IVSTAR= circumferential displacement (0=not slaved, 1=slaved)
        1       $ IWSTAR= radial displacement (0=not slaved, 1=slaved)
```

B-1. Scale model housing data for case 4, Sheet 13.

```
       1       $ ICHI  = meridional rotation (0=not slaved, 1=slaved)
0.6300000E-01  $ D1    = radial component of juncture gap
       0.      $ D2    = axial component of juncture gap
    Y          $ Is this constraint the same for both prebuckling and buckling?
       7       $ INODE = node in current segment (ISEG) of junction, INODE( 2)
       5       $ JSEG  = segment no. of lowest segment involved in junction
       7       $ JNODE = node in lowest segmnt (JSEG) of junction
       1       $ IUSTAR= axial displacement (0=not slaved, 1=slaved)
       1       $ IVSTAR= circumferential displacement (0=not slaved, 1=slaved)
       1       $ IWSTAR= radial displacement (0=not slaved, 1=slaved)
       1       $ ICHI  = meridional rotation (0=not slaved, 1=slaved)
0.3470000      $ D1    = radial component of juncture gap
       0.      $ D2    = axial component of juncture gap
    Y          $ Is this constraint the same for both prebuckling and buckling?
    H          $
    H          $ CONSTRAINT CONDITIONS FOR SEGMENT NO.   11   11   11   11
    H          $ POLES INPUT FOLLOWS...
       0       $ Number of poles (places where r=0) in SEGMENT
    H          $ INPUT FOR CONSTRAINTS TO GROUND FOLLOWS...
       0       $ At how many stations is this segment constrained to ground?
    H          $ JUNCTION CONDITION INPUT FOLLOWS...
    Y          $ Is this segment joined to any lower-numbered segments?
       1       $ At how may stations is this segment joined to previous segs.?
       1       $ INODE = node in current segment (ISEG) of junction, INODE( 1)
      10       $ JSEG  = segment no. of lowest segment involved in junction
      13       $ JNODE = node in lowest segmnt (JSEG) of junction
       1       $ IUSTAR= axial displacement (0=not slaved, 1=slaved)
       1       $ IVSTAR= circumferential displacement (0=not slaved, 1=slaved)
       1       $ IWSTAR= radial displacement (0=not slaved, 1=slaved)
       1       $ ICHI  = meridional rotation (0=not slaved, 1=slaved)
-0.6300000E-01 $ D1    = radial component of juncture gap
       0.      $ D2    = axial component of juncture gap
    Y          $ Is this constraint the same for both prebuckling and buckling?
    H          $
    H          $ CONSTRAINT CONDITIONS FOR SEGMENT NO.   12   12   12   12
    H          $ POLES INPUT FOLLOWS...
       0       $ Number of poles (places where r=0) in SEGMENT
    H          $ INPUT FOR CONSTRAINTS TO GROUND FOLLOWS...
       0       $ At how many stations is this segment constrained to ground?
    H          $ JUNCTION CONDITION INPUT FOLLOWS...
    Y          $ Is this segment joined to any lower-numbered segments?
       1       $ At how may stations is this segment joined to previous segs.?
       1       $ INODE = node in current segment (ISEG) of junction, INODE( 1)
       5       $ JSEG  = segment no. of lowest segment involved in junction
      13       $ JNODE = node in lowest segmnt (JSEG) of junction
       1       $ IUSTAR= axial displacement (0=not slaved, 1=slaved)
       1       $ IVSTAR= circumferential displacement (0=not slaved, 1=slaved)
       1       $ IWSTAR= radial displacement (0=not slaved, 1=slaved)
       1       $ ICHI  = meridional rotation (0=not slaved, 1=slaved)
0.3000000E-02  $ D1    = radial component of juncture gap
       0.      $ D2    = axial component of juncture gap
    Y          $ Is this constraint the same for both prebuckling and buckling?
    H          $
    H          $ CONSTRAINT CONDITIONS FOR SEGMENT NO.   13   13   13   13
    H          $ POLES INPUT FOLLOWS...
       0       $ Number of poles (places where r=0) in SEGMENT
    H          $ INPUT FOR CONSTRAINTS TO GROUND FOLLOWS...
       0       $ At how many stations is this segment constrained to ground?
    H          $ JUNCTION CONDITION INPUT FOLLOWS...
    Y          $ Is this segment joined to any lower-numbered segments?
       1       $ At how may stations is this segment joined to previous segs.?
       1       $ INODE = node in current segment (ISEG) of junction, INODE( 1)
      12       $ JSEG  = segment no. of lowest segment involved in junction
      10       $ JNODE = node in lowest segmnt (JSEG) of junction
       1       $ IUSTAR= axial displacement (0=not slaved, 1=slaved)
       1       $ IVSTAR= circumferential displacement (0=not slaved, 1=slaved)
```

B-1. Scale model housing data for case 4, Sheet 14.

```
       1      $ IWSTAR= radial displacement (0=not slaved, 1=slaved)
       0      $ ICHI  = meridional rotation (0=not slaved, 1=slaved)
0.2170000     $ D1    = radial component of juncture gap
      0.      $ D2    = axial component of juncture gap
     Y        $ Is this constraint the same for both prebuckling and buckling?
     H        $
     H        $ CONSTRAINT CONDITIONS FOR SEGMENT NO.   14   14   14   14
     H        $ POLES INPUT FOLLOWS...
       0      $ Number of poles (places where r=0) in SEGMENT
     H        $ INPUT FOR CONSTRAINTS TO GROUND FOLLOWS...
       0      $ At how many stations is this segment constraired to ground?
     H        $ JUNCTION CONDITION INPUT FOLLOWS...
     Y        $ Is this segment joined to any lower-numbered segments?
       1      $ At how may stations is this segment joined to previous segs.?
       1      $ INODE = node in current segment (ISEG) of junction, INODE( 1)
      13      $ JSEG  = segment no. of lowest segment involved in junction
       5      $ JNODE = node in lowest segmnt (JSEG) of junction
       1      $ IUSTAR= axial displacement (0=not slaved, 1=slaved)
       1      $ IVSTAR= circumferential displacement (0=not slaved, 1=slaved)
       1      $ IWSTAR= radial displacement (0=not slaved, 1=slaved)
       1      $ ICHI  = meridional rotation (0=not slaved, 1=slaved)
      0.      $ D1    = radial component of juncture gap
      0.      $ D2    = axial component of juncture gap
     Y        $ Is this constraint the same for both prebuckling and buckling?
     H        $
     H        $ CONSTRAINT CONDITIONS FOR SEGMENT NO.   15   15   15   15
     H        $ POLES INPUT FOLLOWS...
       1      $ Number of poles (places where r=0) in SEGMENT
      10      $ IPOLE = nodal point number of pole, IPOLE( 1)
     H        $ INPUT FOR CONSTRAINTS TO GROUND FOLLOWS...
       0      $ At how many stations is this segment constrained to ground?
     H        $ JUNCTION CONDITION INPUT FOLLOWS...
     Y        $ Is this segment joined to any lower-numbered segments?
       1      $ At how may stations is this segment joined to previous segs.?
       1      $ INODE = node in current segment (ISEG) of junction, INODE( 1)
      14      $ JSEG  = segment no. of lowest segment involved in junction
       5      $ JNODE = node in lowest segmnt (JSEG) of junction
       1      $ IUSTAR= axial displacement (0=not slaved, 1=slaved)
       1      $ IVSTAR= circumferential displacement (0=not slaved, 1=slaved)
       1      $ IWSTAR= radial displacement (0=not slaved, 1=slaved)
       1      $ ICHI  = meridional rotation (0=not slaved, 1=slaved)
      0.      $ D1    = radial component of juncture gap
      0.      $ D2    = axial component of juncture gap
     Y        $ Is this constraint the same for both prebuckling and buckling?
     H        $ RIGID BODY CONSTRAINT INPUT FOLLOWS...
     N        $ Given existing constraints, are rigid body modes possible?
     H        $ "GLOBAL3" QUESTIONS (AT END OF CASE)...
     Y        $ Do you want to list output for segment( 1)
     Y        $ Do you want to list output for segment( 2)
     Y        $ Do you want to list output for segment( 3)
     Y        $ Do you want to list output for segment( 4)
     Y        $ Do you want to list output for segment( 5)
     Y        $ Do you want to list output for segment( 6)
     Y        $ Do you want to list output for segment( 7)
     Y        $ Do you want to list output for segment( 8)
     Y        $ Do you want to list output for segment( 9)
     Y        $ Do you want to list output for segment(10)
     Y        $ Do you want to list output for segment(11)
     Y        $ Do you want to list output for segment(12)
     Y        $ Do you want to list output for segment(13)
     Y        $ Do you want to list output for segment(14)
     Y        $ Do you want to list output for segment(15)
     N        $ Do you want to list forces in the discrete rings, if any?
```

B-1. Scale model housing data for case 4, Sheet 15.

REPORT DOCUMENTATION PAGE

Form Approved
OMB No. 0704-0188

Public reporting burden for this collection of information is estimated to average 1 hour per response, including the time for reviewing instructions, searching existing data sources, gathering and maintaining the data needed, and completing and reviewing the collection of information. Send comments regarding this burden estimate or any other aspect of this collection of information, including suggestions for reducing this burden, to Washington Headquarters Services, Directorate for Information Operations and Reports, 1215 Jefferson Davis Highway, Suite 1204, Arlington, VA 22202-4302, and to the Office of Management and Budget, Paperwork Reduction Project (0704-0188), Washington, DC 20503.

1. AGENCY USE ONLY *(Leave blank)*	2. REPORT DATE	3. REPORT TYPE AND DATES COVERED
	May 1993	Final

4. TITLE AND SUBTITLE

EXPLORATORY STUDY OF JOINT RINGS FOR CERAMIC UNDERWATER PRESSURE HOUSINGS

5. FUNDING NUMBERS

PE: 0603713N
PROJ: S0397
ACC: DN302232

6. AUTHOR(S)

R. P. Johnson, R. R. Kurkchubasche, and J. D. Stachiw

7. PERFORMING ORGANIZATION NAME(S) AND ADDRESS(ES)

Naval Command, Control and Ocean Surveillance Center (NCCOSC)
RDT&E Division
San Diego, CA 92152–5000

8. PERFORMING ORGANIZATION REPORT NUMBER

TR 1586

9. SPONSORING/MONITORING AGENCY NAME(S) AND ADDRESS(ES)

Naval Sea Systems Command
Washington, DC 20362

10. SPONSORING/MONITORING AGENCY REPORT NUMBER

11. SUPPLEMENTARY NOTES

12a. DISTRIBUTION/AVAILABILITY STATEMENT

Approved for public release; distribution is unlimited.

12b. DISTRIBUTION CODE

13. ABSTRACT *(Maximum 200 words)*

The motivation for utilizing ceramic hull components in the design of pressure-resistant housings for underwater applications is well documented. Practical ceramic housing designs require joining techniques that can be used to assemble housing components. These joints may be for permanent bonding of adjacent ceramic components in order to build up hull sections or for service joints that allow adjacent ceramic hull sections to be disassembled for internal access or inspection. One approach to the design of joint interfaces for ceramic pressure hulls uses metallic joint rings to encapsulate the ends of ceramic housing components. This document describes issues that the designer of such joint rings for ceramic housings must address and documents the results of four cylindrical housing configurations that have been designed, fabricated and tested to destruction.

14. SUBJECT TERMS

ceramics
external pressure housing
ocean engineering

15. NUMBER OF PAGES

98

16. PRICE CODE

17. SECURITY CLASSIFICATION OF REPORT	18. SECURITY CLASSIFICATION OF THIS PAGE	19. SECURITY CLASSIFICATION OF ABSTRACT	20. LIMITATION OF ABSTRACT
UNCLASSIFIED	UNCLASSIFIED	UNCLASSIFIED	SAME AS REPORT

21a. NAME OF RESPONSIBLE INDIVIDUAL	21b. TELEPHONE *(include Area Code)*	21c. OFFICE SYMBOL
R. P. Johnson	(619) 553–1875	Code 9402

THE AUTHORS

RICHARD P. JOHNSON presently is an engineer with the Structural Mechanics, Analysis and Design Branch and Ocean Technology Branch. He has held this position since 1987. Before that, he was a Laboratory Technician for the Ocean Engineering Laboratory, University of California at Santa Barbara from 1985–1986, and Design Engineer in the Energy Projects Division of SAIC from 1986–1987. His education includes a B.S. in Mechanical Engineering from the University of California at Santa Barbara in 1986, and an M.S. in Structural Engineering from the University of California, San Diego, in 1991. He has published "Stress Analysis Considerations for Deep Submergence Ceramic Pressure Housings," *Intervention '92*, Marine Technology Society. He is a member of the Marine Technology Society.

RAMON R. KURKCHUBASCHE is a Research Engineer at Naval Ocean Systems Center and has worked since November 1990 in the field of deep submergence pressure housings fabricated from ceramic materials. His education includes a B.S. in Structural Engineering from the University of California at San Diego, 1989; and an M.S. in Aeronautical/Astronautical Engineering from Stanford University in 1990. His experience includes conceptual design, procurement, assembly, testing, and documentation of ceramic housings. Other experience includes buoyancy concepts utilizing ceramic, nondestructive evaluation of ceramic components. He is a member of the Marine Technology Society, and has published "Elastic Stability Considerations for Deep Submergence Ceramic Pressure Housings," *Intervention '92*, Marine Technology Society.

DR. JERRY STACHIW is Staff Scientist for Marine Mammals in the Ocean Engineering Division of the Engineering Department. He received his undergraduate engineering degree from Oklahoma State University in 1955 and graduate degree from Pennsylvania State University in 1961.

Since that time he has devoted his efforts at various U.S. Navy Laboratories to the solution of challenges posed by exploration, exploitation, and surveillance of hydrospace. The primary focus of his work has been the design and fabrication of pressure resistant structural components of diving systems for the whole range of ocean depths. Because of his numerous achievements in the field of ocean engineering, he is considered to be the leading expert in the structural application of plastics and brittle materials to external pressure housings.

Dr. Stachiw is the author of over 100 technical reports, articles, and papers on design and fabrication of pressure resistant viewports of acrylic plastic, glass, germanium, and zinc sulphide, as well as pressure housings made of wood, concrete, glass, acrylic plastic, and ceramics. His book on "Acrylic Plastic Viewports" is the standard reference on that subject.

For the contributions to the Navy's ocean engineering programs, the Navy honored him with the Military Oceanographer Award and the Naval Ocean Systems Center with the Lauritsen-Bennett Award. The American Society of Mechanical

Engineers recognized his contributions to the engineering profession by election to the grade of Life-Fellow, as well as the presentation of Centennial Medal, Dedicated Service Award and Pressure Technology Codes Outstanding Performance Certificate.

Dr. Stachiw is past-chairman of ASME Ocean Engineering Division and ASME Committee on Safety Standards for Pressure Vessels for Human Occupancy. He is a member of the Marine Technology Society, New York Academy of Science, Sigma Xi and Phi Kappa Honorary Society.

END

FILMED

DATE: 10-93

DTIC